November 2015

Impacts of Land Cover and Climate Change on Water Resources in Suasco River Watershed

Ammara Talib
University of Massachusetts Amherst

IMPACTS OF LAND COVER AND CLIMATE CHANGE ON WATER RESOURCES IN SUASCO RIVER WATERSHED

A Thesis Presented

by

AMMARA TALIB

Submitted to the Graduate School of the
University of Massachusetts Amherst in partial fulfillment
of the requirements for the degree of

MASTER OF SCIENCE

September 2015

Department of Environmental Conservation
Water, Wetlands and Watersheds

IMPACTS OF LAND COVER AND CLIMATE CHANGE ON WATER RESOURCES IN SUASCO RIVER WATERSHED

A Thesis Presented

by

AMMARA TALIB

Approved as to style and content by:

_____
Timothy Randhir, Chair

_____
Allison Roy, Member

_____
Paula Rees, Member

_____
Curt Griffin, Department Head,

Environmental Conservation

ACKNOWLEDGEMENT

I would never have been able to finish my dissertation without the guidance of my committee members, support from my family and help from friends. I would like to express my deepest gratitude to my advisor, Dr. Timothy Randhir, for his excellent guidance, patience, and providing me with an excellent support all the way from when I was first considering applying to the MS program in the Department of Environmental Conservation, through to completion of this degree. I would like to thank him, who let me experience the research of water resources, simulation models and practical issues beyond the textbooks, patiently corrected my writing and. I am grateful to Fulbright and International Institute of Higher education for financially supported my research. Dr. Tim' intellectual heft is matched only by his genuinely good nature and down-to earth humility, and I am truly fortunate to have had the opportunity to work with him.

I would also like to thank Dr.Yumna Saddaf, Muhammad Afzal, Muhammad Jamal Qureshi, Dr. Neveed, Dr. Nawaz and Dr. John Finn for guiding my research for the past several years and helping me to develop my background in Hydrology, physiology, biochemistry, and ecology. Special thanks go to Dr. Allison Roy, and Dr. Pula Rees who was willing to participate in my final defense committee. I would like to recognize my lab mates Luisa, Wulan, Ronak, Patrick, Havier and Hla Na and Nathali Costa who as good friends were always willing to help and give their best suggestions during my years of study at the University of Massachusetts Amherst. It would have been a lonely lab without them. Many thanks to the developers of HSPF model and I would like to

recognize Anurag Mishra, Brian Bicknell, Paul Hummel, Paul Duda, Tony Donigian and Robert burgholzer to help me with coding and other problems related to my model. My research would not have been possible without their helps.

I would also like to thank my parents, one elder brother Abdul Sami, and a family friend Naeem Khalid. They were always supporting me and encouraging me with their best wishes. Finally, I would like to thank my best friend, Saira Jamil. She was always there cheering me up and stood by me through the good times and bad.

A special thank you to all those support and friendship helped me to stay focused on this research and who have provided me with the encouragement to continue when the going got tough.

ABSTRACT

IMPACTS OF LAND COVER AND CLIMATE CHANGE ON WATER RESOURCES IN SUASCO RIVER WATERSHED

SEPTEMBER 2015

AMMARA TALIB, BS., PUNJAB UNIVERSITY LAHORE

MS., UNIVERSITY OF MASSACHUSETTS AMHERST

Directed by: Professor Tim Randhir

Hydrological balance and biogeochemical processes in watershed are significantly influenced by changes in land use land cover (LULC) and climate change. Those changes can influence interception, evapotranspiration (ET), infiltration, soil moisture, water balance and biogeochemical cycling of carbon, nitrogen and other elements at regional to global scales. The impacts of these hydrological disturbances are generally reflected in form of increasing runoff rate and volume, more intense and frequent floods, decreasing groundwater recharge and base flow, elevated levels of sediments and increase in concentration of nutrients in both streams and shallow groundwater. Water quality of Sudbury, Assabet and Concord (SuAsCo) watershed in Massachusetts is also compromised because of influx of runoff, sediments and nutrients. There is a crucial need to evaluate the synergistic effects of LULC change and climate change on the water quality and water quantity in a watershed system. A watershed simulation model is used to simulate hydrologic processes and water quality changes in sediment loads, total nitrogen (TN), and total phosphorus (TP). The model is calibrated and validated with field-measured data. Climatic scenarios are represented by downscaled regional projections from Global Climate Model (GCM) models and regional built out scenarios of LULC are used to assess the impacts of projected LULC and climate change on water

quality and water quantity. Simultaneous changes in LULC and climate significantly affect the water resources in the SuAsCo River watershed. Change in climate increased ET (4.7 %) because of high temperature, but independent change in land cover reduced ET (6.5%) because of less available vegetation. Combined change in land cover and climate reduced ET (2.1%) overall, which indicates that land cover change has significant impact on ET. Change in climate increased total run off (6%) and this increase is more significant as compared to 2.7 % increase in total runoff caused by land cover change. Change in land cover increased surface runoff more significantly (69.2%) than 7.9 % increase caused by climate change. Combined change in land cover and climate further increased the average storm peak volume (12.8 percent) because of high precipitation and impervious area in future. There is a potential for reducing runoff, sediments and nutrients loads by using conservation policies and adaptation strategies. This research provides valuable information about the dynamics of watershed system, as well as the complex processes that impair water resources.

TABLE OF CONTENTS

LIST OF TABLES

Table **Page**

LIST OF FIGURES

Figure **Page**

CHAPTER 1

INTRODUCTION

1.1 Background

This section describes about the issues regarding water quality and water quantity in watershed systems. Information about stressors such as LULC and climate change that impact hydrological processes significantly has been provided. This chapter includes general objectives, specific objectives, null and alternative hypothesis.

Inadequate water quantity and poor water quality is becoming an increasing concern in the United States and other parts of the world [Kosmas et al., 1997 and Kim et al., 2013; Santhi et al., 2006]. The water quantity issues are in form of increase in evapotranspiration (ET), decrease in infiltration and soil moisture, increasing runoff rate and volume, changes in timing of spring and winter runoff event, decreasing groundwater recharge and base flow , more intense and frequent floods in some areas and droughts in the others [Pielke and Avissar, 1990; Moscrip and Montgomery, 1997]. Poor water quality is another concern. In United States, 35%, 45%, and 44% of the assessed rivers and streams, lakes, and estuaries, respectively, are impaired by one or more pollutants according to recent report to Congress regarding water quality [US Environmental Protection Agency, 1999]. In addition, the impairment of 30% or 135,000 km^2 of the nation' s impaired rivers and streams,44% of the impaired lakes, and 23% of the impaired estuaries is caused by two prime nutrients: Nitrogen and phosphorus [Sauer et al.,2008]. These changes in hydrological balance and biogeochemical processes in watershed also

influence earth-atmosphere interactions, biodiversity, water budget, biogeochemical cycling of carbon, nitrogen and other elements at regional to global scales [Tang et al., 2005].

LULC change is one of the stressors that significantly affect hydrological balance and then aggravate water quantity issues [Fu et al., 2009]. Hydrological processes such as infiltration, groundwater recharge, base flow and surface runoff are influenced by land use changes in a watershed [Lin et al., 2007]. LULC modification such as changes in vegetation cover, alter surface roughness and Leaf Area Index (LAI) that can lead to disturbance in surface energy balance and evapotranspiration (ET) [Pielke and Avissar, 1990]. The changes in energy balance and ET may significantly affect the timing and magnitude of evaporative losses to the atmosphere and the amount of water yield that governs soil moisture content, runoff and base flow patterns of regional hydrologic responses [Hendersen-Sellers et al., 1993; Jones and Post, 2004]. Hence these disturbance in hydrological balance lead to increase in runoff rate, volume and more intense and frequent floods [Kosmas et al., 1997;Brath et al., 2006].

In addition to water balance, LULC also impacts water quality, especially sediment loading that is mainly caused by uncontrolled urban runoff and soil erosion [Randhir and Tsvetkova, 2011]. Many studies assess the impacts of LULC change on watershed [Wolter et al., 2006; Randhir and Hawes, 2009; Xia et al., 2012]. These studies show a strong tie between land cover patterns and soil erosion and sediment yield in watersheds. Soil erosion via deforestation, bank edges not protected by fencing, livestock poaching at feeding lots, tillage , and ploughing for afforestation cause loading of sediments in water bodies [Evans et al., 2006; Ozturk et al., 2013; Yang et al., 2013]. Soil

erosion is also caused by inappropriate land use and poor management that can lead to land degradation and deterioration of surface water quality [Singh et al., 2011]. Hence, soil erosion induced by LULC change not only reduces soil productivity but also increases sediment and other pollutants loads to receiving water bodies [Deng et al., 2008]. High suspended sediment loads and the resulting turbidity can impact the use of surface waters for water supply and other designated uses. Mukundan et al., [2013] reports that changes in fluvial sediment loads influence material fluxes, aquatic geochemistry, water quality, channel morphology, and aquatic habitats. Considering the fact that hydrological processes and sediment transport capacity varies for different types of land cover, sediment export to rivers is a function of type of land use [Shi et al., 2013; Yan et al., 2013; Wasige et al., 2013]. Therefore, quantifying spatial and temporal patterns in sediment loads is important both for understanding and predicting soil erosion and sediment transport processes as well as watershed-scale management of sediment and associated pollutants. Having said that, it is necessary to address the issue of sediment loadings in water because the quality of aquatic life and performance and life of reservoirs, canals, drainage channels, harbors, and other downstream structures is determined by sedimentation rates and amounts [Lane et al., 1997].

LULC change also causes excessive nutrient loading or eutrophication [Artola et al., 1995] that leads to lack of potability in drinking water and death of aquatic organisms especially fish. The eutrophication of downstream water bodies are caused by excess nutrient export from natural and anthropogenic sources, which is transported through the fluvial network [Dodds et al., 2011]. The prominent anthropogenic sources of nutrients loads are production and applications of fertilizer, discharge of human waste, livestock

operation and clearing land [Cloern, 2001]. The structure and function of the aquatic ecosystem are affected by high nutrient concentrations which is a threat to the ecosystem integrity [Aguilera et al., 2012]. The increased growth of algae and aquatic weeds is the most obvious consequence of eutrophication that interfere with the use of water for fishing, recreation, industry, agriculture and drinking [Carpenter et al., 1998]. Hence the impairment of aquatic resources by eutrophication can have substantial economic impacts [Carpenter et al., 1998].

Climate change is another stressor [International Panel on Climate Change (IPCC) 2001, 2007].Water cycle is disturbed by climatic change because of feedbacks between rising temperatures and hydrologic processes and the consequences of these disturbances in form of changes in patterns of precipitation and runoff and more frequent occurrence of extreme weather events [Milly et al., 2005; Milliman et al., 2008; Boyer et al., 2010]. According to IPCC Assessment Report 5 (AR5), it is likely that the frequency of heat waves has increased in large parts of Europe, Asia and Australia. There are likely more land regions where the number of heavy precipitation events has increased than where it has decreased. In addition, the frequency or intensity of heavy precipitation events has likely increased in North America and Europe. Change in climate disrupts the climate–runoff relationship, water budget and, vegetation responses to higher temperature (ET) that leads to changes in the timing and intensity of rainfall [Vaze et al., 2010]. Over several decades, climate change impacts on the hydrological cycle, e.g. leading to changes of precipitation patterns, have been observed. Higher water temperatures and changes in extremes hydro-meteorological events (including floods and droughts) are likely to aggravate different types of pressures on water resources with possible negative

impacts on ecosystems and human health [Mozumder et al., 2011. In addition, climate-related changes in water quantity are expected to affect food availability, water access and utilization, especially in arid and semi-arid areas, as well as the operation of water infrastructure (e.g. hydropower, flood defenses, and irrigation systems) [Forsee and Ahmad, 2011; Quevauviller, 2011].

In addition to characteristics of the water that are influenced directly by climate change, land surface processes that regulate the production, release, and transport of natural materials and anthropogenic contaminants to ground and surface waters are also affected by climate change [Williams et al., 2008; Campbell et al., 2009]. Water and air temperature, precipitation amount and intensity, and droughts are the hydroclimatic factors that affect water quality by influencing the transfer of contaminants [Kundzewicz et al., 2007; Park et al., 2010]. Water temperature can directly influence temperature-dependent water quality parameters including dissolved oxygen, redox potentials, pH, and lake stratification, mixing, and microbial activity [Park et al., 2010; Luo et al., 2013; Shrestha et al., 2012]. Analyses on the combined impact of climate and land use changes showed that the impact of land development on stream flow will be enhanced by climate change [Kosmas et al., 1997; Li et al., 2009]. The combined effects of modifications in river hydrology and geomorphological processes will likely impact riparian ecosystems [Wilson and Weng., 2011; Kim et al., 2013]. Changes in the LULC and climate regime can influence natural processes of a watershed ecosystem [Abbaspour et al., 2007; Shen et al., 2011; Singh et al., 2011] and have long-term implications on economic and ecological processes [Singh et al., 1999; Albek et al., 2004 ;Santhi et al., 2006].

Many studies show that mitigation measures that are effective for soil erosion can be assumed to control diffuse pollution losses, because of the strong relationships between runoff, sediment and the transport of P, N, pesticides, pathogens, and metals [Ahiablame et al, 2013; Dechmi and Skhiri et al., 2013]. Low impact development (LID) practices have been utilized to mitigate hydrologic and water quality impacts of urbanization. To reduce non-point source pollution and improve water quality, land management practices such as conservation tillage and optimum irrigation are also routinely used [Barrington et al., 2013; Delgado et al., 2013]. BMPs and better fertilizer application management is needed to control NPs of TN, TP. As compared to employ individual crop and tillage management practices and structural controls, combinations of crop, tillage and structural control scenarios revealed to have more potential to reduce sediment yield [Chen et al., 2012; Hong et al., 2012].The interaction of land use and climate change varies greatly in time and in space, as fluxes of water within a catchment move both vertically (e.g. evapotranspiration) and laterally (through soils, hill slopes, aquifers and rivers). Thus, as water moves through the catchment any impacts of the climate change and land use can be transmitted through the catchment [Falkenmark, 2003]. So the assessment of LULC and climate change usually includes evaluation of spatial patterns of hydrological consequences to different LULC maps, temperature, precipitation, comparison of simulated hydrological components to LULC and climate changes at the basin scale, and examination of temporal responses in channel discharge with changes in LULC and climate [Stohlgren et al., 1998; Nie et al., 2011].

Modeling has become one of the most powerful tools for watershed management in the last decades [Albek et al., 2004]. To predict/or forecast storm water quantity, storm

water runoff models have been widely used but due to the complexities of the processes affecting storm water quality current modeling efforts have had limited success in accurately predicting storm water quality (Obropta and Kardos, 2007). Most hydrological studies have focused on results from simplified models [Horton et al., 2006; Zhang et al., 2012]. But as land use and meteorological forcing such as heat waves, droughts, heavy precipitation and floods may dramatically evolve, one can however question the adequacy of such models in a changing climate [Hock et al., 2005; Magnusson et al., 2010]. While an adequate amount of research has been conducted on the potential impacts of LULC change on hydrology [White and Greer, 2006; Tran et al., 2010; Carey et al., 2011; Girolamo and Porto et al., 2012], and future climate on water resources, most of these studies did not integrate future land use configurations in their analysis .There are very few studies that have analyzed the combined effects of climate and land use changes on water quality and water quality [Wilson and Weng, 2011; Tong et al., 2012; Kim et al., 2013]. As a result, the synergistic impacts of future detailed urban land use configurations and trends, under various climate emission scenarios, on surface water quality at the sub-basin level are currently fuzzy [Wilson and Weng, 2011; Cuo et al., 2013; Tran and Neill., 2013]. Hence to assess the impacts of LULC and climate change on catchment hydrological response, there is a need of an appropriate approach, that is sensitive to LULC and climate changes and which adequately represent hydrological processes [Ewen, J. and G. Parkin, 1996; Choi and Deal, 2008]. Having said that there is a need of an integrated approach involving hydrological modeling is required to quantify the contributions of changes in individual land use types to changes in stream flow and sediment yield. Those integrated hydrological simulation models provide information

about watershed that helps in making decisions regarding the development and management of water and land resources in a watershed.

In this study, we use integration of GIS and simulation modeling to investigate the hydrological response of a semi urban watershed to a changing climate and land cover. The physically based models are particularly useful in estimating the major components of the water balance at a daily time step (evapotranspiration, surface runoff, baseflow and interflow) from rainfall, pan evaporation and gauged total stream flow. These model requires input information on LULC, soil properties, sources of nitrogen (N) and phosphorus (P), stream reach characteristics, and time series of precipitation, temperature, solar radiation and potential evapotranspiration. The models predict flow rate, sediment loads, TN and TP loads. Then calibrated model can be used to project the future changes in streamflow, TN and TP load under different climate and land use change scenarios the watershed. Water quality of the SuAsCo watershed is compromised because of influx of sediments and nutrients [Smith, 2000; Riskin et al., 2003; Giles, 2005]. There is a crucial need to analyze source, transfer, and fate of sediments and nutrients at watershed scale.

Therefore, this study will examine the potential combined effects of climate and LULC changes on watershed system. One study by Zarriello et al [2010] in SuAsCo watershed has examined the impacts of land use land cover change, but there is no study about combined impacts of landuse and climate change on water resources in SuAsCo. This study quantifies contributions of change for individual LULC and climate change to different hydrological responses. Understanding how land-use and climate change will affect water resource quantity and quality, in the context of watershed geomorphology,

will aid watershed managers and stream ecologists in the protection of adequate water supply for human needs and habitat availability for stream biota.

A comprehensive deterministic, distributed and physically based modeling system capable of simulating all major hydrological processes in the land phase of the hydrological cycle [Zarriello and Ries, 2000; Albek et al., 2004] is used in this study. Unlike other empirical and conceptual hydrological model, HSPF is a physically based model that is able to explicitly represent the spatial variability of some, if not most, of the important land surface characteristics such as topographic elevation, slope, aspect, vegetation, soil as well as climatic parameters including precipitation, temperature, and evapotranspiration distribution. The HSPF model is chosen for this study from the range of existing water quality models for two main reasons: (1) its comprehensive catchment description, which accounts for the numerous different factors influencing flow and water quality [Ribarova et al.,2008] and (2) its capability to run at time steps of less than a day (Bicknell et al., 2001). A rigorously calibrated and validated physically-based macroscale hydrological model over the SuAsCo, aims to identify changes in observed streamflow at several locations and to explore the causes of streamflow changes by examining climate change impacts on water balance terms, and land cover/use change impacts on streamflow.

1.2 Research Objectives

Both general and specific objectives are given below.

1.2.1 General Objective

The general objective of my research is to evaluate the synergistic effects of LULC change and climate change on the water quality and water quantity in a watershed system.

1.2.2 Specific Objectives

Specific objectives of my research are to:

i. Simulate baseline biophysical processes (such as runoff, sediment, TN, TP loads) in the watershed system using continuous-time, process model;
ii. Evaluate impacts of land use land cover (LULC) change on runoff, sediments, TN and TP loads;
iii. Assess the impacts of climate change on runoff, sediments, TN, and TP loads;
iv. Quantify the combined effects of both (LULC) and climate change on runoff, sediments, TN and TP loads;

1.2.3 Hypothesis

1st objective:

Ho: O_{bs}-S_{im} =0

Baseline simulations are significantly close to observed information

Ha: O_{bs}-S_{im} ≠0

Baseline simulations significantly deviate from observed information

2nd objective

Ho: $\Delta W_Q/\Delta LULC = 0$

LULC changes have no impacts on water quality and water quantity

Ha: $\Delta W_Q/\Delta LULC \neq 0$

LULC changes have significant impacts on water quality and water quantity

3rd objective

Ho: $\Delta W_Q/\Delta CC = 0$

Climate change has no impacts on water quality and water quantity.

Ha: $\Delta W_Q/\Delta CC \neq 0$

Climate change has significant impacts on water quality and water quantity.

4th objective

Ho: $\Delta W_Q/\Delta\ \Delta LULU = 0$

Combined impacts of LULC change and climate change on water quality and water quantity are insignificant.

Ha: $\Delta W_Q/\Delta\ \Delta LULU \neq 0$

Combined impacts of LULC change and climate change on water quality and water quantity are significant.

1.3 Thesis Plan

Thesis is divided into four chapters. The first chapter presents the introduction, and background information about water quality and water quantity issues. The second chapter describes about literature review, general objectives, and specific objectives, null

and alternative hypothesis. Third chapter is about description of study area, database and HSPF calibration. Forth chapter is about results and discussion about assessment of the impacts of climate change and LULC on water quality and water quantity. Fifth chapter is about conclusion and identification of the mitigation strategies to minimize the impacts of LULC and climate change on watershed system. Appendices, tables and figures are presented at the end of thesis.

CHAPTER 2

LITERATURE REVIEW

This section provides a review of background literature related to LULC and climatic impacts on watershed systems. The review is presented in five categories: watershed modeling, LULC change, climate change, combined LULC and climate change, and policy adaptation.

2.1 Watershed Modeling

Hydrological modeling is important for watershed management as hydrology is the driving force behind many processes occurring on the watershed. In order to explain the mechanisms governing processes in a water body (streams, lakes or groundwater), hydrology and hydrological relationships must be investigated and simulated. Many different large-scale watershed flow models exist which describe processes related to the movement of runoff, sediments and nutrients through large drainage networks of river basins. Equations of such models can be applied on different scales.

[Singh et al., 1999] applied, MIKE SHE, the physically based distributed modeling system, to simulate the hydrological water balance of a small watershed. Soil Water Assessment Tool (SWAT) was used by Santhi et al., [2006]; Abbaspour et al., [2007] and Chen et al., [2012] to simulate all related processes affecting water quantity, sediment, and nutrient loads and to evaluate the long-term impact of implementation of Water Quality Management Plans (WQMPs) on nonpoint source pollution at the farm

level and watershed level using a modeling approach. Agricultural Pollution Potential Index (APPI) and Pollution Load (PLOAD) model was used for non-point priority source area and pollution load estimation in Fujiang watershed, China [Shen et al., 2011]. Water erosion prediction project (WEPP) model was used to develop appropriate vegetative as well as structural measures to control sediment yield from a small multi-vegetated watershed in high rainfall and high land slope conditions of eastern Himalayan range in India [Singh et al., 2011]. Albek et al., [2004] used a mathematical modeling program called Hydrological Simulation Program—FORTRAN (HSPF) for the hydrological modeling of the Middle Seydi Suyu Watershed in Turkey.

[Singh et al., 1999] applied, MIKE SHE, the physically based distributed modeling system, to simulate the hydrological water balance of a small watershed in the western part of the Midnapore district of West Bengal, India, with the objective of developing the irrigation plan for paddy crops. Results showed that it is possible to meet the irrigation demand of the crops with the proper planning. That study indicated the applicability of a comprehensive hydrological modeling system for the management of water resources for agricultural purposes in a watershed.

Albek et al., [2004] used a mathematical modeling program called Hydrological Simulation Program—FORTRAN (HSPF) for the hydrological modeling of the Middle Seydi Suyu Watershed in Turkey. They conducted base simulations for the 1991–1994 water years to determine and compare the response of the watershed to various scenarios. The findings showed that the watershed outflows will decrease by 21% due to an annual mean temperature increase of 3 °C caused by climate change.

Santhi et al., [2006] used Soil Water Assessment Tool (SWAT) to evaluate the long-term impact of implementation of Water Quality Management Plans (WQMPs) on nonpoint source pollution at the farm level and watershed level using a modeling approach. The results showed that the benefits of the WQMPs were greater (up to 99%) at the farm level and the benefits due to WQMPs were 1–2% at the watershed level. This study also showed that a modeling approach can be used to estimate the impacts of water quality management programs in large watersheds.

Abbaspour et al., [2007] used the program SWAT to simulate all related processes affecting water quantity, sediment, and nutrient loads in the Thur River basin (area 1700 km^2) which is located in the north-east of Switzerland and is a direct tributary to the Rhine. They concluded that it is feasible to use SWAT as a flow and transport simulator for a watershed with good data quality and availability and relatively small model uncertainty. They observed that simulation of particulates such as sediment and phosphorus are subject to large model uncertainties because of the "second-storm" effect, among others. They found large-scale watershed models effective for simulating watershed processes and therefore watershed management studies.

Shen et al., [2011] used Agricultural Pollution Potential Index (APPI) and Pollution Load (PLOAD) model for non-point priority source area and pollution load estimation in Fujiang watershed, China. The study indicated that in order to achieve the regional goal of water quality, the agricultural activity and effective treatment of the human and livestock discharge should both be carried out to control the non-point source pollution. They found out that, based on the NPS pollution evaluation in subbasins, the land use was the major contributor for total nitrogen (TN), whereas human and livestock

discharge was the main cause for total phosphorus (TP). They also propose that in order to control the non-point source pollution (NPS) pollution, best management practices (BMPs) regarding the agricultural activity and effective treatment of the human and livestock discharge should both be carried out.

Singh et al., [2011] used water erosion prediction project (WEPP) model to develop appropriate vegetative as well as structural measures to control sediment yield from a small multi-vegetated watershed in high rainfall and high land slope conditions of eastern Himalayan range in India. Simulations of combinations of management practices indicted that sediment yield can be reduced up to 78.40%, by replacing traditional upland paddy crop with maize, soybean, and peanut, because that soybean and peanut in upland situations with field cultivator or drill-no-tillage system, and structural control in the drainage line has potential to make agriculture sustainable in the watershed.

Chen et al., [2012] identified the spatial and temporal distribution of nitrogen (N) in the upstream watershed of a typical drinking water reservoir, in the city of Ningbo, Zhejiang province. They estimated the N load for the 254 km2 upper stream watershed by using a watershed model, Soil and Water Assessment Tool (SWAT). The findings of this study revealed that, in order to protect soil and water resources, modeling and monitoring of NPS at multiple scale, provides information to assess trends and the status of NPS both long-term and short-term trends.

Hong et al., [2012] used a combined socio-economic–ecological toolbox (ArcECON, ArcGEOMOD, and ArcGWLF), running on the ArcGIS platform, is used for two New York State catchment areas, Onondaga Creek watershed and Wappinger Creek,

to analyze subsequent impacts on stream flow and nutrient export using the spatial pattern of urbanization in response to anticipated socio-economic conditions and scenarios through a year 2020. They predicted higher flashier stream flow as well as worsening stream condition caused by estimated higher economic growth to induce increased new housing permits and spread of impervious surface areas, which was aggravated when only the forest lands were allowed to be developed.

Most approaches to assess the LULC and climate change impacts showed that integrated approaches that model the combined effect of LULC and climate changes can be used for scenario analysis, because most of the integrated models simulate hydrology, sediment, and nutrient loads with reasonable accuracy. TN and TP increase under all future climate and land use scenarios. BMPs and better fertilizer application management is needed to control NPs of TN, TP. As compared to employ individual crop and tillage management practices and structural controls, combinations of crop, tillage and structural control scenarios revealed to have more potential to reduce sediment yield.

2.2 Land Use Land Cover (LULC) Change

Wolter et al., [2006] studies the Land Use/Land Cover (LULC) change to understand the near shore ecology of U.S Great Lakes Basin, for the U.S. portion of the Great Lakes basin for 1992 and 2001.) They observed the 33.5% increase in low-intensity development and 7.5% increase in road area and on the other hand 2.3% decrease in agricultural and forest land. They results revealed the loss of 38% of wetlands caused by new developments near coastal areas of the Great Lakes.

Randhir and Hawes [2009] used dynamic model that links land use, overland flow, suspended sediment, and an aquatic species to evaluate alternate land use policies in Hatfield Mill River watershed. They used dwarf wedge mussel that is classified as endangered in the region as an indicator species of aquatic health in a watershed in Massachusetts. The simulation model was used to evaluate spatial nature of processes and land use policies. Spatial and temporal changes in runoff, sediment loading, and mussel population were modeled over a period of 4 years. Scenarios with an increase in sediment loading above the baseline mean exhibited an irregular recovery of the mussel population from high loading events. The results showed the need for best management practices to decrease runoff and sediment loading in the watershed, through education and incentive programs.

Xia et al., [2012] used the landscape pattern index method using GIS tools, to compare the landscape patterns of Baiyangdian Watershed in 2002 and 2007, and to determine the transformation rules of landscape essential factors, and analyze the correlation between the changes of landscape patterns and water quality in Baiyangdian Watershed. Their findings revealed that urbanization could lead to decrease in the degree of fragmentation of man-made landscape and increase in the natural landscape of watershed. This study showed that river pollution is mostly contributed by construction land and farmland; however water quality can be improved by higher percentage of forest cover.

Shi et al., [2013] used hydrological modeling and partial least-squares regression (PLSR) to investigate the landscape patterns within watersheds in the Upper Du River watershed (8973 km^2) in China. They examined how the spatial patterns of land cover are

related to the soil erosion and sediment yield of watersheds. Their study showed that in order to provide quantitative information to allow decision makers to make better choices regarding landscape planning, partial least-squares regression PLSR can be used to simply determine the relationships between land-cover patterns and watershed soil erosion and sediment yield.

Yan et al., [2013] used an integrated approach involving hydrological modeling and partial least squares regression (PLSR) was used by to quantify the contributions of changes in individual land use types to changes in stream flow and sediment yield. They used land use maps from four time periods for the Upper Du watershed in China to study the changes in stream flow and sediment yield. The changes to farmland, forest and urban areas were the major land use changes that affected streamflow in that watershed.

Wasige et al., [2013] used a combination of ancillary data and satellite imagery to study the impacts of large-scale human induced land use and land cover changes (LUCC), on sustainable agriculture and water quality of Kagera Basin in the Lake Victoria watershed. The results showed that the rates of LUCC observed were higher than those reported in Sub Saharan Africa (SSA) and other parts of the world. This study combined the multi-source spatio-temporal data on land cover to enable long-term quantification of land cover changes.

Yang et al., [2013] investigated the relation of variation of dissolved organic carbon (DOC), total phosphorus (TP) and dissolved nitrogen (DN) in surface runoff water with varying land uses in the Saint Lucie Estuary and Indian River Lagoon, Florida. They observed that rainfall events were largely responsible for temporal fluctuation of DOC and DN, and loads of DOC, TP, TN, and metals in runoff water from

agricultural fields. Results showed that Ranch had the greatest DOC and DN concentrations in runoff water out of eight investigated land uses, followed by vegetable farm and forest, and golf course usually had the lowest DOC in runoff water.

Ozturk et al., [2013] studied the land use dynamics in a rural watershed, Bartin spring, located in the northwestern Turkey. They land use dynamics model coupled with a spatially distributed three-dimensional surface–subsurface hydrologic model. Based on alternative land use and forest management scenarios, the coupled model was used to simulate the water budget. Their investigation showed that the water budget is most sensitive to variations in precipitation and conversion between forest and agricultural lands. They found coupled model to be a useful tool for assessing the impact of land use change on the watershed hydrological processes.

All of these studies showed that there are strong ties between land cover patterns and soil erosion and sediment yield in watersheds. Absence of protective land cover largely determines soil erosion, whereas on-site sediment production and the connections between sediment sources and rivers determine sediment export to rivers. Considering the fact that hydrological processes and sediment transport capacity varies for different types of land cover, sediment export to rivers is a function of land use.

2.3 Climate Change

Merritt et al., [2006] studied the hydrologic response to scenarios of climate change in sub watersheds of the Okanagan basin, British Columbia. They used three global climate models (GCMs) to generate high and low emission scenarios. The models predicted an increase in winter temperature of 1.5–4.0 °C and a precipitation increase of

the order of 5-20% by the 2050s. Summer temperatures were simulated to increase by approximately 2–4 °C. The scenarios raise questions over the availability of future water resources in the Okanagan Basin, particularly as extended periods of low flows into upland reservoirs are likely to coincide with increased demand from agricultural and domestic water users.

Marshall and Randhir., [2008] used a continuous simulation model to evaluate potential implications of increasing temperature on water quantity and quality at a regional scale in the Connecticut River Watershed of New England. They observed that climate change can have significant effects on streamflow, sediment loading, and nutrient (nitrogen and phosphorus) loading in a watershed. Climate change also influences the timing and magnitude of runoff and sediment yield. Changes in variability of flows and pollutant loading that are induced by climate change have important implications on water supplies, water quality, and aquatic ecosystems of a watershed. Potential impacts of these changes include deficit supplies during peak seasons of water demand, increased eutrophication potential, and impacts on fish migration.

Park et al., [2010] studied the potential effects of climate change on the watershed biogeochemical processes and surface water quality in mountainous watersheds of Northeast (NE) Asia. The results from a four-year intensive study at a forested watershed in Chongquing province showed that during the years with lower precipitation, when year to year variations in precipitation was a key factor in modulating the effects of acid deposition, the concentrations of sulfate and nitrate in soil and surface waters were generally lower.

Boyer et al., [2010] studied the important modifications into the hydrological regimes of the St. Lawrence tributaries (Quebec, Canada), induced by projected changes in temperature and precipitation for the next century. They used three General Circulation Models and two greenhouse gas emissions scenarios to create a range of plausible scenarios. Most of the hydrological simulations projected an increase in winter discharges and a decrease in spring discharges. They suggested that higher winter discharges are expected to have an important geomorphological impact mostly because they may occur under ice-cover conditions. On the other hand, lower spring discharges may promote sedimentation into the tributary and at their confluence with the St. Lawrence River.

Mozumder et al., [2011] conducted a survey to draw out responses from experts and decision makers serving the Florida Keys regarding vulnerability to global climate change. They concluded that proactive adaptation measures can assist vulnerable community's better cope with adverse environmental and socioeconomic impacts. They propose that a large majority of respondents consider additional funding and assistance for climate science and adaptation, better intergovernmental organization and public workshops will be highly effective to support adaptation.

Shrestha et al., [2012] investigated the climate-induced hydrologic changes in the Lake Winnipeg watershed (LWW), Canada. The hydrologic model, Soil and Water Assessment Tool (SWAT), was employed to simulate a 21-year baseline (1980–2000) and future (2042–2062) climate. They found the future increases in annual precipitation and temperature in various seasons and regions of this catchment and such changes are expected to influence the volume of snow accumulation and melt, as well as the timing

and intensity of runoff. The effects of future changes in climatic variables, specifically precipitation and temperature, are clearly evident in the resulting snowmelt and runoff regimes. The most significant changes include higher total runoff, and earlier snowmelt and discharge peaks. Some of the results also revealed increases in peak discharge intensities. They proposed that such changes will have significant implications for water availability and nutrient transport regimes in the LWW.

Luo et al., [2013] investigated the climate change impacts on water supply and ecosystem stressors .They applied the Soil and Water Assessment (SWAT) model to quantify the impacts of projected 21st century climate change in the northern Coastal Ranges and western Sierra Nevada. Proportional to the projected increases in air temperature, increases in annual average stream temperature was predicted by model. Compared to the present-day conditions, 30–60 more days per year were predicted with average stream temperature > 20 °C during 2090s.

Climate change and increased variability, including extreme events, have been suggested to have significant impacts on water quality around the world through various studies. Climate-induced increase in surface temperatures can impact hydrologic processes of a watershed system.

Climate change can impact human health and aquatic ecosystems through water quality deterioration caused by higher water temperatures, increased precipitation intensity, and longer periods of low flow. Climate change can affect water quality, not only by directly changing the characteristics of the water, but also by influencing land surface processes that regulate the production, release, and transport of natural materials and anthropogenic contaminants to ground and surface waters.

2.4 Combined Land Use Land Cover (LULC) and Climate Change

Kosmas et al., [1997] studied the effect of land use and precipitation on annual runoff and sediment loss in eight different sites along the northern Mediterranean region and the Atlantic coastline located in Portugal, Spain, France, Italy and Greece. The investigation showed that that runoff and soil erosion could greatly be affected by land use. They also found out that erosion in shrub lands increased with decreasing annual rainfall and then it decreased with decreasing rainfall.

Li et al., [2009] studied the impacts of land use change and climate variability on hydrology in an agricultural catchment on the Loess Plateau of China. They assessed the impacts of land use change and climate variability on surface hydrology (runoff, soil water and evapotranspiration) Using the SWAT (Soil and Water Assessment Tools) model. SWAT proved to be a useful tool for assessing the effects of environmental changes including land use change and climate variability in the Loess Plateau. They observed that overall; climate variability influenced surface hydrology more significantly than land use change.

Wilson and Weng., [2011] investigated that the future land use and climate changes have the potential of dramatically changing the concentration levels of total suspended sediments and phosphorus at both the general watershed and sub-basin scales in the Des Plaines River watershed. They also found out that future climate change exerts a larger impact on the concentration of pollutants than the potential impact of land use change. They suggested that modeling the effects of past and current land use composition and climatic patterns on surface water quality provides valuable information for environmental and land planning.

Kim et al., [2013] investigated the separate and combined impacts of future changes in climate and land use/land cover (LULC) on stream flow in the Hoeya River Basin, South Korea. They simulated the stream flow in future periods under three scenarios (climate change only, LULC change only, and climate and LULC change combined) by the Soil and Water Assessment Tool (SWAT) model. They observed that stream flow increased in spring and winter but decreased in summer and autumn under climate change, on the other hand high flow during wet period increased but low flow decreased in dry periods under LULC change. The results showed that although the LULC change had less effect than climate change on the changes in stream flow, but stream flow is significantly affected by LULC. Larger seasonal changes in stream flow were observed under combined scenario; however the result for the combined scenario was similar to that of the climate change only scenario. They inferred that the problems of increased seasonal variability in stream flow caused by climate change may heightened by LULC changes.

Tran and Neill., [2013] employed a nonlinear model applied to a spatial dataset of more than 180,000 catchments to study the effects of land use/land cover (LULC) along with other climate and geomorphologic factors on mean annual stream flow in the Upper Mississippi River Basin (UMRB). The results showed that the magnitude of the impact on stream flow varies from one LULC to another. It is not a simple function of a LULC's spatial extent but arguably a result of complex interactions among various LULCs as well as other climate and geomorphologic factors.

Cuo et al., [2013] examined the observed stream flow over the past decades in the upper Yellow River Basin (UYRB) to better understand the climate change impact and

long-term and recent land cover/use change impact. They employed the modified variable infiltration capacity (VIC) model. VIC simulations suggest that these changes in observed stream flow were due to the combined effects of changes in precipitation, evapotranspiration, rainfall runoff, and base flow. They observed that the areas where human activity was relative intense, the impacts of land cover change/use including agriculture, industry, urbanization, and reservoir operations became important.

Analyses on the combined impact of climate and land use changes showed that the impact of land development on stream flow will be enhanced by climate change. The combined effects of modifications in river hydrology and geomorphological processes will likely impact riparian ecosystems. Changes in the LULC and climate regime can influence natural processes of a watershed ecosystem and have long-term implications on economic and ecological processes. Hence to protect the water resources and environmental quality, assessment of hydrologic responses these changes is also required.

2.5 Policy Adaptations

Ghimire and Johnston [2013] studied the impacts of domestic and agricultural rainwater harvesting systems on watershed hydrology for Albemarle-Pamlico river basin (USA). Results indicated that a 100% rain water harvesting (RWH) caused a reduction in average monthly water yields by up to 16%, 9%, and 19% for Back Creek, Sycamore, and Green Mills watersheds, respectively.

Delgado et al., [2013] studied about the conservation practices for water resources. They propose that for adaptation to LULC change and climate change impacts on watershed resources, conservation practices will be key and must be used, such as the

use of conservation tillage, management of crop rotations and crop residue (including use of cover crops where viable), management of livestock grazing intensities, improved management of irrigation systems, use of technologies, and precision conservation. They propose that projected spatial changes in the hydrological cycle, such as wetter and drier regions, and periods of drought should be considered as an important adaptation practice. Soil and water conservation policies should also consider conservation practices that contribute to increased water-holding capacity in the soil profile, improved drainage practices, and the development of new crop varieties and cropping systems that are more resistant to drought.

Barrington et al., [2013] proposed that there is a need of an overarching company policy to minimize water use and effluent discharge and the use of alternate water sources such as rainwater runoff and reuse of water within process units will help in water conservation They also suggested that water auditing has an important role in achieving water conservation in industries and to improve water conservation through technical, cultural and behavioral adaptations, many opportunities existed.

Ahiablame et al, [2013] investigated the effectiveness of low impact development practices in two urbanized watershed. The 2–12% reduction in runoff and pollutant loads is achieved by various application levels of barrel/cistern and porous pavement for the two watersheds. Reduction in runoff not only led to reduction in total stream flow but also associated pollutant loads by 1–9% in the watersheds.

Dechmi and Skhiri et al., [2013] evaluated best management practices under intensive irrigation for outlet Del Reguero watershed in sapin. The results showed that the

load reductions were increased when individual BMPs were combined. The BMP scenario combining optimum irrigation application, conservation tillage and reduced P fertilizer dose was the best, leading to a TP load reduction of about 22.6%.

Many studies showed that mitigation measures that are effective for soil erosion can be assumed to control diffuse pollution losses, because of the strong relationships between runoff, sediment and the transport of P, N, pesticides, pathogens, and metals,. Low impact development (LID) practices have been utilized to mitigate hydrologic and water quality impacts of urbanization. To reduce non-point source pollution and improve water quality, land management practices such as conservation tillage and optimum irrigation are also routinely used.

CHAPTER 3

METHODOLOGIES

This section describes about study area, baseline of HSPF model, database and methods used to calibrate and validate HSPF.

3.1 Description of Study Area

SuAsCo is a small semi urban watershed in eastern Massachusetts about 25 mi west of the Boston metropolitan area and is one of the 27 major watersheds in Massachusetts. SuAsCo stands for the Sudbury, Assabet, and Concord Rivers and is the land area surrounding these three rivers. The total drainage area of SuAsCo is 391 mi^2 (249,782 acres). Lower Concord River Basin is the portion of the basin that drains directly to the Concord River, which is formed at the confluence of the Sudbury and Assabet Rivers in the town of Concord. Sudbury River Basin composes 162 mi^2 and is about 44% of the total SuAsCo basin, and the Assabet River Basin 177 mi^2 is about 41% of SuAsCo basin, while the Lower Concord River Basin 60 mi^2 is about 15 percent of the total SuAsCo River Basin area (Figure 1). Mean annual streamflow from the basin at outlet NWIS gaging station CONCORD R BELOW R MEADOW BROOK (station no. 1099500) is about 650 ft^3/s (421 Mgal/d)**.** SuAsCo watershed encompasses partially or wholly 36 Massachusetts town**.** About 400,000 people lived in the SuAsCo Basin in 2000. In Assabet river Basin, an estimated 129,000 people were residing and 185,200 people lived in the Sudbury River Basin in 2000 (Zarriello et al., 2010). Population per

unit area in the Sudbury River Basins (1,140 people/mi^2) was estimated to be about 60 percent greater than in the Assabet River Basin (730 people/mi^2).

3.1.1 Climate

SuAsCo watershed is characterized with humid continental climate, with warm summers and cold, snowy winters. Annual average precipitation in SuAsCo is 47.71 inches. Mean annual temperature and evapotranspiration is 48.57 F^O and 25.47 inches respectively. The index of dryness, i.e. the ratio of potential evapotranspiration to precipitation is 0.53. Three weather stations were used for climate data in SuASco. Worcester WSO AP (Station no. MA 199923) weather station located about 22 mi southwest from the center of the Sudbury and Assabet River Basins. Walpole 2 (Station no. 198757) is located about 19 miles southeast from the center of Sudbury and Assabet River Basins. Bedford (Station no. MA 190535) is located about 5 miles to the south east of lower Concord river basin.

3.1.2 Soil Type

Based on texture predominant soil types in SUASCO include fine sandy loam (34%), outcrop and urban land complex (24%), loamy sand (11%) and muck (10%). Other soil types include pit quarry, dumps, sand and gravel, loamy coarse sand, loamy, loam, sandy, loamy sand, loamy fine sand, mucky fine sand, loam, mucky silt loam, sandy loam, silt loam and very fine sandy loam (all combined 20%). Soil with hydrologic group A and D covers about 34.6 % and 25.6 % of watershed respectively. While about 23.8% and 16.1% of watershed comprises of hydrologic group C and B respectively. A complete list of soil types, associated texture and hydrologic group used in simulation runs is given in Table 1.

3.1.3 Topography

SuAsCo Basin is located in the coastal lowlands near the border with the central highlands along the southwestern portion of the basin [Denny, 1982]. The hillier terrain more common, in the southwestern part of the basin, particularly in the Assabet River Basin, The Sudbury River drops from a maximum elevation of about 700 ft to about 100 ft at its confluence with the Assabet River. Along its 33 mi length, the river gradient averages about 5.2 ft/mi, but low-gradient reaches are common in wetlands and reservoirs found in many reaches. The Assabet River drops from a maximum elevation of about 750 ft to about 100 ft at its confluence with the Sudbury River. Over its 32 mi length, the river gradient averages about 6.8 ft/mi, but low-gradient reaches behind impoundments are common. The river gradient flattens considerably below the Maynard streamgage [Zarriello et al., 2010]. The Concord River drops from a maximum elevation of about 348 ft to about 118 ft at its confluence with the Sudbury and Assabet River.

3.1.4 Land Use Land Cover

Forest is the predominant land use in watershed. About 43% of watershed is forest (Figure 2). Wetlands, both forested and non-forested, constitute to about 13 % of the watershed. 5% of the land use is for agriculture, pasture and brushland. About 35 % of the watershed is urban land. The rest of the area includes barren land, public/transitional areas and cemeteries (Table 2).

3.1.5 Surface-Water Resources and Streamflow

The upper Sudbury River Basin was once a major source of drinking water for the Boston metropolitan area. Eight reservoirs were built in the Sudbury basin to meet the rapidly growing demand of water. These reservoirs include Lake Cochituate, Ashland, Hopkinton, Whitehall, Sudbury, Foss, Brackett, and Stearns Reservoirs. However, after Wachusett Quabbin Reservior to the northwest and Quabbin Reservoir to the west were constructed in 1939, water from Sudbury basin was no longer needed and also of less desirable quality [Zarriello et al, 2010]. MWRA (Massachusetts Department of Conservation and Recreation, 2008) classified Sudbury and Foss Reservoirs are classified as reserve water. The operation of these reservoir for reactional and maintenance can still effect streamflow in this part of the basin, even though withdrawals are no longer made from these reservoirs. The Assabet River Basin contains several water-supply reservoirs—Lake Williams and Millham Reservoir that, along with MWRA, supply water to the city of Marlborough and Gates Pond that supplies water to the town of Hudson. Along with number of reservoirs for mill power, Warner Pond in Concord, Lake Boon in Stow, and Fort Meadow Reservoir in Marlborough were built in the 18th and 19th centuries and now these reservoirs are regulated for recreational purposes. More recently built reservoirs, such as A1 in Westborough, provide flood control. Streamflow below impoundments can be directly altered by flow regulation and indirectly through evaporation losses. About 13% of the SuAsCo watershed consist of wetlands that can affect streamflow through storage and evapotranspiration (ET) losses. In addition, withdrawals, diversions, and wastewater-treatment facility discharges can also affect streamflow. Figure 3 shows the location of lakes and impoundments in SuAsCo.

3.2 Conceptual Model

Conceptual framework for assessing impacts of LULC changes and climate change on watershed system is presented in Figure 4. Watershed system consists of three components: 1) Abiotic, 2) Biotic, and 3) Socio-economic component. The interaction among those components impacts water quality and water quantity. Those change i.e. changes in LULC and climate can not only lead to increased runoff, declined percolation, increased ET, but also elevate sediment and nutrient levels. Hence climate change and LULC change are the stressors for watershed. However policy adaptation e.g. use of best management practices (BMPs) can help to reduce the impacts of those stressors.

3.3 Empirical Model

Empirical model (Figure 5) is combination of specific methods that assess particular components and changes in watershed system. These methods are explained below in detail:

HSPF is a continuous simulation model based on the principle of conservation of water mass, that is, inflow equals outflow plus or minus any change in storage [Zarriello and Ries; 2000]. In HSPF, watershed is divided into subbasins to represent the spatial heterogeneity of the study area. Based on unique soil-landuse combination, each subbasin is further discretized into a series of hydrologic response units (HRUs). HRUs are divided into pervious-area land segments (PERLNDs) and impervious-area land segments (IMPLNDs). PERLNDs and IMPLNDs have zones that retain precipitation at the surface as interception storage or snowpack storage. All water that is not evaporated produces surface runoff from IMPLNDs. In PERLNDs storage volumes and processes are

represented by upper, lower, and groundwater zones, since PERLNDs allow excess precipitation to infiltrate into the subsurface. Because of that processes that control the rate of infiltration and change in subsurface storage make simulation of PERLNDs considerably more complex than simulation of IMPLNDs [Zarriello and Ries, 2000]. The length of stream channels, lakes and reservoirs is represented by RCHRESs. For each HRU and RCHRES in the model, water budgets (inflows, outflows, and changes in storage) are calculated for each time step. In the model simulation, surface runoff from PERLNDs and IMPLNDs and subsurface discharge from PERLNDs are typically directed into reaches. The hydraulic properties of the reaches are defined by the relationship between depth, storage, and discharge in function table (FTABLE) of the model input [Barbaro and Sorenson, 2013].

Two primary input files are required for HSPF operation, the User Control Input (UCI) file and the Watershed Data Management (WDM) file. The UCI file directs the process actions used by the model and sets input parameter variables. Process actions or algorithms in the model calculate the movement of waterand changes in storage. To simulate different processes, the three main blocks of the UCI file are (1) PERLNDs, (2) IMPLNDs, and (3) RCHRESs. Modules and sub-modules are present within each block. Some of these modules and sub-modules are mandatory for simulations and others are optional. For example, the PWATER modules are required to simulate the hydrology of pervious areas, but the SNOW module is optional for simulating snowpack buildup and melt.

The SCHEMATIC or NETWORK blocks are used to represent the physical layout of the basin. The area of each IMPLND and PERLND that drains to a RCHRES

(also referred to as a reach) is defined in this section of the model to formulate subbasins. The SCHEMATIC or NETWORK blocks also are used to area of each IMPLND and PERLND that drains to a RCHRES. The MASSLINK section associated with a SCHEMATIC block or NETWORK block controls the linkage of flow components between model elements. Typically, this linkage involves routing (1) surface runoff from PERLNDs and IMPLNDs to reaches, (2) interflow and base flow from PERLNDs to reaches, and (3) streamflow from reach to reach. The physical layout of the basin is represented by the SCHEMATIC or NETWORK blocks. This section of the model is used to define the area of each IMPLND and PERLND that drains to RCHRES to formulate subbasins. The MASSLINK section associated with a SCHEMATIC block or NETWORK block controls the linkage of flow components between model elements. Typically, this linkage involves routing (1) surface runoff from PERLNDs and IMPLNDs to reaches, (2) interflow and base flow from PERLNDs to reaches, and (3) streamflow from reach to reach [Barbaro and Zarriello, 2007].

Surface runoff can discharge to a reach from impervious surfaces (SURI) and pervious surfaces (SURO). Infiltrated water can discharge to the reach through the subsurface as interflow (IFWO), which is analogous to a fast-responding shallow subsurface flow, or from active ground water (AGWO), which is analogous to a slow-responding base-flow component, or, optionally, exit from an HRU as a deep ground-water flow that discharges outside of the basin (IGWI). Inflow to a reach also can come from upstream reaches (IVOL), direct precipitation, and other user-specified point sources such as treated wastewater [Zarriello and Ries, 2000].

Five outflow exits (or gates) can be used to direct volumetric outflow from a reach. Water was routed downstream through the third outflow exit (OVOL 3) in reaches with withdrawals; in reaches with no withdrawals, a single outflow exit representing outflow to the downstream reach was specified. Water from the time series of cumulative withdrawals was directed through the second outflow exit (OVOL 2) in reaches. When two outflow gates are specified (OVOL 1), the volume time series of water withdrawals (OUTDGT 1) for each reach is read from the EXT SOURCES block (external sources).

3.4 Conceptual Parameters used in HSPF

Three conceptual parameters are used in HSPF to separates moisture inputs (precipitation and snowmelt) into infiltrating and non-infiltrating fractions. Those three conceptual parameters include, a surface storage capacity value (UZSN), an interflow–inflow index (INTFW), and an infiltration-capacity index (INFILT) (Johnson et al., 2003). Chezy–Manning equation and average values of the surface roughness, length, and slope for the overland flow plane of each HRU are used to generate overland flow [Donigian et al., 1999].

Subsurface lateral flow also known as interflow–outflow (IFWO) in HSPF is calculated on the basis of a linear relation between the conceptual interflow-storage volume and lateral flow as a function of the interflow-recession coefficient (IRC). IRC, which is the ratio of the present rate of IFWO to the value 24 h earlier, can be input on a monthly basis to allow for annual variations in soil-moisture and the timing of IFWO [Bicknell et al., 1997]. Subsurface lateral flow has a substantial effect on stormflow

hydrographs, particularly in areas where vertical percolation is retarded by bedrock or a shallow, poorly permeable soil layer [Johnson et al., 2003].

HSPF computes evapotranspiration (ET) as a function of moisture storage and PET, which is adjusted for vegetation cover, and estimates actual ET from the potential demand from five sources (1) interception storage, (2) upper-zone storage; that is, some or all the moisture in depressions and near-surface retention, (3) vegetation demand, which is satisfied from lower-zone storage through the parameter LZETP, which can be adjusted monthly to account for seasonal changes in the plant growth stage and soil moisture, (4) deeply rooted vegetation demand, which is satisfied from active groundwater storage through the parameter AGWETP, and (5) riparian-vegetation demand, which is satisfied by active groundwater outflow as stream baseflow through the parameter BASETP [DeGaetano et al., 1994, and Johnson et al., 2003].

3.5 Database

A list of database is given below.

3.5.1 Watershed Data Management (WDM)

Watershed Data Management (WDM) file is used to store time-series data required for simulations and time series generated by the model [Kittle et al., 1998]. The WDM data base is organized by data sets with a unique data set number (DSN) assigned to separate time series. Each data set also has attributes that describe the data type, time step, location, and other important features. In the SuAsCo WDM file, the first 100 DSNs are used for input meteorologic time-series and observed streamflow. Data sets with numbers larger than 100 are generally organized by reach. Table describes the general

organization of the WDM file. The sum of individual ground-water withdrawals plus any surface-water withdrawals provides the total water withdrawal time series for given reach and these time series (OUTDGT) are entered into the WDM file in data set. Time series for point source loading (effluent volume, sediments, nutrients, BOD and temperature of effluent) are also entered in WDM.

3.5.2 Stream Flow Data

Observed daily-flow data were obtained for the USGS gaging stations at four gaging stationsv (Figure 7). Gaging station at Concord River below R Meadow Brook at Lowell (station no. 01099500) was used for calibration for a time period 1973-2008. Gaging station at Nashoba Brook near Acton (station no. 01097300) for time period 1973-2008, Assabet River at Maynard (station no. 01097000) for time period 1973-2008 and Sudbury River at Saxonville (station no. 01098530) for time period 1980-2008 were used for validation. Streamflows for these four gaging stations are in DSN 1, 2,5,18 in WDM file (Table 3).

3.5.3 Meteorological Data

Meteorological data, including precipitation, air temperature, dew-point temperature, solar radiation, and wind speed for the SuAsCo watershed was gathered from National Climatic Data Center (NCDC) for three USGS stations; Bedford, Worcester WSO AP and Walpole 2 for duration of January 1973 to December 2008. Annual average precipitation (1973-2008) recorded at Bedford weather station is about 48.01 inches with minimum and maximum precipitation is 33.5 and 62.2 inches respectively. Walpole 2 weather station recorded annual average precipitation of 47.7 inches with minimum and maximum precipitation is 30.6 and 60.8 inches respectively for

a period from 1973 to 2008. Annual average precipitation (1973-2008) recorded at the Worcester WSO AP is about 47.42 inches with minimum and maximum precipitation is 32.01 and 64.3 inches respectively. Annual Average temperature is 48.6 $F^{O,}$ 49.7 F^{O} and 47.4 F^{O} at Bedford, Walpole 2 and Worcester WSO AP respectively. Mean annual potential evapotranspiration was 25.8 inches, 26.5 inches and 24.1 inches at Bedford, Walpole 2 and Worcester WSO AP weather station respectively for the simulation duration. HSPF algorithms use hourly values meteorological data. The Thedatabase contained both this Pan Evaporation dataset and a computed Potential Evapotranspiration (PEVT) dataset. The PEVT dataset is appropriate as an input to the HSPF model for both potential evapotranspiration applied to the land surface and for lake evaporation applied to water surfaces

3.5.4 Water Withdrawals and Return Flows

Most of the water withdrawals are for municipal use and from ground water. 38 withdrawals are from ground water and 12 are from surface water in Assabet River (Table 4). In Sudbury River there are 27 ground water withdrawals and 4 surface water withdrawals. 5 withdrawals are from ground water and 1 withdrawal is from surface water in Concord River Basin (Table 5). The total annual water withdrawals during 1973-2008 average about 11 Mgal/d from Assabet River Basin, 14 Mgal/d from Sudbury River Basin and 4 Mgal/d from Concord River Basin. Table 6 present locations of withdrawals for agricultural, commercial and industrial uses. Daily discharges records were obtained from 14 WWTP (Figure 8) in SuAsCo for the period of 1973-2008 and cross checked with the monthly wastewater discharges reported to the U.S. Environmental Protection Agency (USEPA) for the period January 1, 1993, through December 31, 2003.

Average annual discharges ranged from 0.008 to 2.99 Mgal/d at Raytheon Sudbury Factory WWTP and Billercia WWTP respectively. Shrewsbury WWTP diverted to Westborough WWTP in 1987 and Digital Equipment Corporation Company WWTP stopped working after 1995 and the facility was used by senior citizen. Overall Wastewater discharge averaged 8.3 Mgal/d in the Assabet River Basin, 2.8 Mgal/d in the Sudbury River Basin and 4.6 Mgal/d in Concord River Basin (Table 7).

3.5.5 Representation of the Basin

The physical and spatial representation of the basin in the model is defined by the combination of HRUs (PERLNDs and IMPLNDs), their contributing area to a reach, and the linkage of one reach to another. The process of defining HRUs, their linkage to reaches, and the linkage of reaches to each other often is referred to as the schematization or discretization of a basin. A Geographic Information System (GIS) was used to discretize the watershed. To build a basin project, Universal Transverse Mercator coordinate (UTM), zone 18 projection was used. The watershed delineation process defines a boundary around the entire land area contributing to flow in a stream. Automatic delineation tool in BASIN (Better Assessment Science Integrating point & Non-point Sources) 4.1 will be used to define 157 hydrologically connected subwatersheds within study area. Watershed was delineated based on Networked Hydro Centerlines. Cataloging unit boundaries were used as a focusing mask. Other data layers used in the discretization process were obtained from MassGIS, and include 1:25,000-scale MassGIS Soil Survey Geographic (SSURGO)layer, 1:25,000-scale land use and 1:25,000-scale hydrography. The spatial data were simplified and grouped to obtain categories that were considered important to the hydrology of the watershed. The soil

data layer was was simplified into 4 on the basis of permeability and storage characteristics: Soil type A (2) Soil type B (3) Soil type C and (4) Soil type D. Watershed delineation was done by using threshold method by using different threshold values (Figure 6). The threshold area was set to 1.4 sq. mi. for 780 numbers of cells, because this value most accurately modeled the stream network.The watershed was segmented based on three meteorological stations (Bedford,Worcester WSO AP and Walpole 2) different landuse types and soil types by using intersect tool in ArcGIS 10.1 and watershed segmentation tool in BASINS 4.1.

3.6 Hydrologic Processes Represented by HSPF

The detail of hydrologic processes is given below.

3.6.1 Hydrologic Response Units

The land-use data layer was simplified from 32 categories to 9 land-use categories: (1)agriculture/grassland/shrubs, (2) commercial/industrial,(3) Forest, (4) high density residential area, (5) low density residential area, (6) medium density residential area, (7), Public/institutional (mixed residential) (8)water, and (9) wetlands. HRUs were obtained by combining the soil and the simplified land-use data layers. Intersection of the combined soil and land-use data layers with the subbasin delineations yielded the area of each HRU for each subbasin. Commercial, industrial, and transportation areas are generally referred to herein as commercial because this is the dominant land-use type. 30 possible combinations of soil and land use covered areas to warrant unique HRUs for pervious land and 5unique HRUs for impervious land for each of three segments (based on met stations) were used in model.

3.6.2 Impervious Areas (IMPLNDs)

Some impervious surfaces drain runoff onto surrounding pervious surfaces that allow infiltration, hence water can infiltrate into the ground. In the HSPF model, IMPLNDs are used to simulate effective impervious areas, which are impervious surfaces that drain directly to streams and thus produce only surface runoff. Five IMPLND types were used in the model—commercial, high density, low density, medium density and mixed residential area. Initial estimates of effective impervious area were obtained from Zarriello and Ries [2000] for similar land-use types.

Sutherland Equations [Sutherland, 2000] were used to determine final effective impervious area. Overall, about 35.4 percent of the basin is classified as developed, and 12.1 percent of basin area in impervious area (IA) but only 7.6 percent of basin area is simulated as effective impervious area (EIA). Hence IMPLND areas ranged from 59.5 percent for commercial, transportation, and industry to 33 percent for high-density residential, 18.6 percent for medium-density residential, 16.4 percent for public/transitional area and 7.6 percent for low density area (Table 8).

3.6.3 Pervious Area (PERLNDs)

Of the 30 unique PERLND HRUs defined for the basin 4 represent forested areas over soil type A, B, C,D. Cropland, pasture, orchards, nurseries and brushland/successional were included in one class and that class named as agriculture/pasture. 4 unique HRUs represent agriculture/pasture over 4 soil types. One HRU represent open water and one HRU represent wetlands and these two HRUs were not further distinguished by the underlying soil types. Twenty HRUs represent various combinations of residential-area densities and soil types. Four HRUs represent

commercial/industrial areas over four combinations of soil types. Commercial/industrial HRUs include commercial and industrial areas. HRUs for residential areas represent public/institutional, low-, medium-, and high-density development. High-density residential HRUs represent multi-family residential and single-family residential on lots smaller than or equal to 0.25 acre. Medium-density residential HRUs represent transportation and single-family homes on lots between 0.25 and 0.5 acre. Public/Institutional HRUs include mining, open land, participation recreation, transitional, waste disposal, power line utility, golf course, urban/public/institutional, cemetery and junkyard. Low-density residential HRUs represent single-family homes on lots larger than 0.5 acre. Forest HRUs are the dominate HRU type in the basin (43 percent) more than collective developed HRUs (35 percent). Most developed areas are classified as low- to medium-density residential (21 percent). In general, hydrologic characteristics are similar for PERLNDs with similar surficial geology; however, upper- and lower-zone storage and infiltration are less for developed PERLNDs than for forested PERLNDs. The decreased storage allows developed PERLNDs to respond more rapidly to precipitation than the same surficial geology type undisturbed by development.

3.6.4 Stream Reaches

The Assabet, Sudbury and Concord River Basins were discretized (divided) into 157 stream reaches on the basis of hydrologic features. Tributaries at Assabet River were divided into 67 reaches; 17 of which are on the main stem of the river. Thirteen tributaries (North Brook, Beaver Brook, Hog Brook, Fort Meadow Brook, Danforth Brook, Taylor brook, Elizabeth Brook, Inch Brook, Heath Hen Meadow Brook, Spring Brook, Fort Pond Brook, gates pond Brook and Grassy Pond Brook) upstream of

Maynard gaging station (station no. 1097000) and one tributary (Spencer Brook) downstream of that gaging station, were divided to create reaches at reservoirs and major tributary confluences. Three tributaries (Nagog Brook, Connant Brook and Nashoba Brook) are at upstream of Nashoba Brook gaging station (station no. 1097300) near action at Assabet river basin, and one tributary (Butter Brook) is at downstream of gaging station.

Sudbury River Basin is divided into 65 reaches, 38 of which are upstream from the Saxonville streamgage (station no. 01098530). 11 of the 38 upstream Sudbury River reaches are on the main stem. Fifteen tributaries upstream from the Saxonville streamgage (Snake Brook, Angelica Brook, Stony Brook, Jenny Dugan Brook, Rutters Brook, Course Brook, Munroe Brook, Waushakum Pond brook, Denny Brook, Indian Brook, Jackstraw Brook, Whitehall Brook and Dunsdell Brook, Cochituate Brook and Peppermint brook) and nine tributaries (Hop Brook, baiting Brook, Cold brook, Dudley Brook, Landham-Allowance Brook and Mill Brook 1) downstream of Saxonville streamgage were subdivided to create reaches at reservoirs and major tributary confluences.

Tributaries at Concord River basin are divided into 26 reaches. Seven tributaries (Russel Millpond brook, Cold Spring brook, Farley Brook, marginal Brook, Pages Brook, River meadow Brook, Sawmill Brook) upstream of Concord river below R meadow brook at Lowell gaging station (station no. 1099500) were subdivided to create reaches at reservoirs and major tributary confluences. "Manning's "n" Values and REACHES names are presented in Table 9.

3.6.5 Hydraulic Characteristics (FTABLEs)

The hydraulics of a river reach or reservoir (RCHRES) segment was described in FTABLE by defining the functional relationship between water depth, surface area, volume, and outflow in the segment. The number of rows in the FTABLE depend on the range of depth to be covered and the desired resolution. The SuAsCo watershed topography is piedmont, so FTABLES are computed for the piedmont province by using alternative method of FTABLES that is based on power regression equations. Power regression equations for Piedmont province are: $Q=xDA^{y}$ (x =0.015, y= 0.989); $A=uQ^{d}$ (u=3.53, d =0.65); $W_m=aQ^{b}$ (a=11.95, b= 0.47); $Y_m=cQ^{f}$ (c=0.28, f= 0.22); $V=KQ^{m}$ (k= 0.35, m=0.25); n = 0.77;$(uQ^{d})(cQ^{f})^{2/3}$ $(S^{1/2})/xDA$;Where: A= Cross-sectional area (m^2); Q=Discharge (m^3/s); DA=Drainage Area (Km^2); W_m=Mean flow width (m); Y_m=mean flow depth (m); n= Manning's Roughness coefficient; V= velocity (m/s); (x, y, u, d, a, b, c, f, k, m)=Empirical constants, n = Manning's coefficient (uses Manning's equation assuming a parabolic shape with a hydraulic radius equal to 0.67.Y_m.

The cross-section geometry and Manning's roughness coefficients were obtained from surveys conducted at river reaches for flood-insurance studies, and from streamflow measurements made at continuous- and partial-record stations in the basin (U.S. Army Corps of Engineers, 1966; FEMA, 1979; FEMA, 1982). When this detailed information was not available, channel widths and cross-section elevations were obtained from USGS 1:24,000-scale digital topographic maps and field observations.

3.7 Model Calibration

The model was calibrated for 36 year period from January1, 1973, to December 31, 2008, by minimizing the differences between simulated and observed streamflow at the four streamgages in the model area. HSPF models by USGS for similar landuse type watersheds Ipswich [Zarriello and Ries , 2000], Blackstone [Barbaro and Zarriello, 2007] and Taunton River [Barbaro and Sorenson, 2013] were used as a guide for parameters values.

The optimum parameter values that reflect watershed-specific physical processes are generally obtained through the calibration process. To assist with the calibration process in watershed HSPEXP tool [Lumb et al., 1994] was used. HSPEXP statistical criteria, monthly flow, cumulative flow and regression of observed vs. simulated flow were used for calibration. Hydrologic parameters necessary for HSPF simulation are estimated using guidance provided by BASINS Technical Note 6 (Estimating Hydrology and Hydraulic Parameters for HSPF). An iterative process was then used to adjust variable values for HRUs. Discharge measured at Concord River below R Meadow Brook at Lowell (station no. 01099500) for a time period 1973-2008 provided the main data sets for model calibration.

For validation, discharges measured at Nashoba Brook near Acton (station no. 01097300) for time period 1973-2008, at Assabet River at Maynard (station no. 01097000) for time period 1973-2008 and at Sudbury River at Saxonville (station no. 01098530) were used. Calibration is done by adjusting relevant parameters to reduce differences between simulated and observed streamflow characteristics, such as volume error, highest flows and lowest flows, storm and seasonal volume error, low flow

recession, summer and winter volume. Parameters that influence the simulate infiltration, interflow, surface and soil moisture storage and losses through evapotranspiration, and interflow and groundwater recession rates during simulation have generally large effect on runoff volume and error [Johnson et al., 2003]. The R^2 and the Nash-Sutcliffe model-fit efficiency coefficient (E) were used to measure the quality of the model fit. The Nash-Sutcliffe E provides a more rigorous evaluation of the fit quality than R2 does because E is sensitive to differences between the observed and simulated means and variances, whereas R2 measures only the differences between mean values [Legates and McCabe, 1999]. Hydrographs and flow-duration curves of the daily mean flow reflect climate, topography, and hydrogeologic conditions of the basin.

Calibration mainly focused on minimizing differences between simulated and observed flows at at Lowell gaging station at Concord River below R Meadow Brook. Hence, fitting the model to the Lowell was weighed against the benefits of fitting the model to the Maynard streamgage, which was less affected by reservoir operations. Simulated flows at the nashoba Brook near Acton streamgage showed least goodness of fit because that reach is not present on the main stem of Assabet River.

For sediments, JRER (exponent in soil detachment equation) approximates the relationship between rainfall intensity and incident energy to the land surface for the production of soil fines. Wischmeier and Smith [1978] proposed the following relationship for the kinetic energy produced by natural rainfall. $Y = 916 + 331 \log X$, Where Y = kinetic energy, ft/ton/acre/in.; X = rainfall intensity, inches/hr.

The fraction of solids storage which is removed each day when there is no runoff (per day) is estimated by using REMSDP parameter. These removal processes include

wind, air currents from traffic, aggregation to larger, less transportable particles, and street cleaning activities. The effects of street cleaning can be estimated as*: R = P*(E/D)*; Where: *R* = sediment removal by street cleaning; *P* = fraction of impervious area where cleaning is performed;

E = efficiency of cleaning; *D* = frequency of cleaning.

Critical bed shear stress values (τc) are calculated from Shields' equation using bed and channel properties, as follows: $\tau c = \theta (\gamma s - \gamma)$ D, Where: θ = dimensionless Shields parameter for entrainment of a sediment ;D=Sediment particle of size; γs = the unit weight of bed sediment; γ = the unit weight of water.

Donigian and Love [2005] have used these procedures to estimate τc values and assess channel stability issues in urbanizing watersheds using HSPF. Erosion is primarily a function of the amount of soil exposed directly to rainfall and surface runoff, which in turn is affected by rainfall, land cover, land slope, soil disturbance, and transport properties of the soil [Donigian and Love, 2005]. The USLE is an empirical equation commonly used to estimate erosional rates as a function of these factors.

The USLE formula is expressed as follows: $A = R * K * L * S * C * P$, where: *A* = annual soil loss in tons per acre per year; *R* = rainfall erosivity factor; *K* = soil erodibility factor; *L* = slope length factor; *S* = slope gradient factor; *C* = cover management factor; *P* = erosion control practice factor. In HSPF, if the model reach being simulated is a stream or river, the bed shear stress is determined as a function of the slope and hydraulic radius of the reach, as follows: *TAU = SLOPE*GAM*HRAD*, Where: *TAU* = stream bed shear stress (lb/ft^2 or kg/m^2); *SLOPE* = slope of the RCHRES; *GAM* = unit weight, or density,

of water (62.4 lb/ft^3 or 1000 kg/m^3); *HRAD* = hydraulic radius (ft or m). The hydraulic radius is calculated as a function of average water depth *(AVDEP)* and mean top width *(TWID)* as follows: *HRAD = (AVDEP*TWID)/ (2.*AVDEP + TWID),* Average depth is computed as: *AVDEP = VOL/SAREA*. The mean top width is found using: *TWID = SAREA/LEN,* Where: *LEN* = length of the RCHRES (ft or meter); *SAREA*=Surface area of water in the reach *(m^2)*.

Other parameters necessary for sediment and nutrient calibration were estimated using guidance provided by BASINS Technical Note 8 (Sediment Parameter and Calibration Guidance for HSPF) [*EPA*, 2007].

3.8 Model Statistical Tests

The statistical tests of model results will be performed to compare simulated flow, sediment, TN and TP loads with the observed (field-measurements) flow, sediment, TN and TP loads. Those statistical tests are (1) percent flow difference [calculated as: (total model simulated flow–total observed flow)/total observed flow], (2) regression coefficient: R^2, and (3) the Nash–Sutcliffe efficiency (NSE) [Nash and Sutcliffe, 1970]. The model efficiency or agreement between observed and the simulated daily discharge data series will be measured by the Nash–Sutcliffe model efficiency (NSE). $NS= 1-[\Sigma_i^n (Q_{sim}-Q_{obs})^2]/ [\Sigma_i^n (Q_{obs}-Q_{avg})^2]$; where n is the number of time steps, Q_{sim} and Q_{obs} the simulated and observed streamflow at time stepi, and Q_{avg} the average observed streamflow over the simulation period.

3.9 LULC Change Impacts

The Land Transformation Model (LTM) is used for future land use change prediction. LTM model have been developed and used by Human Environment Modeling & Analysis laboratory (HEMA lab) at Purdue University. The information that is used to conduct forcasting studies via this model include a set of spatial interaction rules and machine learning, through neural net technology, to determine the nature of spatial interactions of drivers, such as transportation, urban infrastructure and proximity to lakes and rivers, that have historically contributed toward land use change in the past.

3.10 Climate Change Impacts

For the Fifth Assessment Report of IPCC, the scientific community has defined a set of four new scenarios, denoted Representative Concentration Pathways (RCPs). They are identified by their approximate total radiative forcing in year 2100 relative to 1750: 2.6 W m-2 for RCP2.6, 4.5 W m-2 for RCP4.5, 6.0 W m-2 for RCP6.0, and 8.5 W m-2 for RCP8.5. These four RCPs include one mitigation scenario leading to a very low forcing level (RCP2.6), two stabilization scenarios (RCP4.5 and RCP6), and one scenario with very high greenhouse gas emissions (RCP8.5). For RCP6.0 and RCP8.5, radiative forcing does not peak by year 2100; for RCP2.6 it peaks and declines; and for RCP4.5 it stabilizes by 2100. Each RCP provides spatially resolved data sets of land use change and sector-based emissions of air pollutants, and it specifies annual greenhouse gas concentrations and anthropogenic emissions up to 2100. RCPs are based on a combination of integrated assessment models, simple climate models, atmospheric chemistry and global carbon cycle models. For all RCPs, additional calculations were

made with updated atmospheric chemistry data and models (including the Atmospheric Chemistry and Climate component of CMIP5) using the RCP prescribed emissions of the chemically reactive gases (CH4, N2O, HFCs, NOx, CO, NMVOC). These simulations enable investigation of uncertainties related to carbon cycle feedbacks and atmospheric chemistry. RCP4.5 is used in this research to assess the impacts of climate change in SuAsCo watershed. According to RCP4.5 projection, average annual temperature will increase 2.7 ^{0}C and precipitation will increase 7 percent by 2100.

3.11 Combined Impacts of LULC and Climate Change

For Objective 4, the combined impacts of LULC and climate change impacts is assessed by using future land use and climate change scenarios for year 2100.

3.12 Management Implication

This research presents information about the fate and transport of runoff, sediments and nutrients in the SuAsCo watersheds. The modeling helps to estimate the impacts and compare levels of stress. All sites provides reliable estimates of water flows in watershed and quantify runoff, sediments and nutrient loads in the HSPF model, which will be valuable in providing a better understanding and in forecasting pollutants concentrations for future. Changes in river hydrology, morphology, and water quality are expected by increasing the magnitude and response time of runoff entering a river system. I expect that baseline simulations closely match with the observed information. LULC changes will have impacts on water quality and water quantity, as well as climate change will have impacts on water quality and water quantity. LULC change and climate

change will have combined impacts on sediments and nutrients loading. This study will provide useful information that could be used in developing watershed management plans for semi urban watershed areas. The watershed modeling is capable of assessing the spatial and temporal variability of runoff, sediments and nutrients fate in the river so that it also can be considered as an auxiliary assessment tool to provide necessary data reference for ecological risk and human health assessments after water pollution occurred. The results of this research will have numerous management implications for the watershed system. A modular approach is an effective way to develop integrated watershed assessment tools. The outputs of the models will provide comprehensive information of the contaminant distribution in a multimedia environment at watershed scale. The significance of the watershed modeling will be for purposes in identifying environmental management opportunities to mitigate water pollution and preserve aquatic and human health. This research will facilitate in-depth analysis of inter-media transports and multimedia system behaviors under dynamic conditions while preserving the requirements of modest data input and rapid scenario analysis.

CHAPTER 4

RESULTS & DISCUSSION

This chapter is about discussion regarding HSPF calibration for runoff, sediments and nutrients. The assessment of impacts of climate change and land cover change has also been discussed in this section.

Watershed is calibrated for runoff and Table 11 gives a list of adjusted parameters for calibration of hydrology in HSPF model. Gaging stations at Concord River below R Meadow Brook at Lowell is used for calibration. Gaging station at Sudbury River at Saxonville, Assabet River near Acton and Assabet River at Maynard is used for validation.

4.1 Water Quantity Calibration

Water quality calibration is give below.

4.1.1 Concord River below R Meadow Brook at Lowell (01099500, RCHRES 157)

Model is calibrated for this gaging station and other three gagging stations are used for validation. Simulated streamflow in the Concord River at Lowell gaging station is generally in good agreement with observed flow over a wide range of flow conditions and seasons (Figure 9A). Simulations during the calibration period captured the observed evolution and magnitude reasonably well for both daily and monthly time scales. Rising limbs of daily hydrographs and baseflow were simulated especially well. Scatter plots of simulated flows in relation to observed flows indicate a slight undersimulation of high flows and over simulation of low flows. Differences between simulated and observed

flows may also be caused by uncounted transfers of water into the Reservoirs at Assabet River from outside the basin or by uncounted regulation of the Assabet Reservoir system. On average, the mean daily flow over the calibration period was undersimulated by about 8.9 percent, which is largely attributed to the inaccurate accounting of transfers of water into the basin. Flows, on average, during summers were undersimulated by about 8 percent and during winters undersimulated by about 10 percent. Summer storm flow is oversimulated by 14.5 %. This difference also may be caused by unaccounted reservoir operations. An oversimulation of stream flow could be caused by uneven distribution of localized connective storms that caused high measurement of precipitation than that recorded by surrounding stations. The model fit for the daily, monthly and yearly mean flow had an R^2 of 0.79 (Figure 10A), 0.84, and 0.88 respectively, and an NSE of 0.78, 0.83, and 0.71 respectively (Table 10). Figure 11A shows hydrograph of percent chance daily exceeded for simulated total runoff and observed flows. For year 1985, there was no difference in observed and simulated stream flow.

4.1.2 Sudbury River at Saxonville (0198530, RCHRES 140)

Simulated streamflow in the Sudbury River at the Saxonville streamgage is generally in good agreement with observed flow over a wide range of flow conditions and seasons (Figure 9 B). Scatter plots of simulated flows in relation to observed flows indicate a slight undersimulation of high flows and low flows. Differences between simulated and observed flows may also be caused by uncounted transfers of water into the Sudbury Reservoir from outside the basin or by uncounted regulation of the Sudbury Reservoir system. On average, the mean daily flow over the calibration period was undersimulated by about 13.3 percent, which is largely attributed to the inaccurate

accounting of transfers of water into the basin. Flows, on average, during summers were undersimulated by about 12 percent and during winters undersimulated by about 13.9 percent. Summer storm flow is oversimulated by 1.8 %. Years with undersimulated or oversimulated flows are consistent with the difference in annual precipitation recorded at the Saxonville station relative to precipitation recorded at nearby surrounding climate stations. The model fit for the daily, monthly and yearly mean flow had an R^2 of 0.75 (Figure 10B), 0.82, and 0.85 respectively, and an NSE of 0.73, 0.79, and 0.54 respectively (Table 10). Hydrograph of percent chance daily exceeded for simulated total runoff and observed flows are presented in Figure 11B.

4.1.3 Assabet River at Nashoba Brook near Acton (01097300, RCHRES 99)

Streamflows at Nashoba streamgage are affected by occasional regulation of an upstream ponds that is unaccounted for in the model and by alteration of the stage-discharge relation by beavers, resulting in streamflow records that are often rated as poor during the calibration period, particularly at low flows. Simulated and observed flow-duration curves (Figure 12A) are generally in close agreement. On average, the mean daily flow over the calibration period was oversimulated by about 2.6 percent .Scatter plots of simulated flows in relation to observe flows indicate a oversimulation of high flows and low flows. Flows, on average, were oversimulated by 22 percent during summer months and undersimulated by about 6 percent during the winter months. Summer storm flow is oversimulated by 27.4 %. The model fit for the daily, monthly and yearly mean flow had an R^2 of 0.69 (Figure13A), 0.76, and 0.62 respectively, and an NSE of 0.67, 0.75, and 0.61 respectively (Table 10). Simulated and observed flow-duration curves are closely matched over the entire exceedance probability (Figure 14A).

4.1.4 Assabet River at Maynard (142) (01097000)

Simulated streamflow in the Assabet River at the Maynard streamgage is generally in good agreement with the observed flow over a wide range of flow conditions and seasons (Figure 12B). On average, the mean daily flow over the calibration period was oversimulated by about 7.97 percent. Scatter plots of simulated flows in relation to observed flows indicate undersimulation of high flows and oversimulation for low flows. Flows, on average, were oversimulated by 4.4 percent during summer months and undersimulated by about 9.5 percent during the winter months. Summer storm flow is oversimulated by 2.6 %. The model fit for the daily, monthly and yearly mean flow had an R^2 of 0.80 (Figure 13B), 0.84, and 0.78 respectively, and an NSE of 0.78, 0.80, and 0.65 respectively (Table 10). Simulated and observed flow-duration curves are closely matched over the entire exceedance probability (Figure 14B).

In general for all gaging stations, the range of seasonal error is from -10% to 22 % and range of mean daily flow error is less than -13.3% to 7.97%. The yearly stream flow differences between simulated and observed flows at Concord river meadow brook and Sudbury Saxonville streamgages are relatively consistent. For example for year 1999 and 2002, stream flow is undersimulated for these two gaging station and over simulated for other years. The yearly stream flow differences between simulated and observed flows at Nashoba Brook and Assabet River at Maynard are somehow consistent. For example for year 1985,1991,1992,1999 and 2002 stream flow is undersimulated for these two gaging station and over simulated during 1973,1975,1979,1980,1982, 1986, 2005 and 2008. However the differences between all streamgages were not always consistent for all years or in relation to precipitation variability. Hence the inconsistent differences did not

warrant further changes to the model because these changes could adversely affect the model calibration in the SuAsCo Basin. These discrepancies can likely be explained by problems either in the input data or the measured discharge values or a combination of both. Table 10 shows that model is able to represent the dynamics of the hydrograph well at the daily, monthly and yearly scale. For the three validation gaging stations, the performance is somewhat reduced as compared to calibration gaging station. The reduction is, however, limited and the model is able to maintain a very good representation of the overall water balance and the interannual and seasonal variability, as well as the general pattern.

4.1.5 Hydrologic Flow Components and Water Budgets

The majority of the outflows in the water budget compose of discharge to streams and the loss of water through ET for each HRU. Various hydrologic flow components that contribute to outflows include discharge to streams through surface runoff (SURO), interflow (IFWO), and baseflow or active groundwater (AGWO), and ET losses through interception (CEPE), upper-zone (UZET), lower-zone (LZET), and active groundwater storages (AGWS). The relative proportion of the three components of the stream discharge (SURO, IFWO, and AGWO) depends on the physical characteristics of the watershed, the land use and the soil characteristics.

Annual water budgets per unit area are generally similar for HRUs with similar soil types, but still differ among land-use types .Annually, discharge to streams per unit area from HRUs overlying soil type A averaged about 90 percent from active groundwater flow, about 9.8 percent from interflow, and a negligible amount (0.12 percent) from surface runoff. High contribution of active ground water and interflow as

compared to surface runoff in water balance is because of the small segment of impervious zones in the catchment, which would otherwise facilitate quick surface overland flow. In effect, the mainly foreseted watershed favors infiltration in the soil zone and thereby lateral subsurface flow along subsurface channels, macro pores in soil type A (that covers about 34.6% of watershed), and fractures in cultivated land. This would explain the relatively small contribution of overland flow to the streamflow.

Discharge to streams from HRUs overlying soil type D about 61 percent from active groundwater, 34 percent from interflow, and 5 percent from surface runoff. Discharge to streams from HRUs overlying soil type B and C are greater than discharges from HRUs overlying soil type A and lesser that discharges from HRUs overlying soil type D. This is because of lesser permeability for soil type D as compared to other soil types. Forest contributes to base flow (active ground water recharge) the most and commercial areas contribute to the base flow the least because impervious area reduces the base flow. Discharges to streams from wetland HRUs are 57% from active ground water, 39 percent from interflow and 4 percent from surface runoff. All discharge to streams from impervious area HRUs (IMPLND) is from surface runoff. Surface runoff and interflow was highest from commercial areas because of high impervious area, low interception and infiltration in commercial land, while surface runoff and interflow produced by forest was lowest because of high infiltration and interception. On average, about 47.7 in. of precipitation fell on the basin during 1973–2008 of which about 35, 47.6 and 46.9 percent per unit area discharged to streams from HRUs overlying soil type A, soil type D and wetlands, respectively. The remainder was mostly lost to ET, per unit area, from interception, upper zone and lower-zone storage transpiration. Loss by LZET

ranged from 27 to 26 percent for soil type A and soil type D HRUs, respectively. LZETP is a bit higher in soil type A and this is because ET losses in the upper and lower zone are assumed to occur at a rate proportional to the relative moisture content of each of the systems. Hence soil type A has more moisture content than soil type D, because fine soils with narrow pore spacing hold water more tightly than soils with wide pore spacing.

ET loss per unit area from interception and upper-zone storages (CEPE and UZET, respectively) accounts for about 16.5% to 10.9 % of the annual moisture supply to the basin. ET loss per unit area from active groundwater (AGWET) accounts for 1.9 percent to 2.5 percent of the annual moisture supply to the basin. Lower-zone evapotranspiration is highest in forested PERLND types and lowest in commercial/industrial PERLND types.

Forested HRUs compose the major portion of the basin water budget (Figure 15), expressed in inches over the basin, because forested HRUs represent about 43 percent of the total basin area. Forested HRUs contributed about 18.2 in. (46 percent), mostly from active groundwater, of the 39.8 in. of total mean annual discharge to streams. Discharge to streams from forested areas came predominantly from HRUs overlying soil type D (3.2 in.). In 2005, highest stream flow was during March and April because of low ET, and lowest stream flow was during July, August and September because of high ET.

4.1.6 Water quality Calibration Results for Sediments and Nutrients

HSPF Model is calibrated for sediments and nutrients (total nitrogen and phosphorus). Observed data was obtained from MassDEP (Division of Water Pollution Control Massachusetts Water Resources Commission). 808 observations are used for

sediments calibration. Out of 808 observations, 509 samples are collected from Assabet River, 158 samples from Sudbury River and 141 samples were collected from Concord River. Figure 16 shows the location of samples for observed data. Table 12 shows a list of adjusted parameters for calibration of Sediments in HSPF model. The mean and variance of observed daily TSS data with 808 observations is 5.92 and 4.08 respectively and mean and variance of simulated daily TSS data for 808 values is 5.34 and 3.66 respectively. The variance in simulated data is little less than that of observed data .The Pearson correlation for t-Test (paired sample for observed and simulated means is 0.84. Paired t-test is a test on the difference between the two values (observed and simulated). Thus, the two-tail p-value for this t-test is p=0.006and t=2.92. Figure 17 (A, B) and Figure 18 shows scatter plot, bar graphs between observed, simulated mean daily sediments and coefficient of variance for observed, simulated mean daily TSS respectively. Regression coefficient R^2 is 0.701 for sediments.

919 observations are used for total nitrogen calibration, out of which 617 samples are collected from Assabet River, 205 samples are from Sudbury River and 97 samples are from Concord River (Figure 16). The mean and variance of observed daily total nitrogen data with 919 observations is 1.81 and 1.72 respectively and mean and variance of simulated daily total nitrogen data for 808 values is 2.26 and 3.14 respectively. Overall model is simulating a little bit higher nitrogen and that could be because of presence of some dams and lakes in the sampling locations. In contrast to sediments, The variance in observed data is less than that of simulated data for total nitrogen .The Pearson correlation for t-Test is 0.87.The two-tail p-value for this t-test is p=0.53and t=0.64. Figure 19 (A,B) and Figure 20 shows scatter plot and bar graphs between observed,

simulated mean daily total nitrogen and coefficient of variance for observed, simulated mean daily total nitrogen respectively. Regression coefficient R^2 is 0.75 for total nitrogen. The t-test shows that the observed and mean values are not significantly different.

For total phosphorus calibration 922 observations are used, out of which 622 samples are collected from Assabet River, 114 samples are from Sudbury River and 186 samples are from Concord River (Figure 16). The mean and variance of observed daily total phosphorus data with 922 observations is 0.17 and 0.024 respectively and mean and variance of simulated daily total phosphorus data for 922 values is 0.076 and 0.026 respectively. In contrast to nitrogen, overall model is under simulating phosphorus that could be because of presence of some dams and lakes in the sampling locations .The Pearson correlation for t-Test is 0.8.The two-tail p-value for this t-test is p=0.000049and t=4.8. Figure 21 (A,B) and Figure 22 shows scatter plot and bar graphs between observed, simulated mean daily total phosphorus and coefficient of variance for observed, simulated mean daily total phosphorus respectively. Regression coefficient R^2 is 0.65 for total phosphorus. The t-test shows that the observed and mean values are not significantly different.

4.2 Assessment of Land Use Land Cover Change in SuAsCo Watershed by Land Transformation Model (LTM)

The LTM is useful for simulating land use/cover changes across large regions. It can be used to simulate land change in areas that contain several million to even a few hundred million cells. It is thus a useful tool to couple to regional climate, hydrologic and

carbon sequestration models. Land-use change from 2000 to the LTM-projected 2035, 2065 and 2100 conditions is illustrated in Figures 23 for the simplified land-use categories used to develop the model HRUs. In general, the majority of land-use change was from forest to low-density residential, development. According to LTM 2100 projection, In SuAsCo watershed agriculture/pasture is decreased by 30 percent (Table 13). Commercial/industrial area and high density area is increased by 72 percent and 62 percent respectively. Medium density and low density residential area is increased by 83 percent and 93 percent respectively. Forested area is decreased by half (50 percent decrease). Wetlands are decreased by 45 percent, while open water remains unchanged.

Stream flow decreased by 9% for month of April by 2100 and increased by 18% for month of September by 2100. The large decrease in stream flow that occurs in April and significant increase in stream flow between July to October. For March, May, June precipitation changes nearly canceled out ET changes and streamflow showed insignificant change during the same time period compared to other months. Hence in hydrological simulation model, both increases and decreases in streamflow occur in both relative and absolute terms at different seasons or time periods, providing clues about causal mechanisms, and geomorphic and ecological consequences, of vegetation change. The largest relative changes in streamflow occurred in summer months and early fall after removal of forest. 75 percent increase in effective impervious area and 50 percent decrease in forest area from 2005 to 2100 causes 2.7 percent increase in total runoff and 69.2 percent increase in surface runoff. 6.5 percent reduction in evapotranspiration leads to 3 percent decline in interflow (Table 14). Base flow is decreased by 11.2 % from 2005 to 2100 because of increase in impervious area. Because

in any series of storms, the larger the percentage of direct runoff, the smaller the amount of water available for soil moisture replenishment and for ground storage. Decrease in ground water recharge and decrease in baseflow is observed because of increase in total runoff as a result of imperviousness, for a given series of storms. Thus, increased imperviousness has the effect of increasing flood peaks during storm periods and decreasing baseflows flows between storms. In addition, water that runs off, particularly if it is channeled through storm sewers, never has a chance to recharge ground water that lead to reduced base flow. Figure 23 and Figure 24 represents changes and percent changes in water budget with future land cover projections. Water-budget outflow components (Figure 25) by hydrologic response unit (HRU) in SuAsCo watershed under 2005 land use and projected 2100 land-use conditions shows about 10 percent reduction in interception because of deforestation. Land use change impacted evaporation by lower zone (16.8 percent reduction) more significantly than evaporation by upper zone (2 percent reduction), because according to the water budget in SuAsCo evaporation by lower zone is more than double than evaporation from upper zone.

10 percent low flows are increased by 10.7 percent by 2100 because of decrease in evapotranspiration. There is a small decrease in storm volume (0.5 percent) but average storm peak volume is increased by 4.1 percent by 2100 because of less infiltration. Due to land cover change sparse vegetation cover which in case of high rainfall intensities may trigger siltation and disconnect macropores from the soil surface, resulting in surface sealing and a drastic decrease in hydraulic conductivity at the soil surface as well as a decline in macropore connectivity [*Niehoff et al.,* 2002]. The increase in siltation, crusting and compaction of surface soil because of land cover change can

lead to reduction in infiltration that caused the increase in storm peak volume. Streamflow winter volume is increased by 5.1 %. But the increase is summer volume (about10 percent) is more significant than winter volume. The increase is summer volume partly due to the fact that the summer potential evapotranspiration is a bit higher in forested and agricultural areas than in urban areas and, therefore, changing some of the forested land into urban land use leads to an increase in the runoff. There is more potential for infiltration in the summer than in the winter, especially, at the early phase of the storm event because storm events in the summer are generally preceded by a dry soil condition [*Hundecha and Bárdossy*, 2004]. The runoff would be higher because of less possibility for infiltration due to surface sealing triggered by land use change from forested/agricultural land to urban areas.

There is a substantial increase in summer storm volume about 90.6 percent and 22.6 percent reduction in winter storm volume. Reduction is winter storm volume may be because of reduction of floods caused by ice-jams or ice-jam breaks. The reduction of ice jams may be partly because of regional warming or in part from increase in salt content and water temperature caused by the inflow of waste water and cooling water. Based on these results human induced land use change reduced evapotranspiration, baseflow and interflow that lead to increase in overland flow. An increased loss of precipitation to runoff (rather than infiltration) leads to increased peak flow (storm flow) and decreased baseflow. It shows how baseflow and peak flow varies as a function of urbanization.

4.3 Assessment of Climate Change in SuASCo Watershed by RCP4.5 Scenario

IPCC produced clime scenarios as a plausible representations of future climate conditions (temperature, precipitation, and other aspects of climate such as extreme events) using a variety of approaches including analysis of observations, models, and other techniques such as extrapolation and expert judgment [*Stocker, et al.,* 2013]. The IPCC's Fifth Assessment Report (AR5) considers new evidence of climate change based on many independent scientific analyses from observations of the climate system, paleoclimate archives, theoretical studies of climate processes and simulations using climate models. It builds upon the Working Group I contribution to the IPCC's Fourth Assessment Report (AR4), and incorporates subsequent new findings of research. The degree of certainty in key findings in this assessment is based on the author teams' evaluations of underlying scientific understanding and is expressed as a qualitative level of confidence (from very low to very high) and, when possible, probabilistically with a quantified likelihood (from exceptionally unlikely to virtually certain). Confidence in the validity of a finding is based on the type, amount, quality, and consistency of evidence (e.g., data, mechanistic understanding, theory, models, and expert judgment) and the degree of agreement1. Probabilistic estimates of quantified measures of uncertainty in a finding are based on statistical analysis of observations or model results, or both, and expert judgment2. Where appropriate, findings are also formulated as statements of fact without using uncertainty qualifiers. Climate change projections in IPCC Working Group I require information about future emissions or concentrations of greenhouse gases, aerosols and other climate drivers. This information is often expressed as a scenario of human activities, which are not assessed in this report. Scenarios used in Working Group

I have focused on anthropogenic emissions and do not include changes in natural drivers such as solar or volcanic forcing or natural emissions, for example, of CH4 and N2O.

According to RCP4.5 climate scenario, the annual average temperature will increase by 1.1^{o}C, 2.1 ^{o}C and 2.7 ^{o}C by 2035, 2065 and 2100 respectively in Eastern North America and there will be 3%, 5% and 7% increase in annual precipitation by 2035, 2065 and 2100 respectively. Model is run for RCP4.5 climate scenario for 2035, 2065 and 2100. Figure 26 shows the changes in stream flow. Total runoff and surface runoff is increased by about 6 and 8 percent respectively because of 4.7 percent increase in evapotranspiration by 2100 (Figure 27). Figure 28 shows a comparison of water budget in SuAsCo watershed under 2005 and projected 2100 Climate Change (RCP 4.5) Scenario. Increased temperature reduced available water resources and increased ET. Stream flow decreased by 18% for month of April by 2100 and increased by 18% for month of February by 2100. The large decrease in stream flow that occurs in April is the result of increased ET and reduced precipitation and significant increase in stream flow between August to February are likely due to increased precipitation. For March, May, June precipitation changes nearly canceled out ET changes and streamflow showed insignificant change during the same time period compared to other months. It is important to note that increased temperature could increase spring and summer actual evapotranspiration, this could counterbalance the effect of a precipitation increase during summer and the change in discharge was the smallest in summer.

2.7 ^{o}C rise in temperature, would considerably reduce the snow storage reservoir during winter and thus largely contribute to a shift of flood events in the SuAsCo from spring and summer to winter.

Interflow is increased by 24.7 by 2100%. Base flow is increased by 1.4 % from 2005 to 2100. 10 percent high flows and 10 percent low flows are increased by 4.6 percent and 9.5 percent respectively by 2100. 7 percent increase in precipitation by 2100 increased storm volume and average storm peak volume by 1.9 and 8.1 percent respectively. Hence increase in precipitation and temperature has major effect on storm flows. Stream flow during summer and winters is increased by 11.3 and 17.1 percent respectively by 2100 (Table 15). Higher winter discharge is a result of intensified snow-melt and increased winter precipitation.

4.4 Assessment of Combined Change in Land Cover Climate in SuASCo Watershed

To assess the combined impact of land cover change and climate change, model is run with LTM projected land cover map for 2100 and climate change scenario (RCP 4.5) for 2100 (Figure 29). Total runoff is increased by 9.2 percent and surface runoff was increased by 81.4 percent (Figure 30). This increase in surface runoff is because of reduced baseflow (about 9% reduction).

While independent change in climate caused a little bit increase in base flow (about 1.42%) because of high precipitation that lead to recharge of subsurface storage, independent change in land cover reduced the baseflow by 11.2 %. But overall base flow is reduced by 9% because of combined influence of land cover and climate change. This is because at local scales, higher summer temperatures and, by extension, evaporation rates, could lead to increased convective precipitation, offsetting baseflow reductions from 11.2 % to 9%. Although baseflow response to changing land use typically are confounded by concurrent climate change, overall combined change in land use and land

cover reduced the baseflow, which indicates land cover change impact the baseflow more significantly than climate change.

Both land use change and climate change increase surface runoff and total runoff. But impact of land cover change on surface runoff is more significant than climate change. Because land cover change reduced the base flow and interflow hence more water is available for overland flow. However climate change increased baseflow and interflow hence more significantly increase the total stream flow or total runoff as compared to land cover. That is why land cover change has more influence on surface runoff and climate change has more significant impact on total runoff or stream flow. Combined change in land use and climate increased total runoff (9.2%) with significant increase in surface runoff (81.4 %). It should be pointed out that the summation of the surface runoff increase by both climate variability and land use change was significantly greater than the independent impact of land cover and climate change. Land use change reduces interflow (3%) in contrast to climate change that increases interflow significantly (24.7%) and overall interflow is increased by 21.6% under the combined influence of land cover and climate change.

Combined change in land cover and climate increased the low flows (20.4%) more significantly than high flows (5.5 %). These changes in high flows and low flows can be explained by rising temperatures. In addition, precipitation more often falls as rain instead of snow. Therefore, thaw happens earlier and less water is stored as snow pack leading to increase winter and summer flood peaks. Summer volume and winter volume is also increased by 22.2 % and 19.1 % respectively. Increase in winter discharge is because of increase of both rainfall and the melt water runoff contribution that will

increase peak flows. Increment in average peak volume is 12.8 % (Table 16). Figure 31 shows water-budget outflow components by Hydrologic Response Unit (HRU) simulated by the Hydrological Simulation Program–FORTRAN (HSPF) in SuAsCo watershed under 2005 and projected 2100 Land Use and Climate Change Scenario. Figure 1 shows comparison of independent change in land cover and climate with combined change in land cover and climate

CHAPTER 5

CONCLUSION

This research presents information about the fate and transport of runoff, sediments and nutrients in the SuAsCo watersheds. The modeling helps to estimate the impacts and compare levels of stress. All sites provide reliable estimates of water flows in watershed and quantify runoff, sediments and nutrient loads in the HSPF model, which will be valuable in providing a better understanding and in forecasting pollutant concentrations for future. Baseline simulations closely match with the observed information. LULC and climate changes have impacts on water quality and water quantity and the impact on watershed is aggravated by combined change in LULC and climate in future. Independent Change in climate increased ET (4.7 %) because of high temperature, but independent change in land cover reduced ET (6.5%) because of less available vegetation (Figure 32). Overall base flow is reduced by 9% because of combined influence of land cover and climate change. Combined change in land use and climate increased total runoff (9.2%) with significant increase in surface runoff (81.4 %) and interflow (21.6%). Land use change reduces interflow (3%) in contrast to climate change that increases interflow significantly (24.7%) and overall interflow is increased by 21.6% under the combined influence of land cover and climate change.

Independent increase in climate change and land use change increased low flows by 9.5 % and 10.7 % respectively and increase in low flows reached to 20.4% when model was run with combined projected land cover and climate data. 10% high flows are decreased (1.1%) by change in land use but increased (4.6 %) with change in climate and that increase become a little more significant (5.5 %) with combined change in land cover

and climate. Independent change in climate and land cover increased summer flows 10 % and 11.3 % respectively and summer stream flow volume increased further (22.2%) with combined change in land cover and climate change. Climate change increase the winter flows (17.1%) more significantly than increment (5.1%) caused by land cover change. Winter flows are increased by 19.1 % by combined change in land cover and climate. Average storm peak volume is increased by 8.1 % and 4.1 % by change in climate and land cover respectively. Combined change in land cover and climate further increased the average storm peak volume (12.8 percent).

This study provides useful information that could be used in developing watershed management plans for semi urban watershed areas. The watershed modeling is capable of assessing the spatial and temporal variability of runoff, sediments and nutrients fate in the river so that it also can be considered as an auxiliary assessment tool to provide necessary data reference for ecological risk and human health assessments after water pollution occurred. The results of this research have numerous management implications for the watershed system. A modular approach is an effective way to develop integrated watershed assessment tools. The outputs of the models provide comprehensive information of the contaminant distribution in a multimedia environment at watershed scale. The importance of watershed modeling is significant in identifying environmental management opportunities to mitigate water pollution and preserve aquatic and human health. This research facilitates in-depth analysis of inter-media transports and multimedia system behaviors under dynamic conditions while preserving the requirements of modest data input and rapid scenario analysis. Better comprehensive and sustainable watershed protection programs, including erosion and sediment control,

storm water management, and best management practices, could be devised by help of information in this research, to minimize the adverse impacts of flow and non-point source pollution in the face of these impending changes. Our understanding of the dynamics of the physical system in a watershed would improve by assessing not only the separate but also the combined impacts of climate and land use changes on water resources A possible range of future flow and water quality conditions are shown by various scenario results, which could be of values to the decision-makers in their development of adaptation and mitigation strategies in preparation for future climate and land use changes.

The efficacy of HSPF in modeling water quantity and quality under a watershed scale is demonstrated by this research. The application of LTM coupling with climate change scenario also proved to be effective in simulating future land use and climate changes, providing a more realistic land use and climate change pattern for the year 2100. This comprehensive approach seemed to be reliable and might provide a reasonable tool for predicting the long-term impacts of land use and climate changes on water resources, useful to environmental scientists, state and local agencies, watershed managers, and regional planners.

However, there are limitations to such modelling studies, since land-use, climate change and hydrological models are accompanied by a high degree of uncertainty. This uncertainty is due to insufficient data availability or quality and related space-time heterogeneity (data uncertainty), insufficient knowledge on the physics and the stochastic features of the processes involved, in particular during extreme precipitation periods (process uncertainty), and simplifications inherent in the model structure (model

uncertainty) [*Niehoff et al*., 2002]. Due to the large number of parameters and long computing times involved, a rigorous procedure for uncertainty analysis is not easily transferable to detailed process-oriented hydrological models like HSPF.

APPENDIX A

TABLES

Table 1: Textural characteristic and associated Hydrologic Group of Soils in SuAsCo Watershed

Soil Texture	Hydrological Group	Percentage area (%)
Sandy Loam	C	0.02
Pit Quarry	A	0.03
Sandy Loam	B	0.05
Silt Loam	D	0.08
Dumps	A	0.09
Very Fine Sandy Loam	C	0.25
Sand & Gravel	A	0.49
Loamy Coarse Sand	A	0.51
Loamy	A	0.58
Loam	B	0.76
Loamy Sand	B	0.86
Silt Loam	B	0.87
Sandy	A	0.94
Loamy Sand	C	0.96
Loamy Fine Sand	B	1.23
Fine Sandy Loam	D	1.24
Silt Loam	C	1.32

Urban-outcrop Land Complex	C	1.66
Mucky Fine Sandy Loam	D	1.72
Sandy Loam	A	1.89
Mucky Silt Loam	D	1.93
Urban-outcrop Land Complex	B	2.38
Very Fine Sandy Loam	B	3.29
Water	A	3.61
Fine Sandy Loam	B	6.63
Fine Sandy Loam	A	6.65
Urban-outcrop Land Complex	A	9.34
Muck	D	9.66
Loamy Sand	A	10.45
Urban-outcrop Land Complex	D	10.96
Fine Sandy Loam	C	19.56

Table 2**:** Land use Land Cover in SuAsCo Watershed

Land use	Area (Acres)	Percentage Area (%)
Agriculture/Pasture	11360	5
Commercial/Industrial	11303	5
High Density Residential	10606	4
Medium Density Residential	22188	9
Low Density Residential	31035	12
Public/Transitional	13347	5
Open Water	8601	3
Wetlands	32948	13
Forest	108394	43
Effective Impervious area	18983	7.6

Table 3: Description of Data Set Numbers (DSNs) in the Watershed Data Management (WDM) system for the SuAsCo Watershed, Mass.

DSN	Purpose
1-12	Observed Stream Flow
101-501	Simulated Stream Flow
1001-1009	Simulated Flow Components for HSPEXP
1010-1231	Simulated Sediment Components
1232-1240	Simulated Stream Flow
1241-1291	Simulated Sediment Components
1292-1297	Simulated Nutrients
1300-1413	Simulated Nutrients
1723-1766	Water Withdrawals
2411-2420	Point Sources Loads
3111-3120	Point Sources Loads
3411-3420	Point Sources Loads
4111-4120	Point Sources Loads
4211-4220	Point Sources Loads
4711-4720	Point Sources Loads
5511-5520	Point Sources Loads
5611-5620	Point Sources Loads
6011-6020	Point Sources Loads
9111-9120	Point Sources Loads
9911-9220	Point Sources Loads

Table 4: Annual Average Withdrawals in SuAsCo Watershed, 1973-2008

River Name	Water System Name	Reach Name in Model	Withdrawals (MG/day)
Concord River	River Meadow Brook Canal Street Well # 1	1	0.19
Assabet River	Marshall well and Kennedy well # 1-4	11	0.41
Assabet River	Fort Pond Brook and Nashoba Brook	15	0.01
Assabet River	Nagog Pond	16	0.42
Assabet River	Whitcomb Well, Clapp Well, Rock Well and Fort Pond Brook Well # 2	19	0.22
Assabet River	Elizabeth Brook Well # 1, Dunster House Well, Eliot House Well and Leverett House Well	21	0.04
Assabet River	Fort Pond Brook Rock Well # 2 and 5	24	0.07
Sudbury River	Jennie Dugan Well and Deaconess Well	25	1.87
Assabet River	Second Division Well	27	0.56
Sudbury River	White Pond Well	29	0.40
Assabet River	Stow Acres Country Club	31	0.16
Assabet River	Old Marlborough Road Wells # 1-3 and Great Road Well # 4	34	0.60
Assabet River	White Pond	35	0.30
Sudbury River	Cranberry Bog Well	39	0.55
Assabet River	Kane Well and Chestnit Street Well # 1- 3	45	1.85
Sudbury River	Lowe Sudbury River GP Wells # 2-7 and 9	51	1.86
Assabet River	Howard Street Wells # 1-3	54	0.14
Assabet River	Crawford Street Well	55	0.33
Assabet River	Lyman Street Well and Chauncy Lake Well # 1 and 2	61	0.22
Assabet River	South Street Well and Smith pond	64	0.01

Sudbury River	Hopkinton Road Well, Morse Street Well and Cedar Swamp	72	0.73
Assabet River	Sandra Pond	75	0.88
Sudbury River	Whithall Brook Well # 4	76	0.11
Sudbury River	Howe Street GP Well # 4-6, Upper Sudbury River Wells # 1 and 2, Whitehall Brook Well # 1 and Weston Nurseries	77	2.12
Sudbury River	Kiddle-Fenwal, Inc	79	0.02
Assabet River	Millham Reservior	83	1.52
Assabet River	Andrews 1, 2 Well, Wilkinson Well	84	0.66
Assabet River	Nashoba Brook Well # 1	85	0.03
Assabet River	Otis Street Well	91	0.30
Concord River	Turnpike Road GP Well # 1 and Mill Road GP Wells # 1-3	101	0.90
Assabet River	Assabet main Stem Wells # 1-3, Elizabeth Brook Well # 1-2 and Fort Pond Brook Rock Well # 1-2	103	0.08
Assabet River	Brigham Street Well and Junpier Hill Golf Course	107	0.49
Sudbury River	Upper Sudbury River Wells # 2-3 and Whitehall Brook Well # 2-5	108	0.63
Sudbury River	Hop Brook GP Well # 3, 8 and 10	110	0.61
Assabet River	Conant Well	111	0.14
Assabet River	Conant 2 Wells # 1-5	112	0.06
Sudbury River	Springvale Well # 1-4 and Lake Cochituate	114	2.46
Assabet River	Bigelow Nurseries at Assabet Head Waters	115	0.10
Assabet River	Nashoba Brook Well # 1	119	0.01
Assabet River	Lawsbrook, Christofferson Well and Scribner Well	122	0.29
Assabet River	Riverneck Road GP Wells # 1-2	123	0.55

Assabet River	Rimkus Well and Gates Pond Reservior	130	0.06
Assabet River	Assabet main Stem-Digital Equipment / Intel	137	0.01
Sudbury River	Happy Hollow Well # 1-2 and Meadowview Well # 1	140	0.93
Assabet River	Assabet Well # 1-2, Assabet Sand & Gravel and Concrete Services at Assabet Main Stem	142	0.76
Sudbury River	Baldwin Pond Well # 1-3 and Campbell Road Well # 1	145	1.05
Sudbury River	Robinson Well, Concord Country Club, Verrill Farm and Nashawtuc Country Club	150	0.29
Concord River	Concord River	155	4.58

Table 5: Water withdrawals Location in SuAsCo Watershed

Community	System Type	System Name	Source Type	Reach Name
Assabet River Basin				
Assabet Headwaters				
Marlborough	MC	Millham Reservoir	SW	83
Northborough	MC	Brigham Street well	GW	107
Northborough	MC	Lyman Street Well	GW	61
Westborough	MC	Andrews 1 Well	GW	84
Westborough	MC	Andrews 2 Well	GW	84
Westborough	MC	Otis Street Well	GW	91
Westborough	MC	Wilkinson Well	GW	84
Westborough	MC	Chauncy Lake Well 1	GW	61
Westborough	MC	Chauncy Lake Well 2	GW	61
Assabet Main Stem				
Acton	MC	Assabet Well # 1	GW	142
Acton	MC	Assabet Well # 2	GW	142
Hudson	MC	Rimkus Well	GW	130
Berlin	MC	Gates Pond Reservoir	SW	130
Maynard	MC	Old Marlboro Road Wells # 1 and 2	GW	34
Maynard	MC	White Pond	SW	35
Maynard	MC	Old Marlborough Road Wells # 3	GW	34
Maynard	MC	Great Road Well # 4	GW	34
Shrewsbury	MC	South Street Well	GW	64
Stow	NMC	Wells # 1-3	GW	103
Concord	MC	Second Division Well	GW	27
Elizabeth Brook				
Boxborough	NMC	Well # 1	GW	21
Boxborough	NMC	Dunster House Well	GW	21
Boxborough	NMC	Eliot House Well	GW	21

Boxborough	NMC	Leverett House Well	GW	21
Stow	NMC	Well # 1	GW	103
Stow	NMC	Well # 1	GW	103
Stow	NMC	Well # 2	GW	103
Fort Meadow Brook				
Hudson	MC	Kane Well	GW	45
Hudson	MC	Chestnut Street Well # 1	GW	45
Hudson	MC	Chestnut Street Well # 2	GW	45
Hudson	MC	Chestnut Street Well # 3	GW	45
Fort Pond Brook				
Acton	MC	Whitcomb Well	GW	19
Acton	MC	Lawsbrook	GW	122
Acton	MC	Christofferson Well	GW	122
Acton	MC	Clapp Well	GW	19
Acton	MC	Scribner Well	GW	122
Boxborough	NMC	Rock Well	GW	19
Boxborough	NMC	Well # 1	GW	21
Boxborough	NMC	Well # 2	GW	19
Boxborough	MC	Well # 2	GW	19
Maynard	MC	Rock Well # 2	GW	24
Maynard	MC	Rock Well # 5	GW	24
Stow	MC	Well # 1-2	GW	103
Howard and Cold Harbor Brook				
Northborough	MC	Crawford Street Well	GW	55
Northborough	MC	Howard Street Wells # 1-3	GW	54
Nashoba Brook				
Acton	MC	Conant well	GW	111
Acton	MC	Marshall well	GW	11
Acton	MC	Kennedy well 1-4	GW	11
Acton	MC	Conant 2 wells # 1-5	GW	112
Acton	MC	Nagog Pond	SW	16
Acton	NMC	Well # 1	GW	119

Westford	NMC	Well # 1	GW	85
Sudbury River Basin				
Cedar Swamp				
Westborough	MC	Hopkinton Road Well	GW	72
Westborough	MC	Sandra Pond	SW	75
Westborough	MC	Morse Street Well	GW	72
Hop Brook				
Hudson	MC	Cranberry Bog Well	GW	39
Sudbury	MC	GP Well # 3	GW	110
Sudbury	MC	GP Wells # 8 and 10	GW	110
Indian Brook				
Ashland	MC	Howe Street GP Well # 4	GW	77
Ashland	MC	Howe Street GP Well # 5	GW	77
Ashland	MC	Howe Street GP Well # 6	GW	77
Lake Cochituate				
Natick	MC	Springvale Well # 1	GW	114
Natick	MC	Springvale Well # 3	GW	114
Natick	MC	Springvale Well # 4	GW	114
Natick	MC	Evergreen Well # 1	GW	114
Natick	MC	Evergreen Well # 2	GW	114
Lower Sudbury River				
Concord	MC	Jennie Dugan Well	GW	25
Concord	MC	Deaconess Well	GW	25
Concord	MC	White Pond Well	GW	29
Concord	MC	Robinson Well	GW	150
Lincoln	MC	Farrar Pond Well	GW	30
Sudbury	MC	GP Wells # 2 and 9	GW	51
Sudbury	MC	GP Well # 4	GW	51
Sudbury	MC	GP Well # 5	GW	51
Sudbury	MC	GP Well # 6	GW	51
Sudbury	MC	GP Well # 7	GW	51

Wayland	MC	Baldwin Pond Well # 1	GW	145
Wayland	MC	Campbell Road Well # 1	GW	145
Wayland	MC	Happy Hollow Well # 1	GW	140
Wayland	MC	Happy Hollow Well # 2	GW	140
Wayland	MC	Meadowview Well # 1	GW	140
Wayland	MC	Baldwin Pond Well # 3	GW	145
Wayland	MC	Baldwin Pond Well # 2	GW	145
Wayland	MC	Chamberlain Well # 1	GW	145
Upper Sudbury River				
Hopkinton	NMC	Wells # 1 and 2	GW	77
Hopkinton	NMC	Well # 3	GW	108
Hopkinton	NMC	Well # 2	GW	108
Whitehall Brook				
Hopkinton	MC	Well # 1	GW	77
Hopkinton	MC	Well # 2	GW	108
Hopkinton	MC	Well # 3	GW	108
Hopkinton	MC	Well # 4	GW	76
Hopkinton	MC	Well # 5	GW	108
Lower Concord River Basin				
Lower Concord Main Stem				
Billercia	MC	Concord river	SW	155
Concord	MC	Hugh Cargill Well	GW	152
River Meadow Brook				
Chelmsford	MC	Turnpike Road GP Well # 1	GW	101
Chelmsford	MC	Mill Road GP Wells # 1-3	GW	101
Chelmsford	MC	Riverneck Road GP Wells # 1-2	GW	123
Chelmsford	MC	Canal Street Well # 1	GW	1

Table 6: Location of Water Withdrawal Location for Commercial, Industrial and Agricultural use in SuAsCo

Subbasin	Use Type	User Name	Water Source	Reach Name
Fort Pond Brook	Agriculture	Idylwilde Farm	SW	15
Nashabo Brook	Industrial	W. R. Grace	GW	15
Assabet Main Stem	Golf	Stow Acres Country Club	SW	31
Elizabeth Brook	Golf	Stow Acres Country Club	SW	31
Assabet Head Water	Agriculture	Berberian Farm/Smith pond	SW	64
Cedar Swamp	Industrial	Tyrolit North American/ Bay State Sterling	GW	72
Cold Spring Brook	Agriculture	Weston Nurseries	SW	77
Cold Spring Brook	Agriculture	Weston Nurseries	GW	77
Indian Brook	Agriculture	Weston Nurseries	SW	77
Cold Spring Brook	Industrial	Kiddle-Fenwal, Inc	GW	79
Reservior 1-3	Industrial	Kiddle-Fenwal Inc.	GW	79
Assabet Head Water	Golf	Junpier Hill Golf Course	SW	107
Lake Cochituate	Industrial	U.S. Army Soldier System Center	GW	114
Assabet Head Water	Agriculture	Bigelow Nurseries	GW	115
Assabet Main Stem	Industrial	Digital Equipment / Intel	GW	137
Elizabeth Brook	Industrial	Digital Equipment / Intel	SW	137
Danforth Brook	Agriculture	Great Oak Farm	GW	139
Assabet Main Stem	Industrial	Assabet Sand & Gravel	SW	142
Assabet Main Stem	Commercial	Concrete Services	SW	142
Lower Sudbury River	Golf	Concord Country Club	GW	150
Lower Sudbury River	Agriculture	Verrill Farm	SW	150
Lower Sudbury River	Golf	Nashawtuc Country Club	SW	150

Table 7: Annual Average Discharges (Mgal/day) from WWTPs in SuAsCo 1973-2008

NPDES	WWTP Facility	Ownership	Receiving Water	Reach Name	Annual Average Discharge (Mgal/day)
MA010049	Marlborough Easterly WWTP	Public	Sudbury River	47	3.28
MA010041	Westborough WWTP	Public	Assabet River	91	3.4
MA010066	Concord WWTP	Public	Concord River	106	1.14
MA0100412	Shrewsbury WWTP	Public	Assabet River	107	1.88
MA000151	Raytheon Sudbury Factory	Private	Sudbury River	116	0.008
MA010048	Marlborough Westerly WWTP	Public	Assabet River	124	1.61
MA0001414	Raytheon Missile System WWTP	Private	Concord River	131	0.19
MA010178	Hudson WWTP	Public	Assabet River	134	2.06
MA002214	Digital Equipment Corporation Company WWTP	Private	Assabet River	141	0.1
MA010100	Maynard WWTP	Public	Assabet River	142	1.41
MA003428	Raytheon Co Wayland	Private	Sudbury River	144	0.03
MA010224	MA Correction Institution (MCI) Concord WWTP	Public	Assabet River	147	0.19
MA003479	Billercia House of Correction WWTP	Private	Concord River	155	0.7
MA010171	Billercia WWTP	Public	Concord River	156	2.51

Table 8: Effective impervious area by developed land-use type for the Hydrological Simulation Program–FORTRAN (HSPF) model of the SuAsCo watershed, Massachusetts

Landuse	Total Impervious Area (IA) acres	Total Area	Percentage of IA	Effective Impervious area (EIA) acres	Percentage of EIA
Commercial/Industrial	7994	11303	70.7	6723	59.5
High Density Residential Area	4192	10606	39.5	3498	33.0
Medium Density Residential Area	7217	22188	32.5	4116	18.6
Public/Transitional	3994	13347	29.9	2185	16.4
Low Density Residential Area	6785	31035	21.9	2352	7.6
Total	30182	88478		18874	

Table 9: Manning's "n" Values and REACHES description for HSPF model

Reach name	Reach number	Channel "n"	Overbank "n"
Branch of River Meadow Brook near Putnam Brook	1	0.045	0.06
Marginal Brook at confluence with Concord River	2	0.04	0.065
River Meadow Brook at Confluence of Farley Brook	3	0.04	0.065
Meadow River Branch at Curve street	4	0.0325	0.1
Farley Brook about 775 feet downstream of Smokerise Drive	5	0.05	0.0625
Branch of Nashoba Brook at upstream of confluence of Butter Brook	6	0.03	0.08
Branch of Nashoba Brook at upstream of confluence of Butter Brook	7	0.03	0.08
Pages Brook at Maple Street	8	0.0315	0.1
Branch of Butter Brook at Confluence with Nashoba Brook	9	0.04	0.0675
Branch of Nashoba Brook at upstream of confluence of Butter Brook	10	0.03	0.08
Butter Brook at Griffin Road	11	0.04	0.0675
Pages Brook at confluence with Concord River	12	0.0315	0.1
Tributary to Cold Spring Brook	13	0.04	0.0675
Spencer Brook about 2000 feet downstream of Lindsay Pond Road	14	0.041	0.061
Fort Pond Brook upstream of confluence of Inch Brook	15	0.0525	0.095
Nagog Brook at confluence with Nashoba Brook	16	0.045	0.07
Conant Brook at confluence with Nashoba Brook	17	0.035	0.06
Sawmill Brook 2 at Monument Street	18	0.035	0.08
Inch Brook at confluence with Fort Pond Brook	19	0.035	0.055
Grassy Pond Brook at confluence with Fort Pond Brook	20	0.0325	0.05
Elizabeth Brook 1 at Delaney Road	21	0.0375	0.085

Spring Brook upstream of Alcott Street	22	0.0345	0.095
Heath Hen Meadow Brook confluence of Fort Pond Brook	23	0.05	0.0625
Branch of Fort Pond Brook at Erikson Dam	24	0.0525	0.095
Tributary of Sudbury River upstream of Lowell Road	25	0.061	0.066
Beaver Brook 4 West Whitcomb Road	26	0.0275	0.09
Branch of Tributary 2 to Assabet River at Baker Avenue	27	0.0275	0.05
Beaver Brook 2 about 1200 feet downstream of High Street	28	0.06	0.0675
Cold Brook at confluence of Pantry Brook	29	0.033	0.075
Farrar Pond at Sudbury River	30	0.045	0.05
Branch of Assabet River approximately 1380 feet downstream of Hudson Road/ Walcott-Randall Road	31	0.0375	0.085
Danforth Brook at confluence of Assabet River	32	0.025	0.08
Branch of Pantry Brook at confluence with Sudbury River	33	0.028	0.075
Taylor Brook at confluence with Assabet River	34	0.0425	0.0675
Boon Pond and branch at Barton Road	35	0.0375	0.085
Hog brook at confluence with Assabet River	36	0.045	0.08
Branch of Beaver Brook 1	37	0.0275	0.09
Run Brook at the confluence of Hop Brook	38	0.0305	0.075
Branch of Hop Brook at Marlborough/Sudbury Corporate Limits	39	0.025	0.0625
Beaver Brook 1 approximately 15 feet downstream of Linden Street	40	0.0275	0.09
Hop Brook at Sudbury/Framingham Corporate Limits	41	0.025	0.0625
Hop Brook at Marlborough/Sudbury Corporate Limits	42	0.025	0.0625
Mill Brook 1 at Lexington and Wayland Corporate Limits	43	0.035	0.0625
Pine Brook at confluence of Mill Brook 1	44	0.035	0.0625
Fort Meadow Brook at Chestnut Street	45	0.0525	0.095
Branch of Beaver Brook 1 approximately 15 feet downstream of Linden Street	46	0.0275	0.09

Hop Brook at Dutton Road	47	0.025	0.0625
Dudley Brook at confluence with Hop Brook	48	0.0305	0.0725
Tributary of Assabet River at Robin Hill Street	49	0.0425	0.0925
Peppermint Brook at Hildreth Street	50	0.035	0.07
Landham-Allowance Brook at the Sudbury/Framingham Corporate Limits	51	0.0255	0.06
Sudbury Reservoir about two mile upstream of Stony Brook Reservoir dam	52	0.061	0.066
Assabet Branch as confluence of Assabet River near Williams Lake	53	0.0375	0.085
Assabet Branch at confluence of Assabet River upstream of Boundary Street near Aluminum City Dam	54	0.0375	0.085
Assabet Branch near Northborough Reservoir	55	0.0375	0.085
Baiting Brook at Constance M. Fiske Dam	56	0.0375	0.0825
Snake Brook at confluence of Lake Cochituate	57	0.035	0.0625
Angelica Brook at confluence with Reservoir No. 3	58	0.0325	0.055
Stony Brook at dam upstream of Deerfoot Road	59	0.0415	0.061
Stony Brook at Sudbury Reservoir	60	0.0415	0.061
Tributary near Chauncy Lake	61	0.0375	0.085
Tributory at confluence of Lake Cochituate	62	0.035	0.0625
Tributary upstream of Smith Pond	63	0.035	0.0625
Tributary at confluence of Smith Pond	64	0.035	0.0625
Jenny Dugan Brook at the confluence with Sudbury River	65	0.0415	0.07
Rutters Brook at Conrail in Westborough	66	0.03	0.0625
Course Brook about 1400 feet downstream of Pond Street	67	0.04	0.056
Munroe Brook at Bryant Road	68	0.065	0.08
Waushakum Pond Brook	69	0.04	0.0675
Tributary at confluence of Waushakum Brook	70	0.04	0.0675

Tributory at confluence of Assabet Reservoir is Westborough	71	0.0375	0.085
Denny Brook	72	0.03	0.0625
Upper Assabet River at Assabet Reservoir in Westborough	73	0.03	0.0625
Tributary to Upper Assabet River	74	0.03	0.0625
Tributary at Westborough Reservoir (Sandra Pond Dam)	75	0.0555	0.065
Tributary at confluence with Whitehall Brook	76	0.0425	0.075
Indian Brook at Hopkinton Reservoir	77	0.0425	0.075
Tributary at confluence with Whitehall Brook	78	0.0425	0.075
Tributary at Ashland Reservoir	79	0.0555	0.065
Branch of Nashoba Brook at upstream of confluence of Butter Brook	80	0.03	0.08
Jackstraw Brook at Hopkinton Road in Westborough	81	0.03	0.0625
Whitehall Brook at confluence with Sudbury River	82	0.0425	0.075
Tributary at Milham Reservoir	83	0.0375	0.085
Tributary at Assabet river Reservoir	84	0.03	0.0625
Nashoba Brook upstream of confluence of Butter Brook	85	0.03	0.08
Course Brook about 190 feet upstream of Merchant Road	86	0.04	0.056
North Brook 10.0 feet upstream of Linden street in Berlin	87	0.034	0.085
Mill Brook 1 at confluence with Pine Brook	88	0.035	0.0625
Branch of Pages Brook at confluence of Concord River	89	0.0315	0.1
Branch of Nashoba Brook upstream of confluence of Butter Brook	90	0.03	0.08
Tributary at Hocomonco Pond	91	0.0375	0.085
Tributary at confluence of Whitehall Brook	92	0.0425	0.075
Tributary at confluence of Cedar Swamp Pond in Westborough	93	0.0555	0.065
Pantry Brook at confluence with Sudbury River	94	0.028	0.075
Tributary at confluence of Hop Brook at Dutton Road	95	0.025	0.0625
Tributary at confluence of Hop Brook near Stearns Mill Pond	96	0.025	0.0625
Tributary near Delaney Complex E Bolton Dam	97	0.0375	0.085

Sudbury Reservoir about 160 feet downstream of Marlborough Road	98	0.061	0.066
Nashoba Brook near State Route 27 at Nashoba Brook Pond	99	0.03	0.08
Tributary at confluence of Assabet River downstream of Hocomonco Pond	100	0.0375	0.085
Russel Millpond Brook	101	0.041	0.066
Tributary at confluence of Fort Pond Brook near Elm Street	102	0.0525	0.095
Elizabeth Brook 1 at Gleasondale Road	103	0.0375	0.085
North Brook at Crosby street in Berlin near Wheeler Pond Dam	104	0.034	0.085
Sudbury River about 460 feet downstream of Cordaville Road	105	0.061	0.066
Tributary at confluence of Heath Hen Meadow Brook	106	0.041	0.0775
Tributary at confluence of Lower Assabet River	107	0.0375	0.0725
Sudbury River approximately 190 feet downstream of Cordaville Street	108	0.0555	0.065
Tributary near Fisk Pond	109	0.0555	0.065
Hop Brook above confluence of Dudley Brook	110	0.0305	0.0725
Elizabeth Brook 1 at Great Road	111	0.0375	0.085
Nashoba Brook at confluence of Fort Pond Brook	112	0.03	0.08
Fort Pond Brook at Erikson Dam	113	0.041	0.0775
Cochituate Brook	114	0.0325	0.055
Tributary near Wallace Pond	115	0.0375	0.0725
Tributary at conflunce of Landham-Allowance Brook	116	0.0255	0.06
Sudbury River downstream of Cordaville Road	117	0.061	0.066
Assabet River about 2500 feet upstream of Boundary Street	118	0.0425	0.0925
Fort Pond Brook at Laws Brook Road	119	0.041	0.0775
Landham-Allowance Brook at Landham Road	120	0.0255	0.06
Sudbury River about 1050 feet downstream of Howe Street	121	0.061	0.066
Tributary downstream of Fort Pond Brook at Laws Brook Road	122	0.041	0.0775
River Meadow Brook at Chelmsford/Lowell Corporate Limits	123	0.045	0.06

Assabet River about 900 feet downstream of Boundary Street	124	0.0425	0.0925
Sudbury River about 500 feet upstream Danforth Street	125	0.061	0.066
Tributary at Warners Pond Brook	126	0.041	0.0775
Tributary at Framingham Reservoir# 3	127	0.061	0.066
Tributary at Tyler Dam	128	0.0425	0.0925
Sudbury River at Myrtle Street	129	0.061	0.066
Gates Pond Brook at interstate Route 495	130	0.0425	0.0925
River Meadow Brook at Lowell	131	0.045	0.06
Sudbury River at Framingham Reservoir # 2	132	0.061	0.066
Tributary downstream of Gates Pond Brook	133	0.0425	0.0925
Assabet River at the Hudson/Stow corporate limits	134	0.0425	0.0925
Sudbury River at Framingham Reservoir # 1	135	0.061	0.066
Dunsdell Brook at Central Street Dam	136	0.061	0.066
Assabet River about 1 mile downstream of Cox Street	137	0.0425	0.0925
Assabet River at confluence of Fort Meadow Brook	138	0.0425	0.0925
Assabet River at confluence of Boon Pond	139	0.0425	0.0925
Sudbury River about 1300 feet upstream of Stonebridge Road	140	0.061	0.066
Assabet River about 1300 feet upstream of Great Road	141	0.0425	0.0925
Assabet River about 190 feet downstream of Acton Street	142	0.0425	0.0925
Sudbury River about 1.9 mile downstream of Stonebridge Road	143	0.061	0.066
Sudbury River at confluence with Wash Brook	144	0.061	0.066
Sudbury River about 0.5 mile downstream of Lincoln Road	145	0.061	0.066
Assabet River about 240 feet downstream of Main Street	146	0.0425	0.0925
Assabet River about 2,000 feet downstream of Concord Turnpike	147	0.0425	0.0925
Assabet River at the confluence with Spencer Brook 1	148	0.0425	0.0925
Sudbury River at the confluence with Pantry Brook	149	0.061	0.066
Sudbury River about 0.5 mile upstream of Sudbury Road	150	0.061	0.066

Sudbury River about 1400 feet downstream of Massachusetts 2A/ Concord Turnpike	151	0.061	0.066
Cold spring brook about 1800 feet downstream of Monument Street	152	0.0425	0.075
Cold Spring Brook about 1.2 miles upstream of Bedford Road	153	0.0425	0.075
Cold Spring Brook about 1 mile downstream of Bedford Road	154	0.0425	0.075
Cold Spring Brook 1400 feet downstream of Nashua Road	155	0.0425	0.075
Concord River at Talbot Mill Dam	156	0.041	0.066
Concord River at Roger Street in Lowell	157	0.041	0.066

Table 10: Model-fit statistics calculated from observed flows and Hydrologic Simulation Program–FORTRAN (HSPF) simulated flows at four streamgages in the SuAsCo River Basins, Massachusetts, 1973 to 2008.

Stream Gage	R^2 (Daily)	NSE (Daily)	R^2 (Monthly)	NSE (Monthly)	R^2 (Yearly)	NSE (Yearly)
Concord River below R Meadow Brook at Lowell	0.79	0.78	0.84	0.83	0.88	0.71
Sudbury River at Saxonville	0.75	0.73	0.82	0.79	0.85	0.54
Assabet River at Maynard	0.8	0.78	0.84	0.8	0.78	0.65
Assabet River at Nashoba Brook near Acton	0.69	0.67	0.76	0.75	0.62	0.61

Table 11: List of adjusted parameters for calibration of hydrology in HSPF model

Process Parameter	Description	Calibrated Value
LZSN	Lower Zone Nominal Soil Moisture Storage (inches)	2-6.4
INFILT	Index to Infiltration Capacity (in/hr)	0.19-0.5
KVARY	Variable groundwater recession ($inches^{-1}$)	0.9-3.3
AGWRC	Base groundwater recession (unitless)	0.945-0.993
INFEXP	Exponent in infiltration equation (unitless)	2
INFILD	Ratio of max/mean infiltration capacities (unitless)	2
DEEPFR	Fraction of GW inflow to deep recharge (unitless)	0.25-0.481
BASETP	Fraction of remaining ET from baseflow (unitless)	0-0.2
AGWETP	Fraction of remaining ET from active GW (unitless)	0.13-0.38
CEPSC	Interception storage capacity (inches)	0.01-0.2
UZSN	Upper zone nominal soil moisture storage (inches)	0.05-2
NSUR (PERLND)	Manning's n (roughness) for overland flow (unitless)	0.15-0.5
INTFW	Interflow inflow parameter (unitless)	1-10
IRC	Interflow recession parameter (unitless)	0.54-0.84
LZETP	Lower zone ET parameter (unitless)	0.12-0.9
NSUR (IMPLND)	Manning's n (roughness) for overland flow (unitless)	0.04-0.16
RETSC	Retention storage capacity (inches)	0.08-0.3

Table 12: List of adjusted parameters for calibration of Sediments in HSPF model

Process Parameter	Description	Calibrated Value
SMPF	Management Practice (P) factor from USLE (unitless)	0.1-0.9
KRER	Coefficient in the soil detachment equation (complex)	0.25-0.53
JRER	Exponent in the soil detachment equation (none)	1
AFFIX	Daily reduction in detached sediment (per day)	0.02-0.3
COVER	Fraction land surface protected from rainfall (none)	0.002-0.98
NVSI	Atmospheric additions to sediment storage (lb/ac-day)	0.3-1
KSER	Coefficient in the sediment washoff equation (complex)	0.3-2.5
JSER	Exponent in the sediment washoff equation (unitless)	1
KGER	Coefficient in soil matrix scour equation (complex)	0
JGER	Exponent in soil matrix scour equation (unitless)	2
KEIM	Coefficient in the solids washoff equation (complex)	0.21-0.3
JEIM	Exponent in the solid washoff equation (unitless)	1.8
ACCSDP	Solids accumulation rate on the land surface (lb/ac/day)	0.13-0.14
REMSDP	DP Fraction of solids removed per day (per day)	0.23-0.27

Table 13: Land use changes changes simulated in the Hydrologic Simulation Program FORTRAN (HSPF) model of SuAsCo Basin, Massachusetts.

Land use	Area (Acres)	Percent Area (%)	Percent Change	Area (Acres)	Percent Area (%)	Percent Change	Area (Acres)	Percent Area (%)	Percent Change
	2035			2065			2100		
Low Density	37850	15	22	46389	19	50	59756	24	93
Medium Density	29271	12	32	34265	14	55	40498	16	83
Public/Transitional	16559	7	24	19655	8	47	24236	10	82
Commercial/Industrial	14410	6	28	16571	7	47	19472	8	72
High Density	13432	5	27	15164	6	43	17185	7	62
Open Water	8078	3	0	8078	3	0	8078	3	0
Agriculture/Pasture	14848	6	31	11924	5	5	7899	3	-30
Wetlands	26933	11	-18	23683	9	-28	17985	7	-45
Forest	88263	35	-19	73913	30	-32	54529	22	-50
Effective Impervious Area	23966	9.6	26.3	27960	11.2	47	33202	13.3	75

Table 14: Summary of Predicted Annual Average Stream Flow Values and Percentage Change for SuAsCo, MA in Future Land Cover Projections for 2005, 2035 and 2100

Stream Flow	Units	2005	2035	Percent Change (%)	2065	Percent Change (%)	2100	Percent Change (%)
Total Runoff	Inches	23.0	23.2	1.0	23.4	1.8	23.6	2.7
Surface Runoff	Inches	3.2	4.0	24.6	4.7	43.7	5.5	69.2
Interflow	Inches	3.443	3.402	-1.2	3.4	-1.5	3.3	-3.0
Evapotranspiration	Inches	20.1	19.6	-2.5	19.2	-4.2	18.8	-6.5
10% High Flows	Inches	7.2	7.1	-0.6	7.1	-0.9	7.1	-1.1
25% High Flows	Inches	13.025	13.003	-0.2	13.0	-0.1	13.0	-0.1
50% High Flows	Inches	18.672	18.747	0.4	18.8	0.8	18.9	1.4
50% Low Flows	Inches	4.3	4.5	3.5	4.6	5.9	4.7	8.8
25% Low Flows	Inches	1.3	1.4	4.4	1.4	7.2	1.4	10.7
10% Low Flows	Inches	0.3	0.342	4.3	0.4	7.0	0.4	10.7
Storm Volume	Inches	6.765	6.755	-0.1	6.7	-0.3	6.7	-0.5
Average Storm Peak Volume	cfs	2045	2070	1.2	2094	2.4	2130	4.1
Baseflow Recession Rate	Inches	0.965	0.962	-0.3	1.0	-0.4	1.0	-0.6
Summer Volume	Inches	3.2	3.4	3.7	3.5	6.4	3.6	10.0
Winter Volume	Inches	6.8	6.9	1.5	7.0	3.1	7.1	5.1
Summer Storms	Inches	0.512	0.531	3.7	0.5	6.4	1.0	90.6
Winter Storms	Inches	1.785	1.787	0.1	1.8	0.4	1.4	-22.6

Table 15: Summary of Predicted Annual Average Stream Flow Values and Percentage Change for SuAsCo, MA in Future Climate Change Projections (RCP4.5) for 2005, 2035 and 2100

Stream Flow	Units	2005	2035	Percent Change (%)	2065	Percent Change (%)	2100	Percent Change (%)
Total Runoff	Inches	23.0	23.6	2.7	23.9	3.9	24.4	6.0
Surface Runoff	Inches	3.2	3.4	3.2	3.4	5.5	3.5	7.9
Interflow	Inches	3.4	3.8	9.3	4.0	16.8	4.3	24.7
Evapotranspiration	Inches	20.1	20.4	1.6	20.8	3.5	21.0	4.7
10% High Flows	Inches	7.2	7.4	2.5	7.4	2.5	7.5	4.6
25% High Flows	Inches	13.0	13.4	2.5	13.55	3.6	13.8	5.8
50% High Flows	Inches	18.7	19.1	2.5	19.4	3.7	19.8	5.8
50% Low Flows	Inches	4.3	4.5	3.1	4.5	4.5	4.6	6.8
25% Low Flows	Inches	1.3	1.3	3.7	1.4	6.0	1.4	8.7
10% Low Flows	Inches	0.3	0.3	3.7	0.3	6.4	0.4	9.5
Storm Volume	Inches	6.8	6.9	1.8	6.8	1.0	6.9	1.9
Average Storm Peak Volume	cfs	2045	2140.8	4.7	2167.6	6.0	2211.1	8.1
Baseflow Recession Rate	Inches	1.0	1.0	-0.2	1.0	-0.2	1.0	-0.4
Summer Volume	Inches	3.2	3.4	4.4	3.5	7.6	3.6	11.3
Winter Volume	Inches	6.8	7.3	7.2	7.7	13.1	8.0	17.1
Summer Storms	Inches	0.5	0.5	5.5	0.6	9.6	0.6	13.9
Winter Storms	Inches	1.8	1.8	3.5	1.9	5.1	1.9	7.1

Table 16: Summary of Predicted Annual Average Stream Flow Values and Percentage Change for SuAsCo, MA for Future Land cover change Climate change Projections (RCP4.5) in 2100

Stream Flow	Units	2005	2100	Percent Change (%)
Total Runoff	Inches	23.0	25.1	9.2
Surface Runoff	Inches	3.2	5.9	81.4
Interflow	Inches	3.4	4.2	21.6
Evapotranspiration	Inches	20.1	19.7	-2.1
10% High Flows	Inches	7.2	7.6	5.5
25% High Flows	Inches	13.0	14	7.2
50% High Flows	Inches	18.7	20.1	7.9
50% Low Flows	Inches	4.3	5.0	14.8
25% Low Flows	Inches	1.3	1.5	19.1
10% Low Flows	Inches	0.3	0.4	20.4
Storm Volume	Inches	6.8	6.9	2.3
Average Storm Peak Volume	cfs	2045	2306.9	12.8
Baseflow Recession Rate	Inches	0.97	1.0	-1.1
Summer Volume	Inches	3.2	4.0	22.2
Winter Volume	Inches	6.8	8.1	19.1
Summer Storms	Inches	0.5	0.6	24.2
Winter Storms	Inches	1.8	1.9	6.4

APPENDIX B

FIGURES

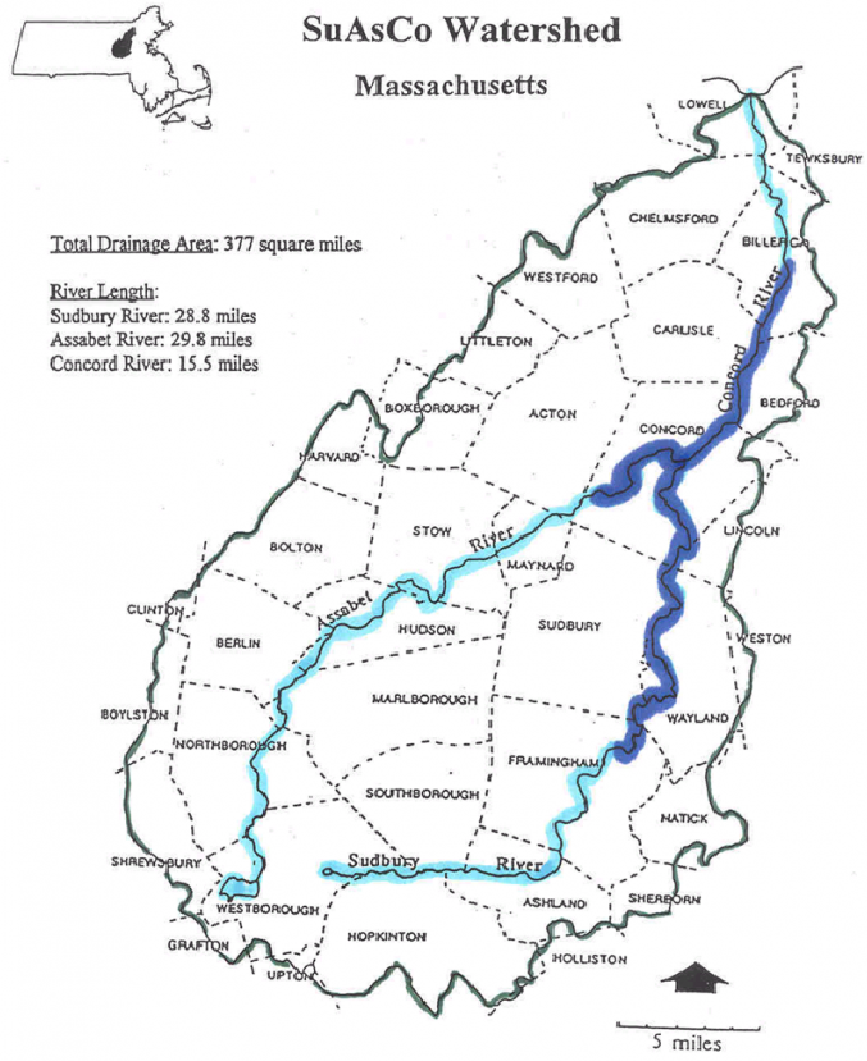

Figure 1: SuAsCo, MA watershed

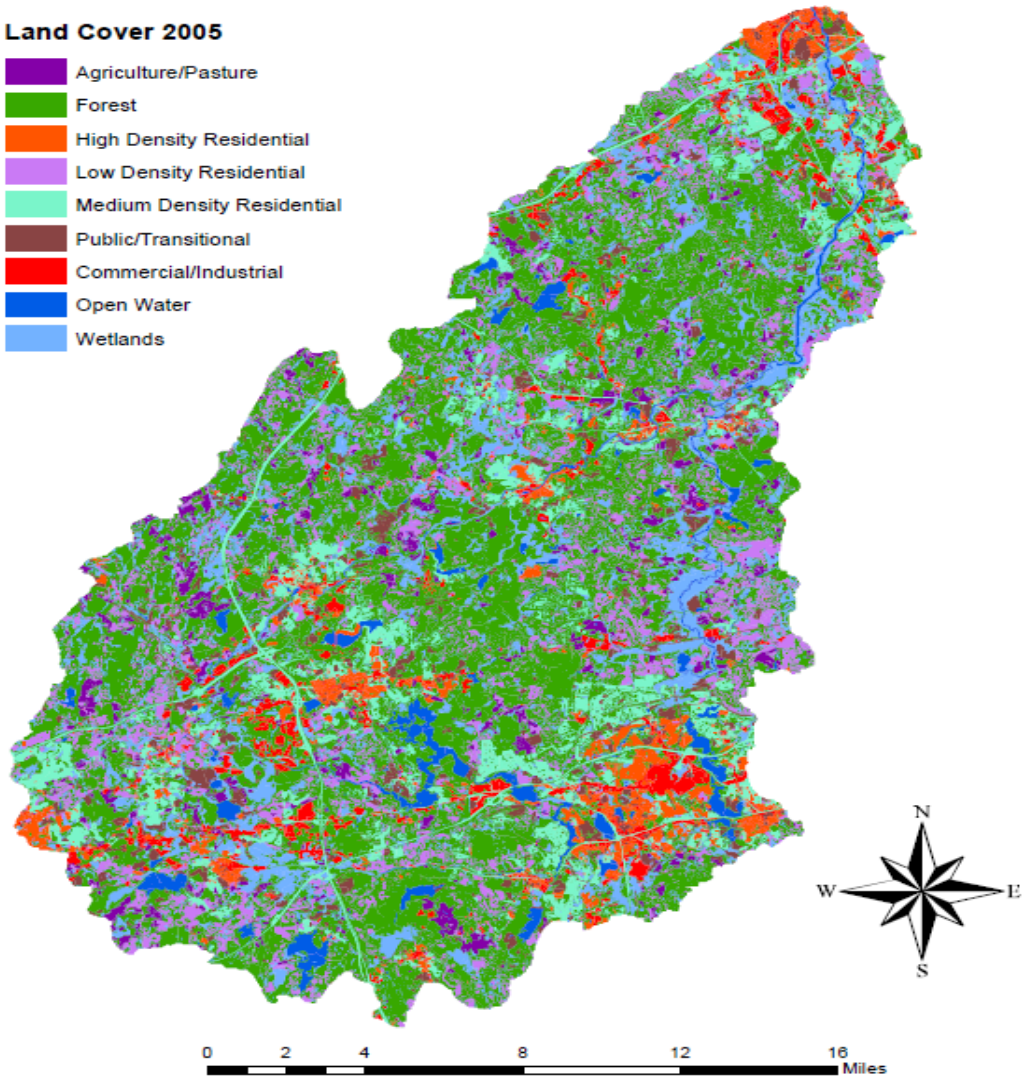

Figure 2: Land Cover types in SuAsCo Watershed, MA

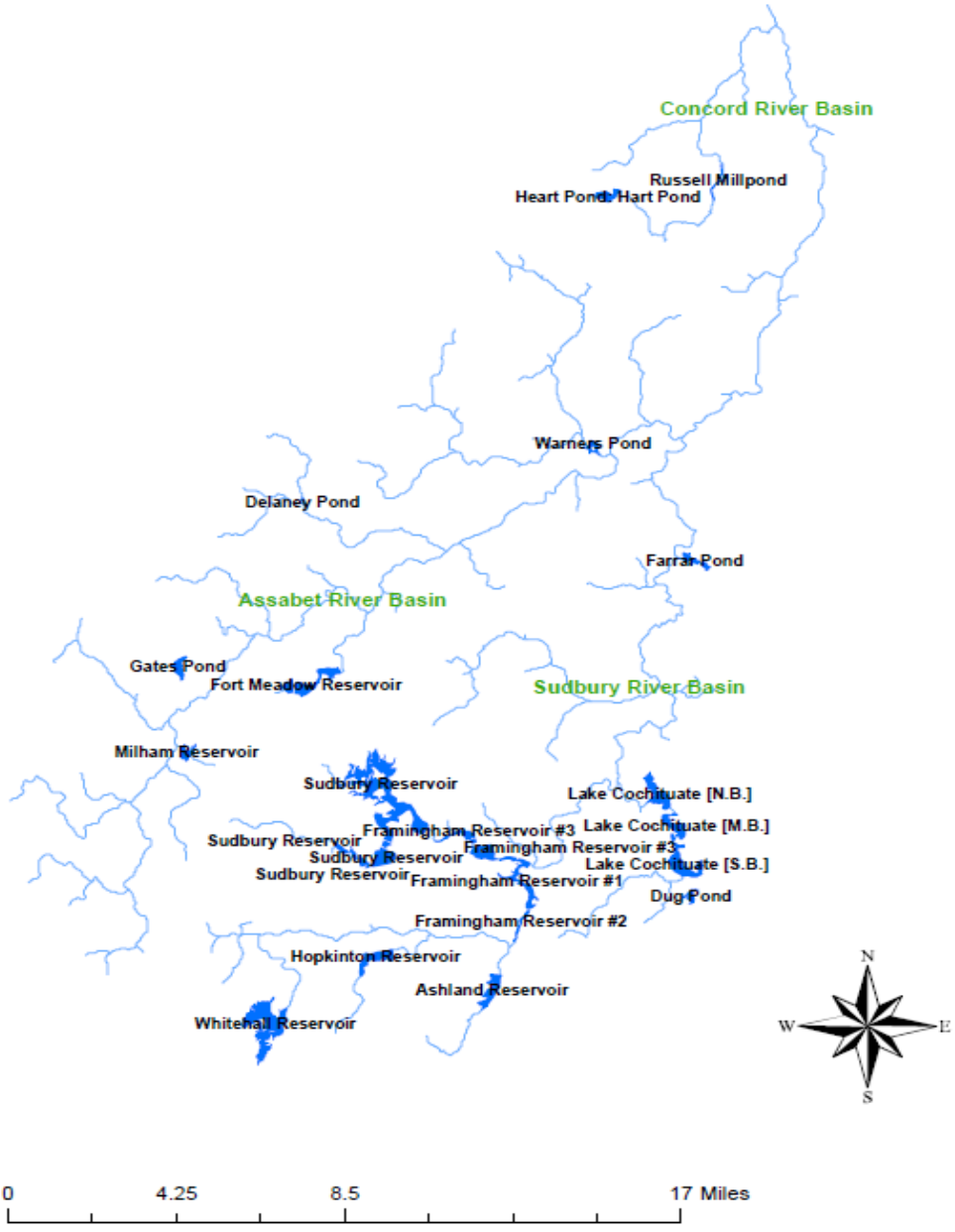

Figure 3: Lakes and impoundments in SuAsCo

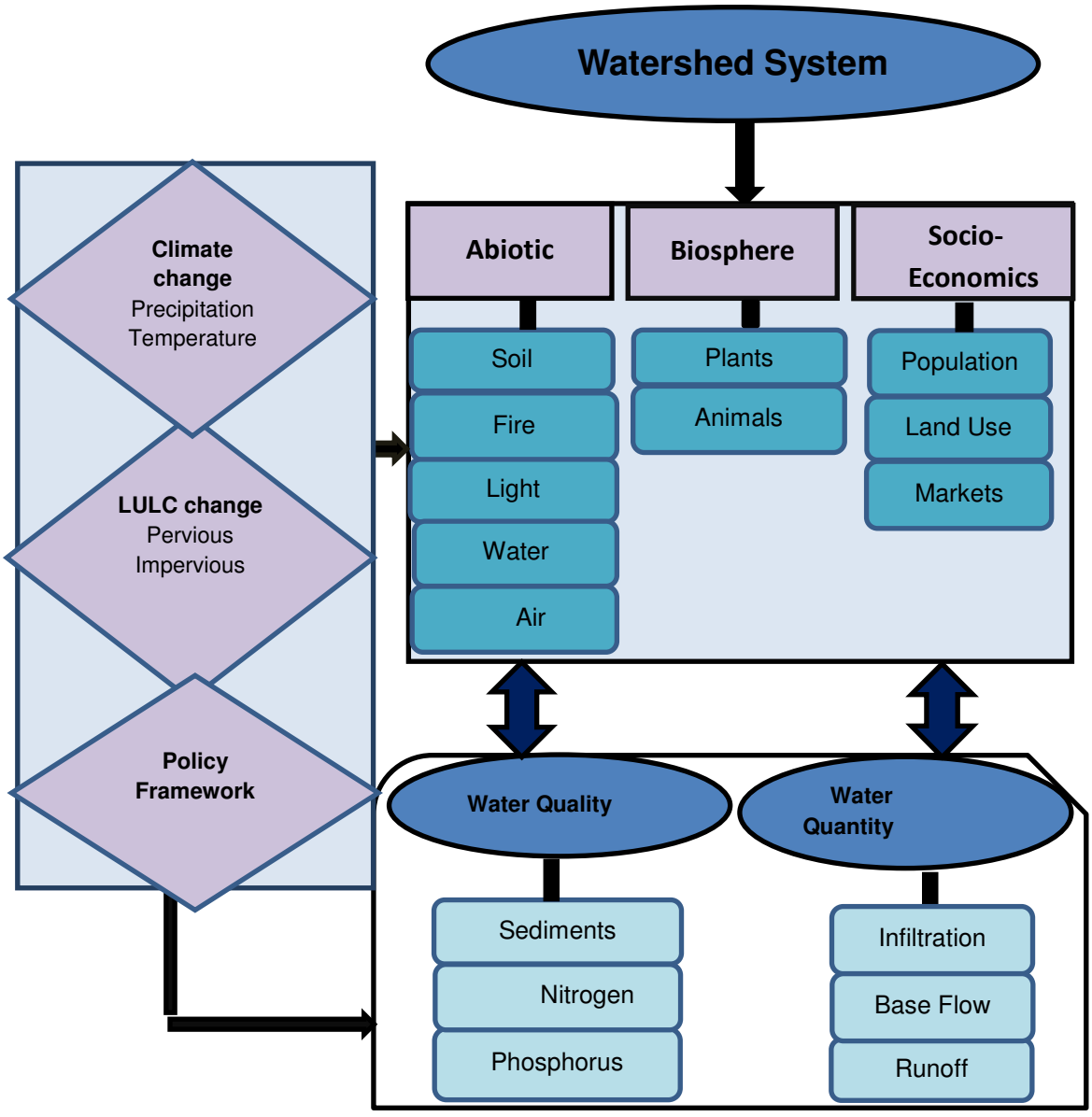

Figure 4: Conceptual framework to study the changes in LULC and climate change on waters systems

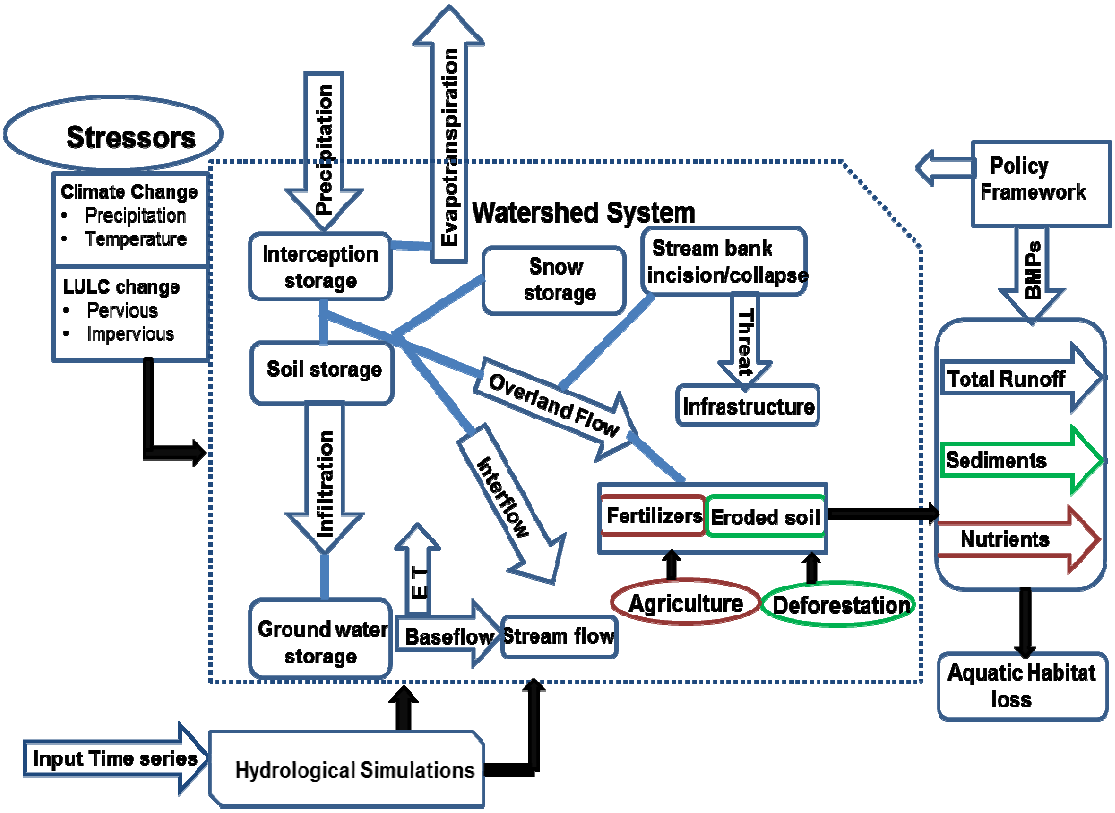

Figure 5: Empirical Model of LULC and climate change impacts

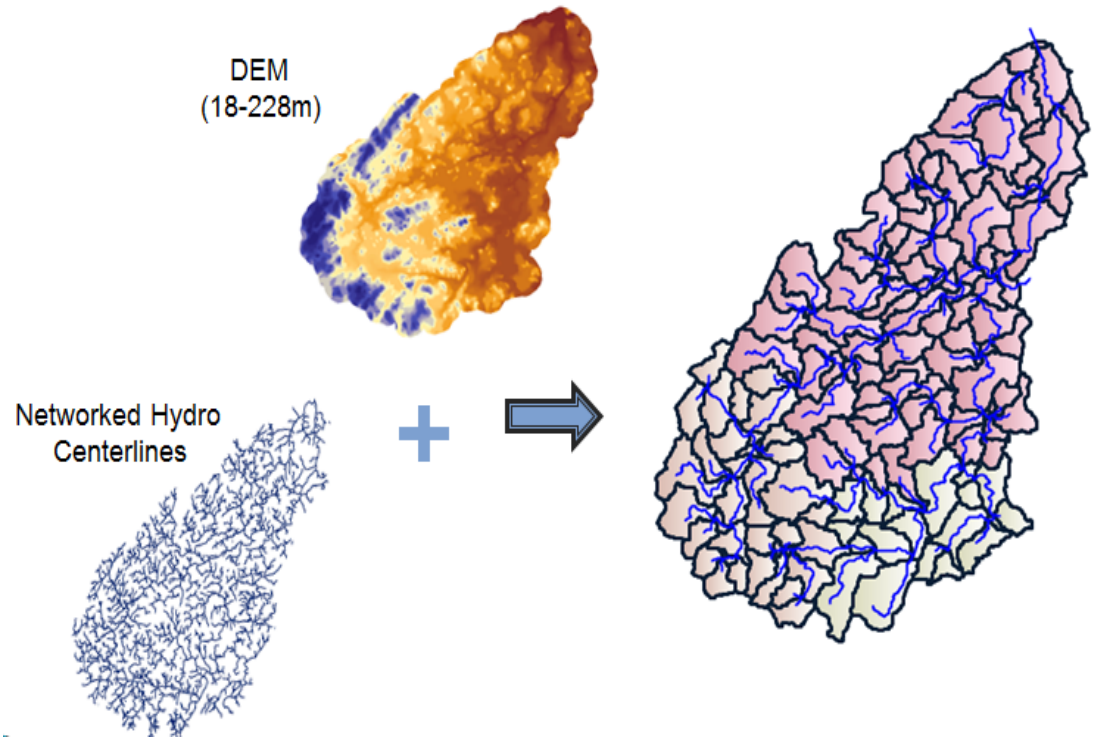

Figure 6: Watershed Delineation

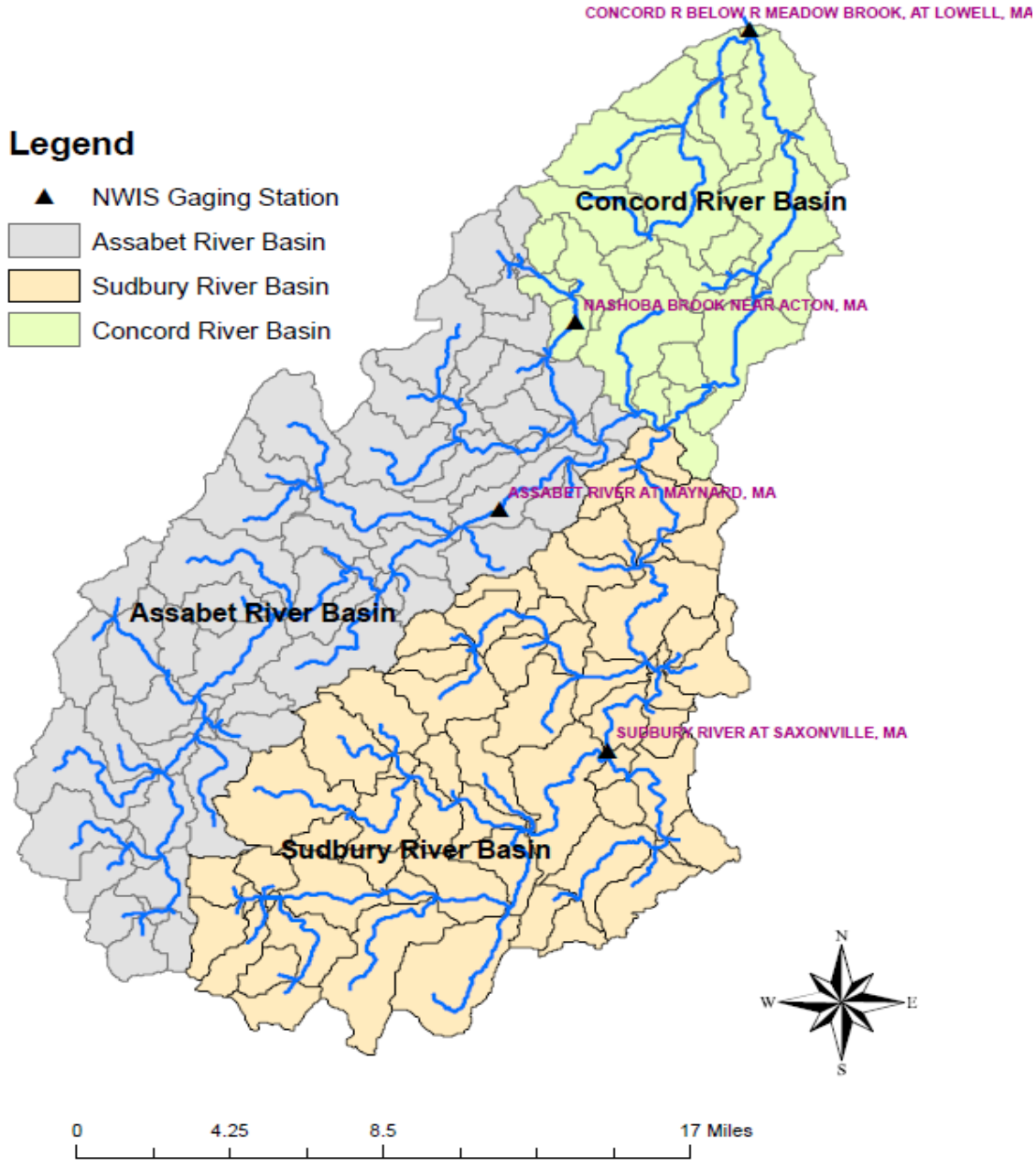

Figure 7: Location of Gaging Station in SuAsCo

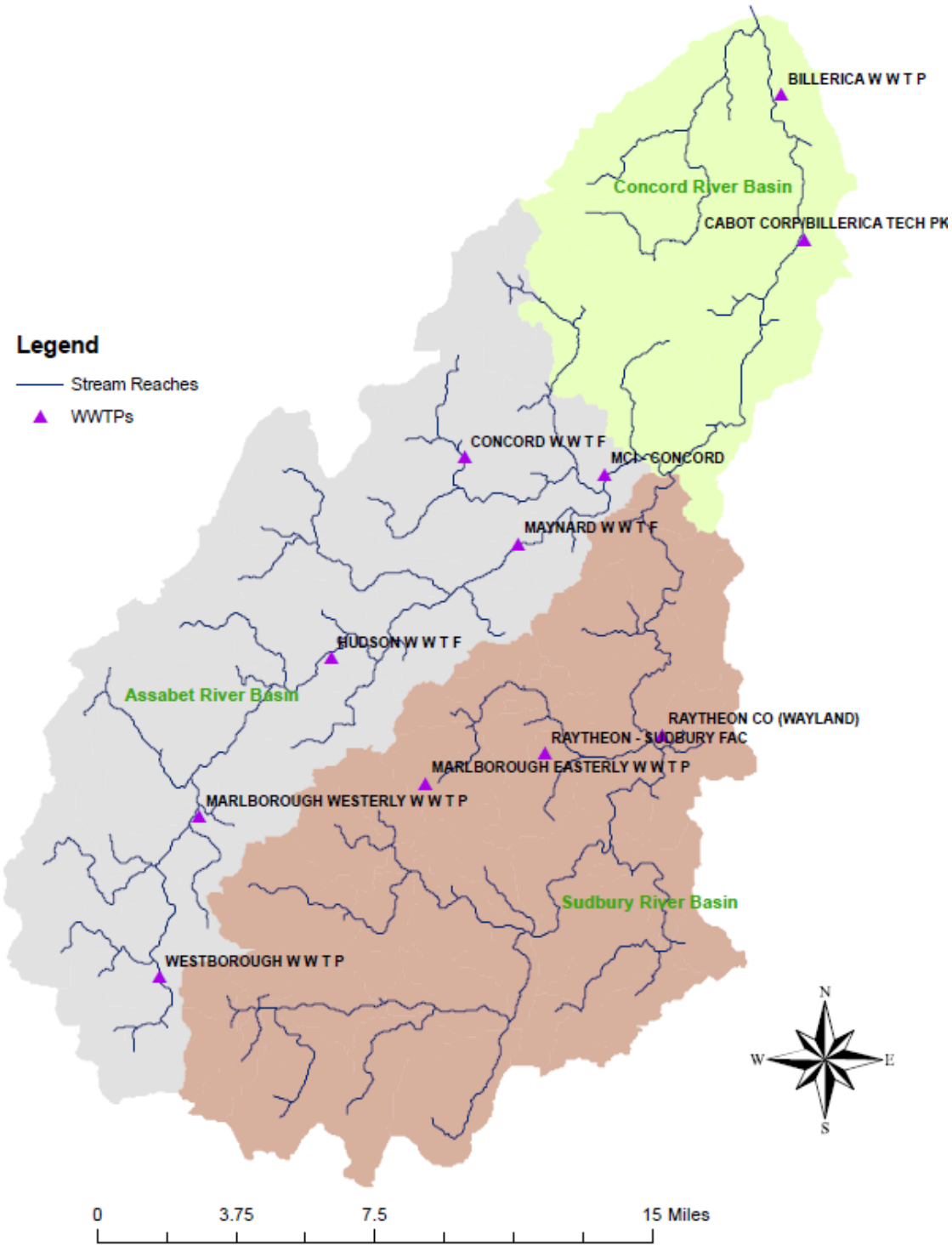

Figure 8: Locations of WWTPs in SuAsCo

A)

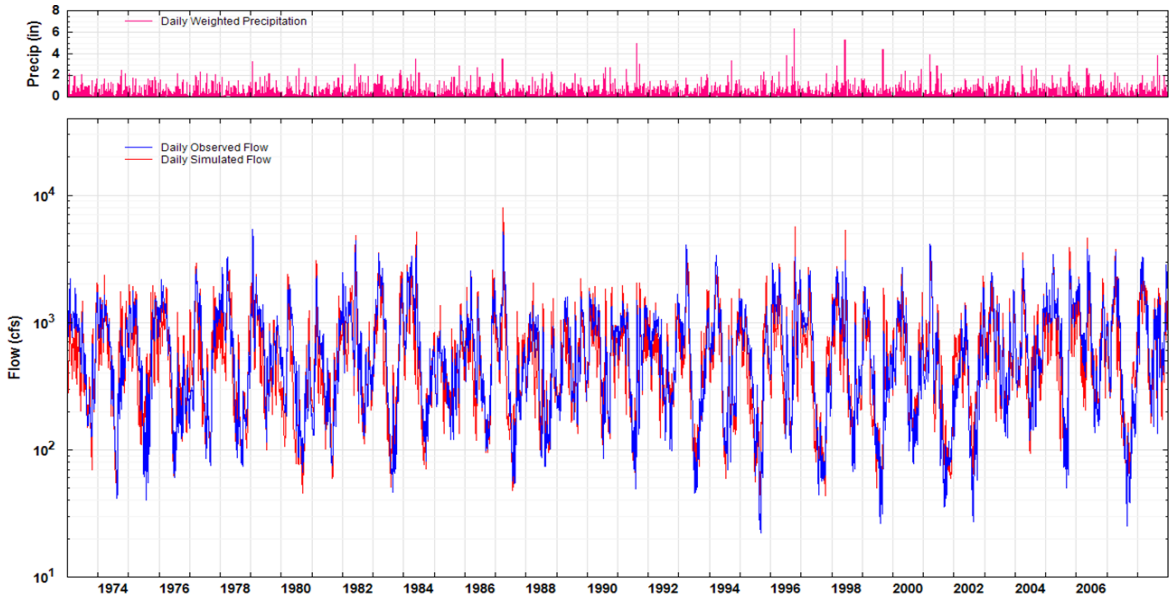

B)

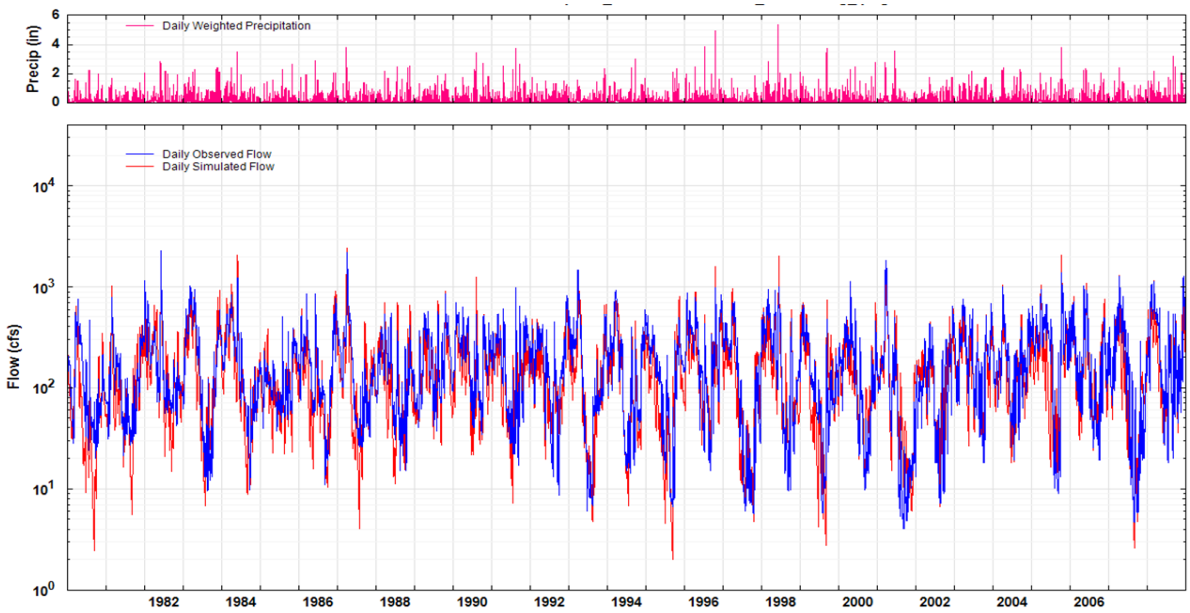

Figure 9: Daily mean Hydrographs at (A) Concord River below Meadow Brook at Lowell streamgage (01099500, RCHRES 157), (B) Sudbury River at Saxonville streamgage (01098530, RCHRES 140)

A)

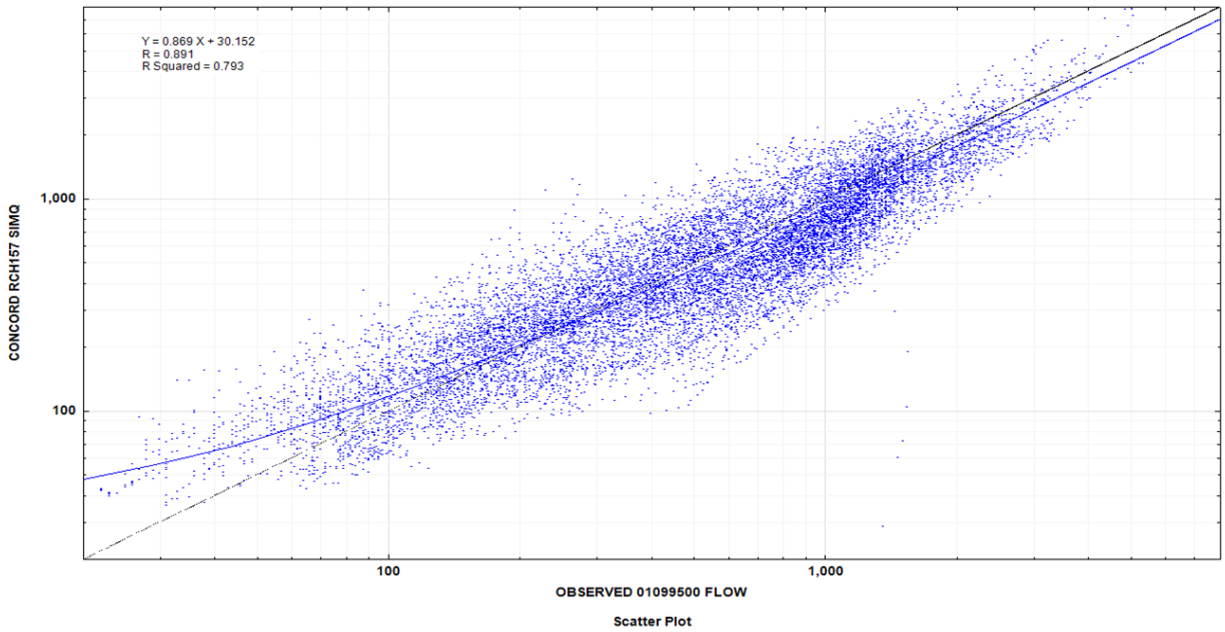

B)

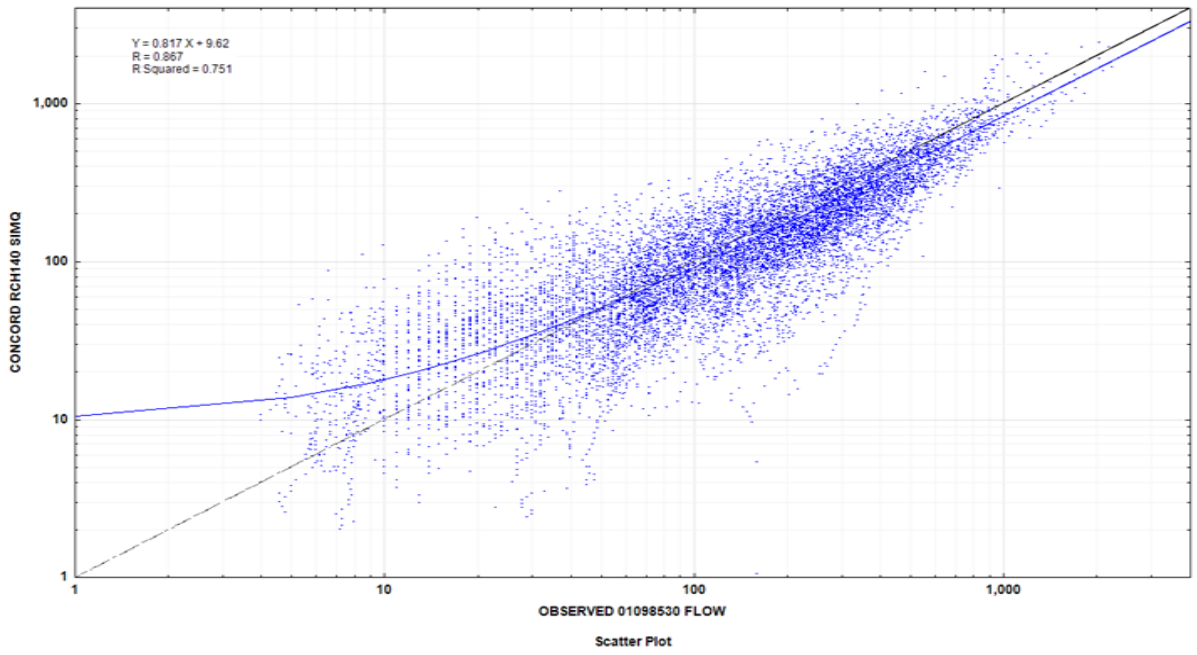

Figure 10: Scatter plot for simulated total runoff and observed flow at (A) Concord River below Meadow Brook at Lowell streamgage (01099500, RCHRES 157), (B) Sudbury River at Saxonville streamgage (01098530, RCHRES 140)

A)

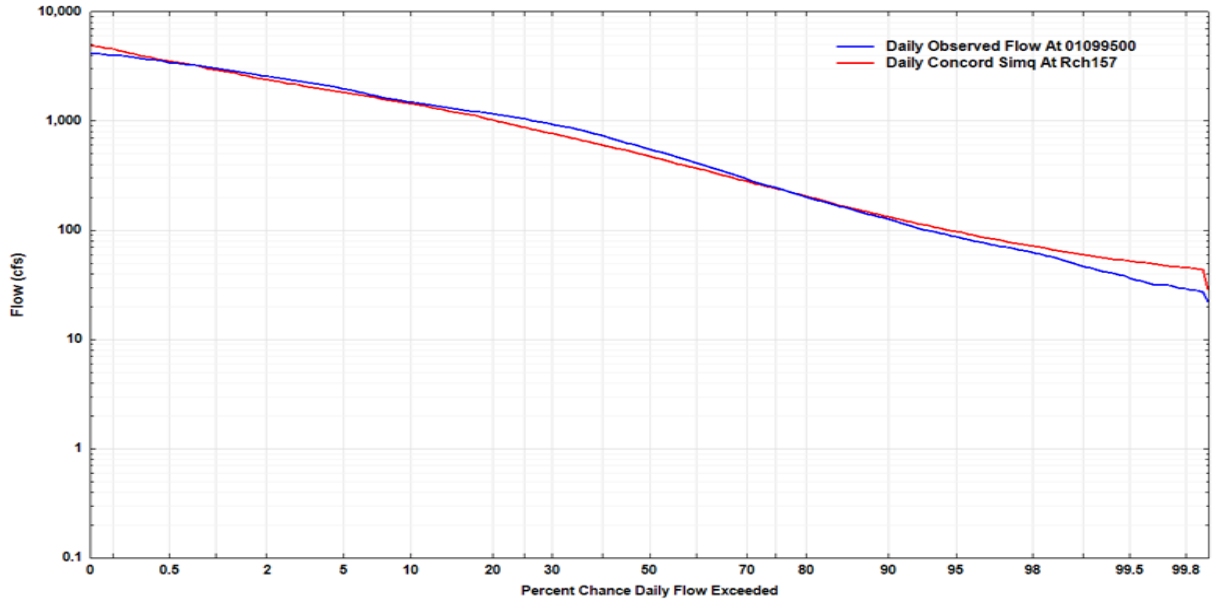

B)

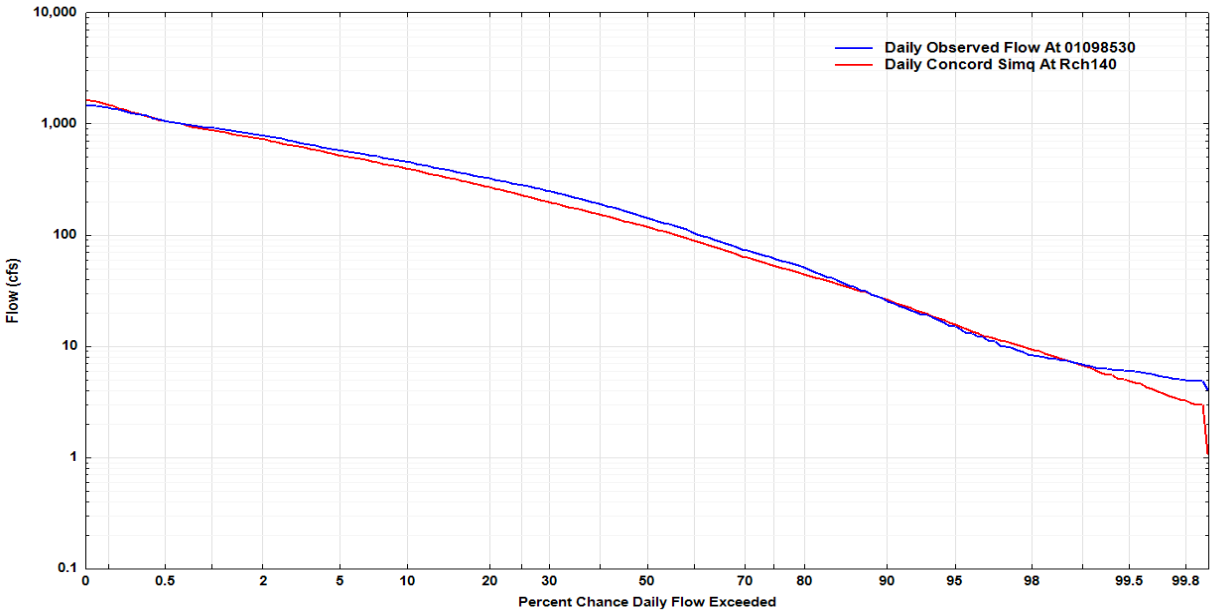

Figure 11: Hydrographs of percent chance daily exceeded for simulated total runoff and observed flow at (A) Concord River below Meadow Brook at Lowell streamgage (01099500, RCHRES 157), (B) Sudbury River at Saxonville streamgage (01098530, RCHRES 140)

A)

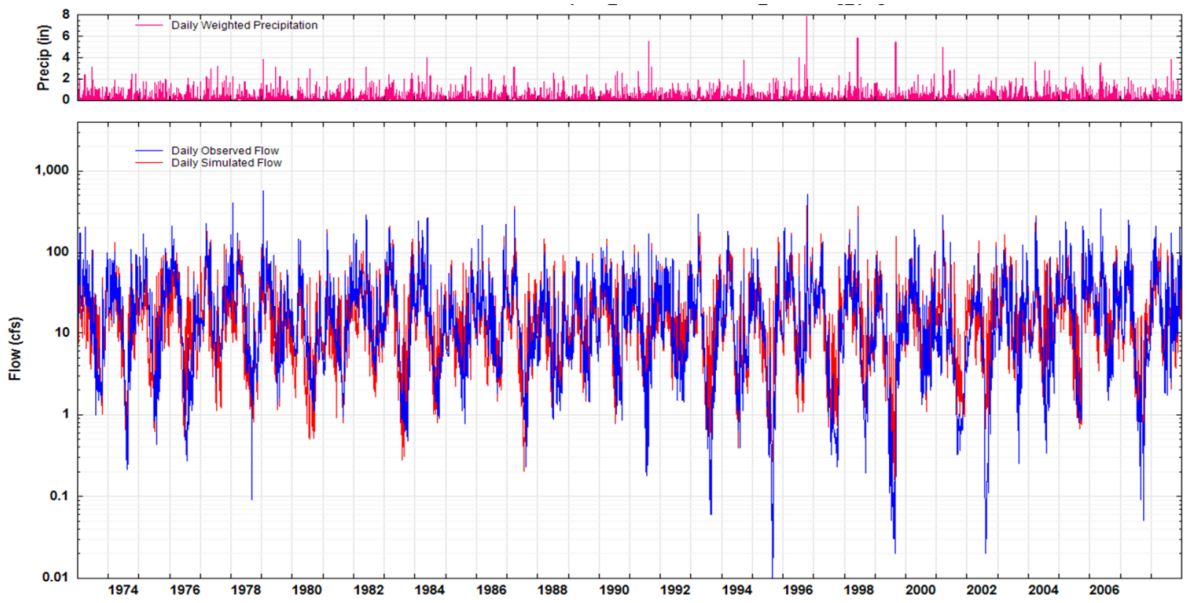

B)

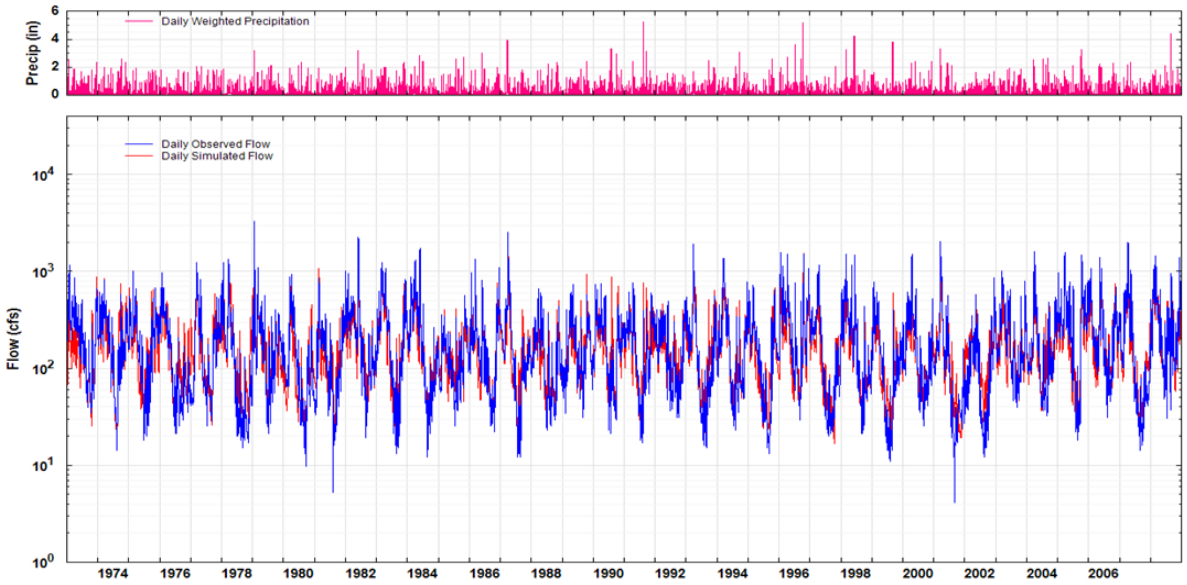

Figure 12: Daily mean Hydrographs at (A) Assabet River at Nashoba Brook near Acton streamgage (01097300, RCHRES 99), (B) Assabet River at Maynard streamgage (01097000, RCHRES 142)

A)

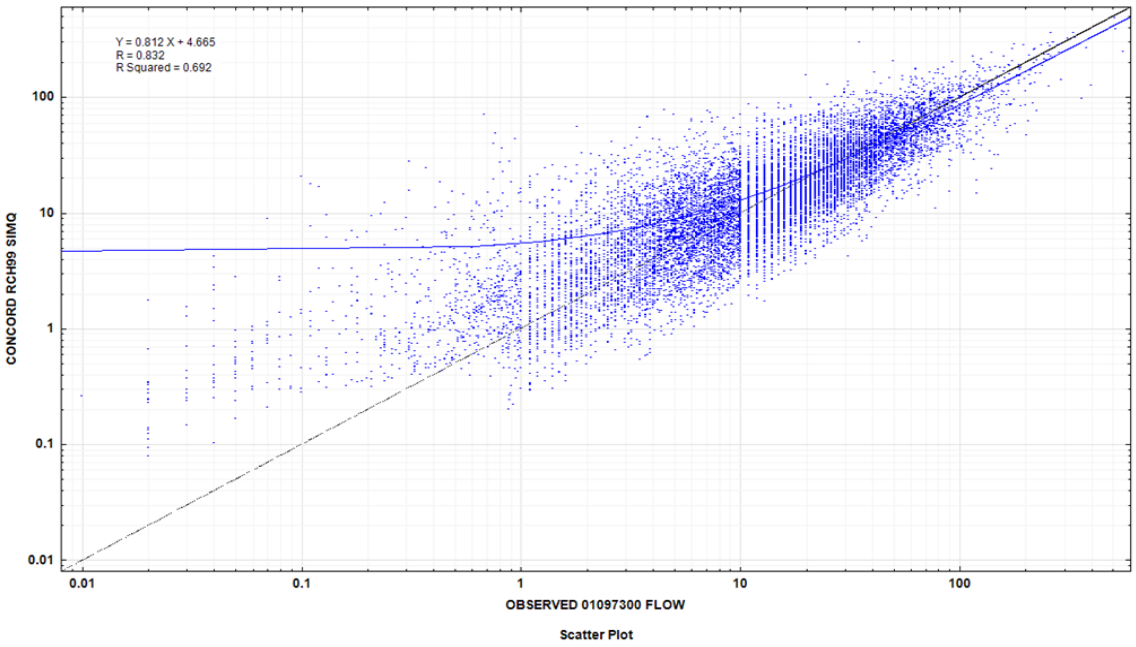

B)

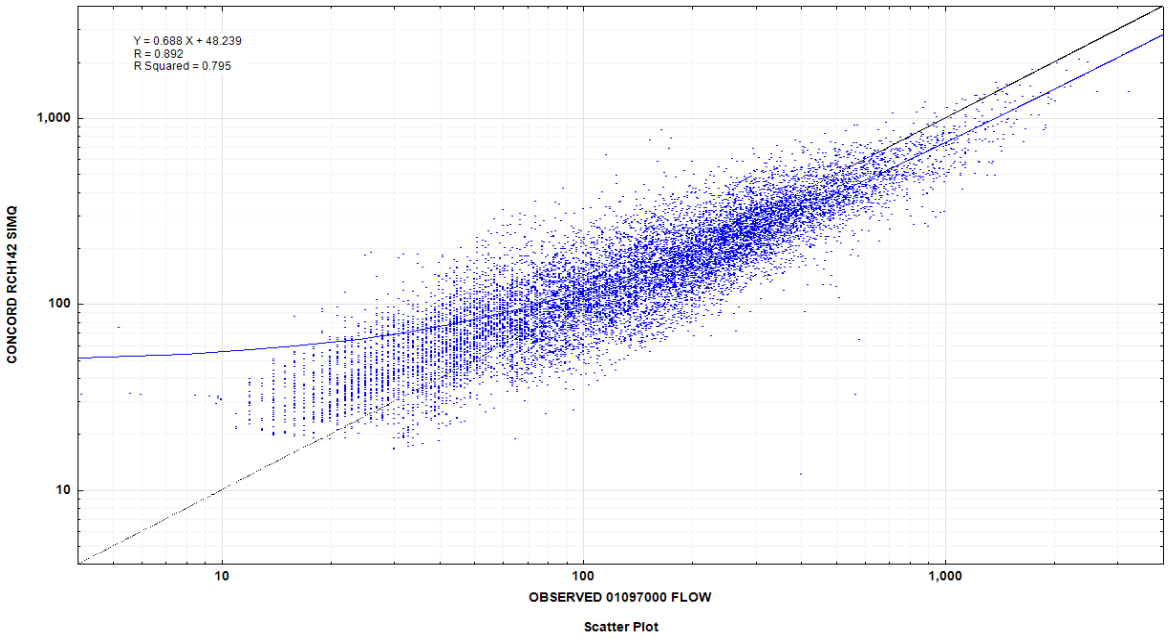

Figure 13: Scatter plot for simulated total runoff and observed flow at (A) Assabet River at Nashoba Brook near Acton streamgage (01097300, RCHRES 99), (B) Assabet River at Maynard streamgage (01097000, RCHRES 142)

A)

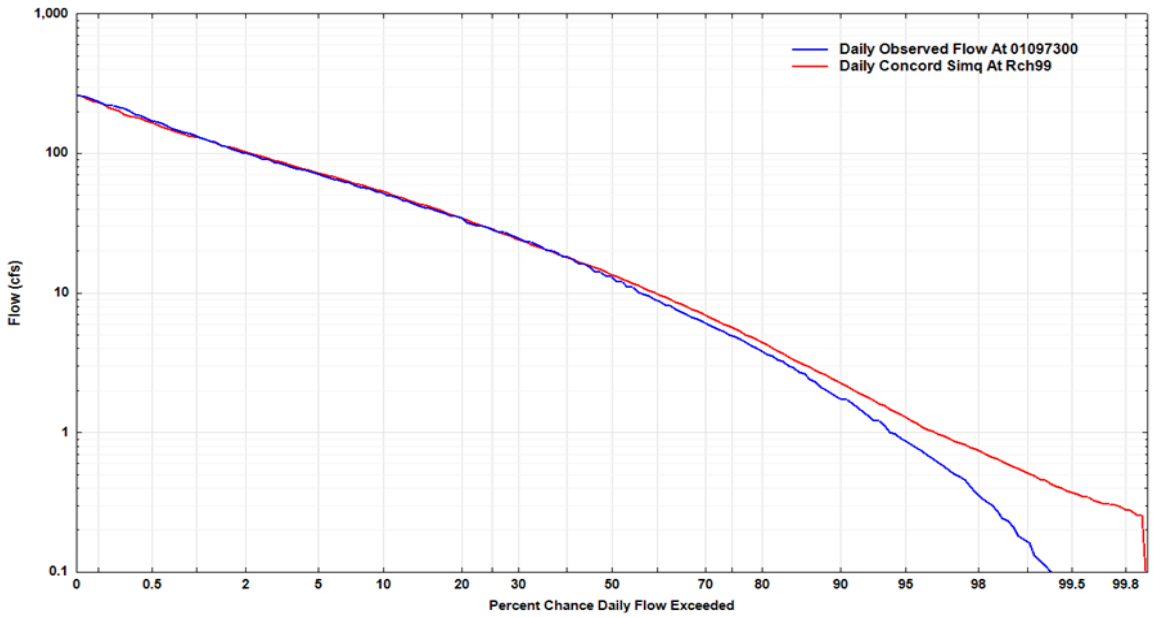

B)

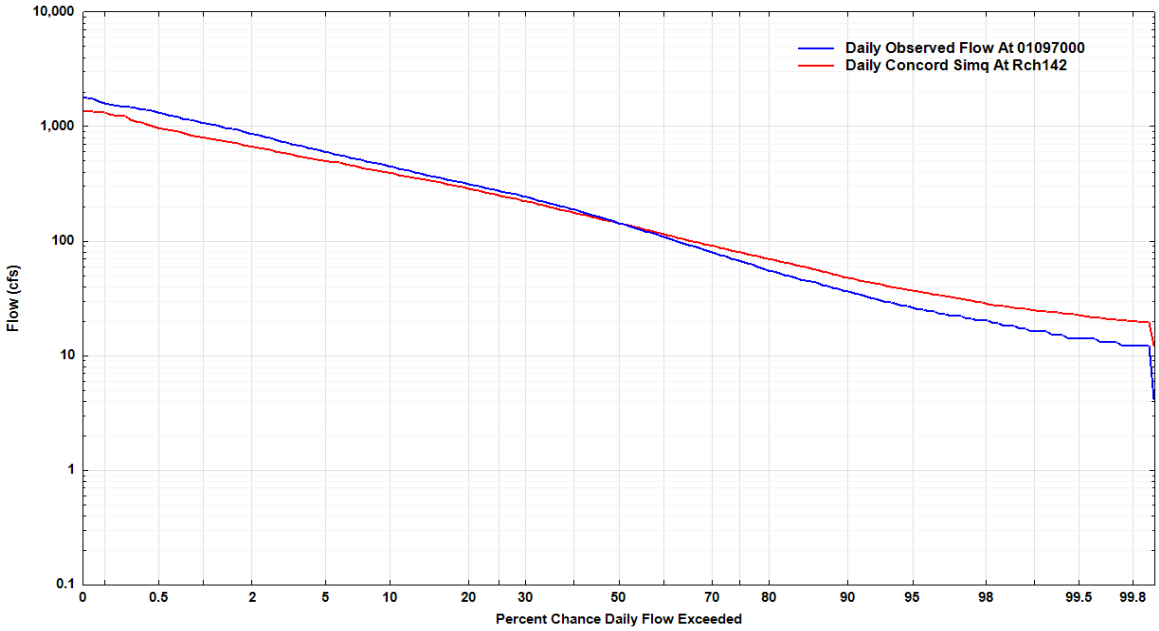

Figure 14: Hydrographs of percent chance daily exceeded for simulated total runoff and observed flow at (A) Assabet River at Nashoba Brook near Acton streamgage (01097300, RCHRES 99), (B) Assabet River at Maynard streamgage (01097000, RCHRES 142)

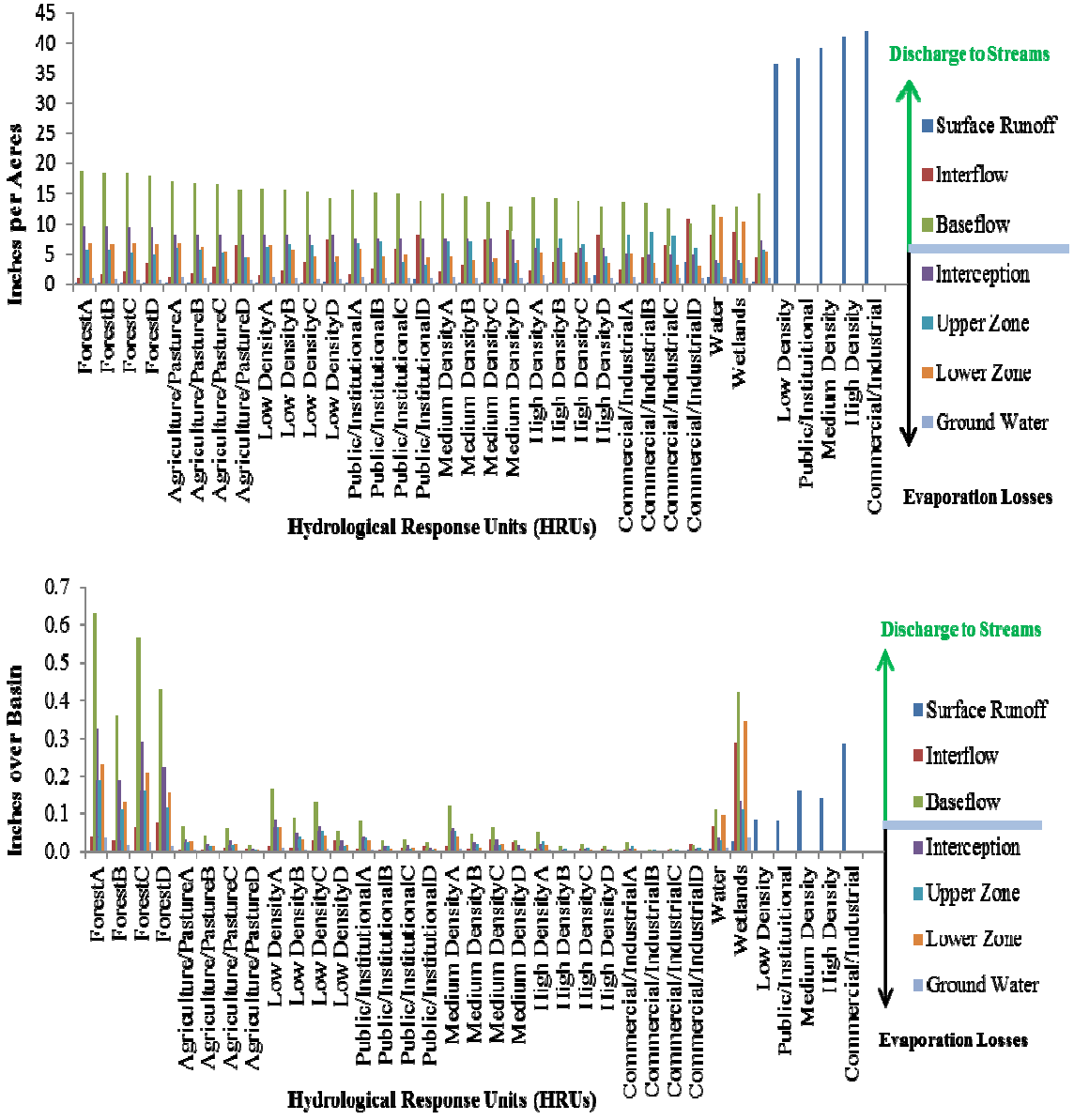

Figure 15: Mean annual 1973–2008 water-budget outflow components in inches per acre and over the entire Basin simulated by the Hydrological Simulation Program–FORTRAN (HSPF) model of the SuAsCo Basin, Massachusetts

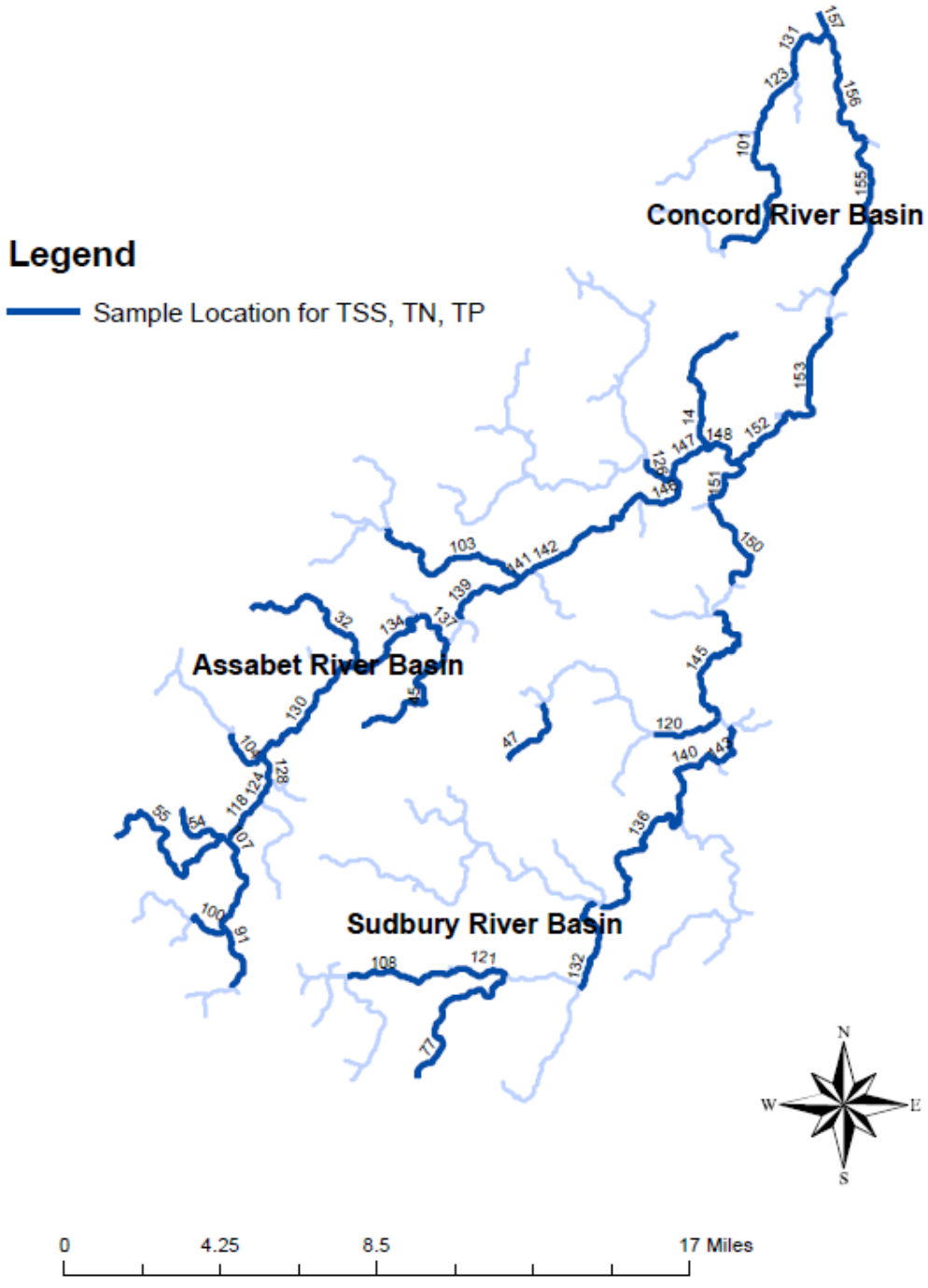

Figure 16: Location of observed samples for sediments, Total nitrogen and phosphorus

A)

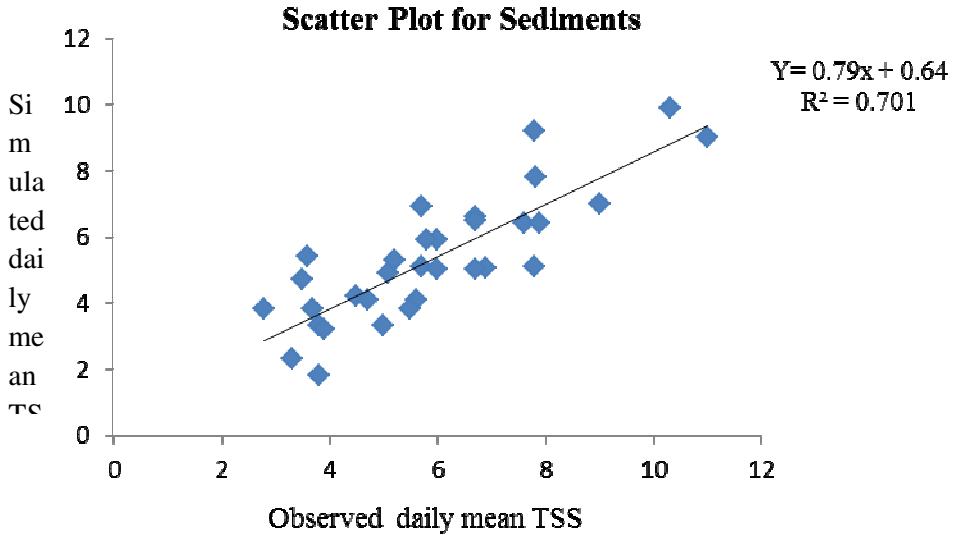

B)

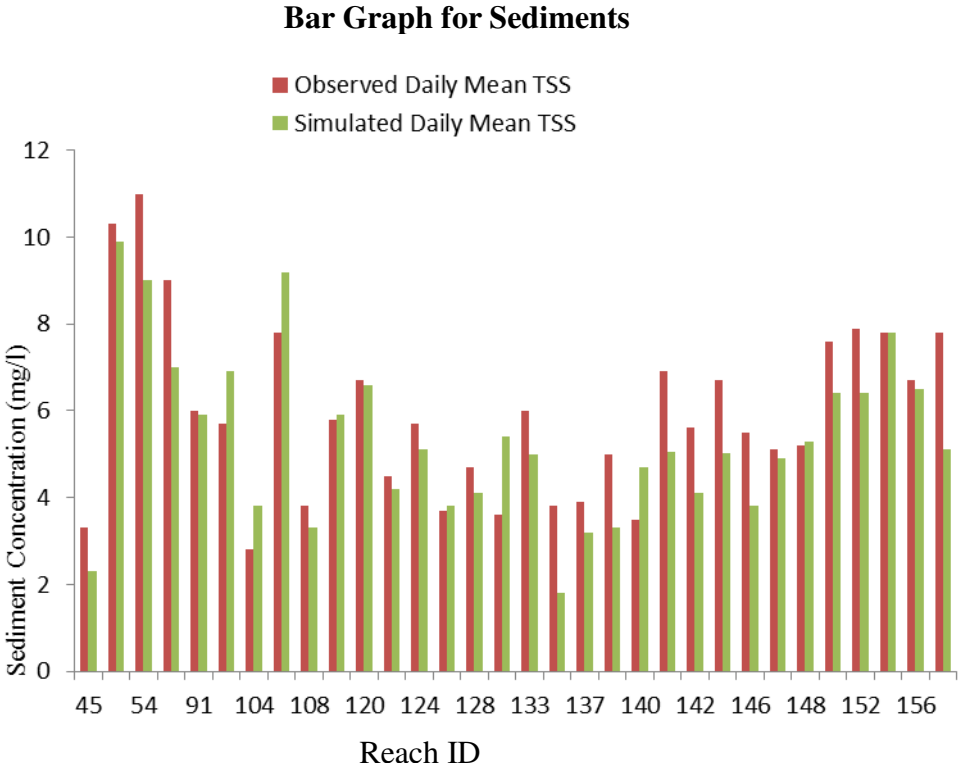

Figure 17: A) Scatter plot between observed and simulated mean daily TSS in SuAsCo (1973-2008) B) Bar graph between observed and simulated mean daily TSS in SuAsCo (1973-2008)

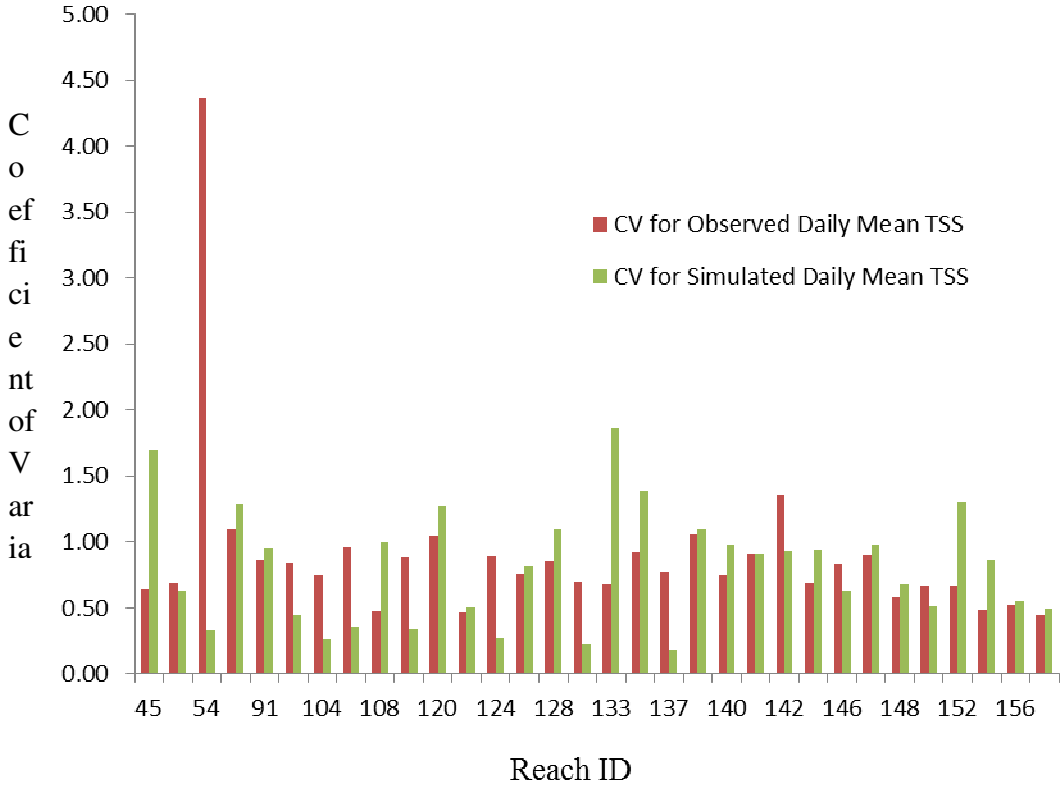

Figure 18: Bar Graph between Coefficient of Variance (CV) of observed and simulated mean daily TSS in SuAsCo (1973-2008)

A)

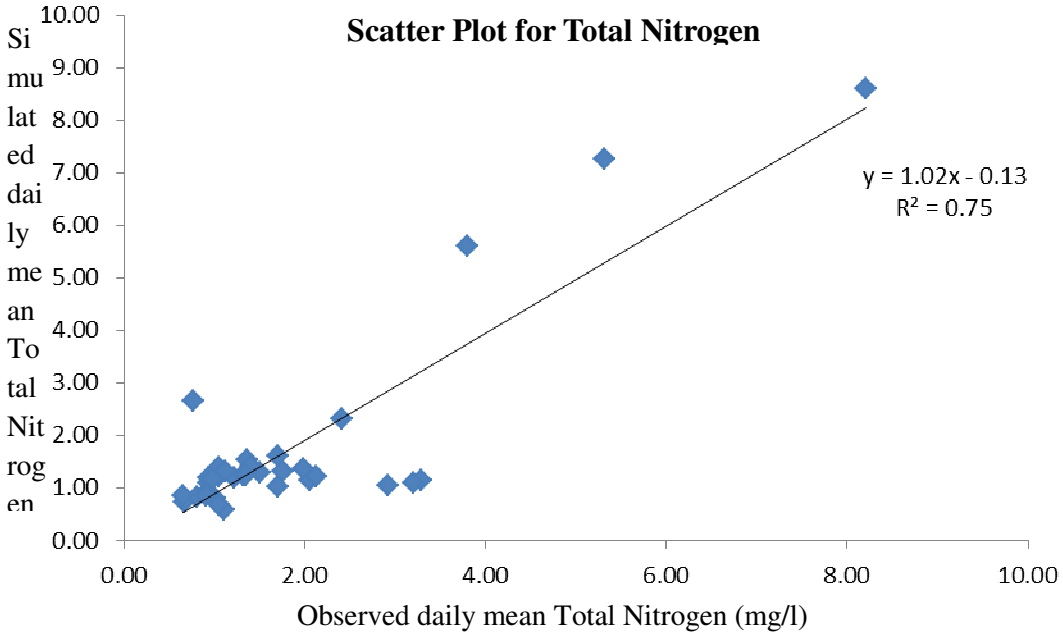

B)

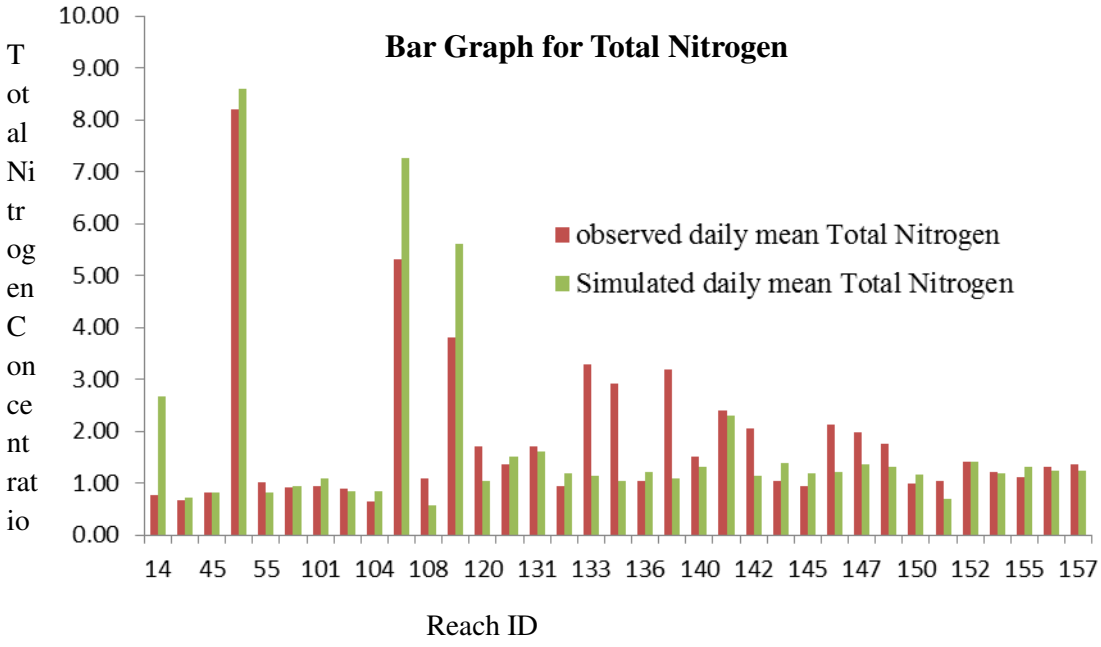

Figure 19: A) Scatter plot between observed and simulated mean daily Total Nitrogen in SuAsCo (1973-2008) B) Bar graph between observed and simulated mean daily Total Nitrogen in SuAsCo (1973-2008)

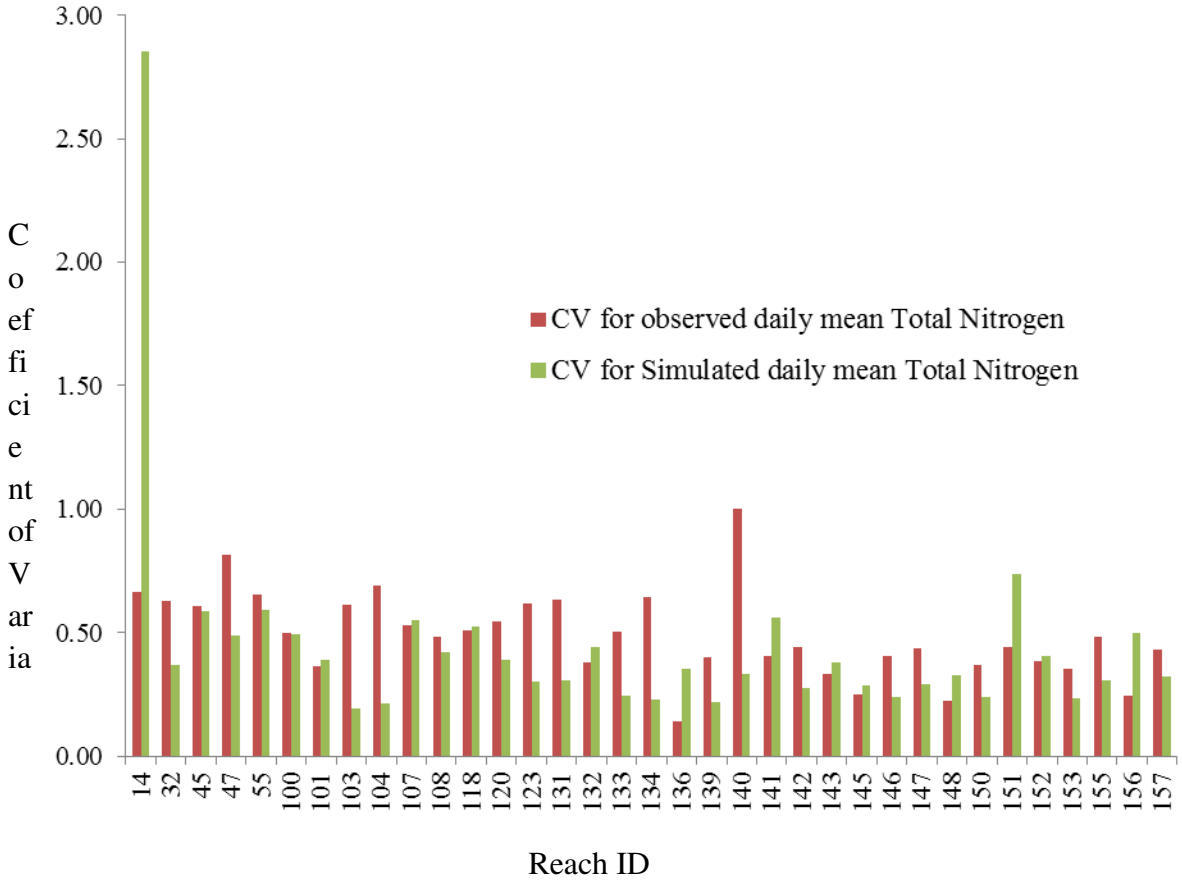

Figure 20: Bar Graph between Coefficient of Variance (CV) of observed and simulated mean daily total nitrogen in SuAsCo (1973-2008)

A)

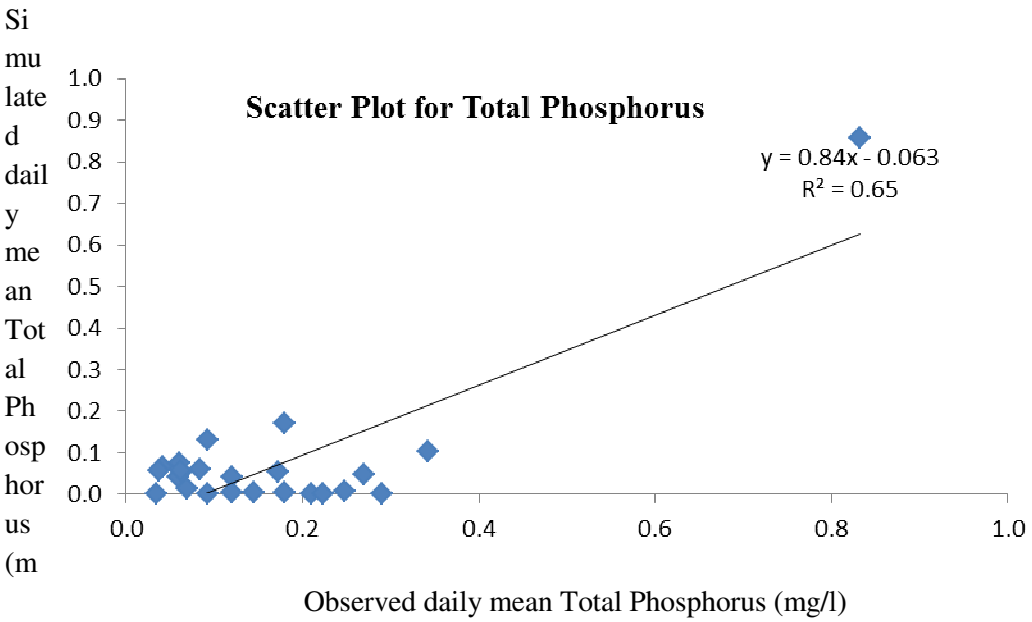

B)

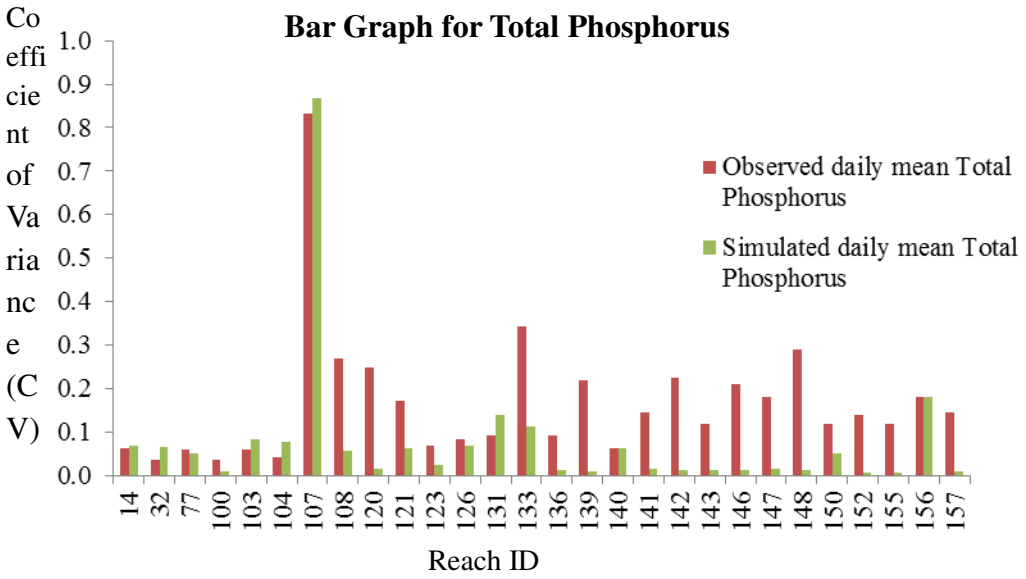

Figure 21: A) Scatter plot between observed and simulated mean daily Total Phosphorus in SuAsCo (1973-2008) B) Bar graph between observed and simulated mean daily Total Phosphorus in SuAsCo (1973-2008)

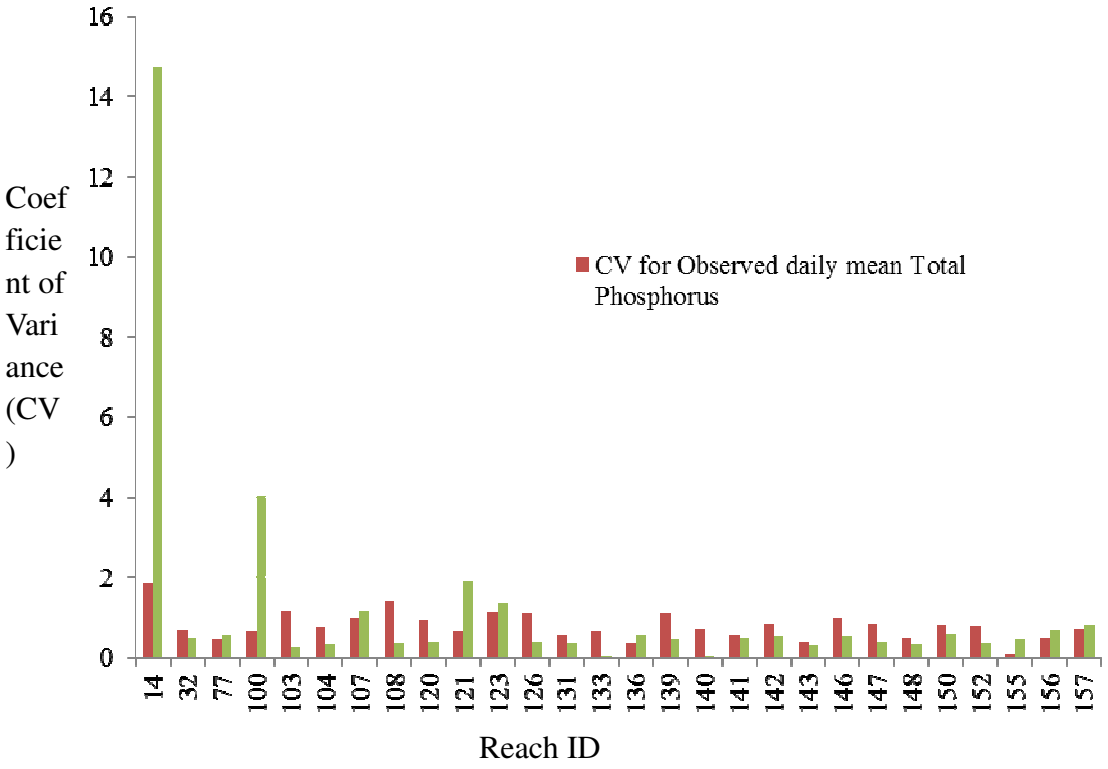

Figure 22: Bar Graph between Coefficient of Variance (CV) of observed and simulated mean daily Total Phosphorus in SuAsCo (1973-2008)

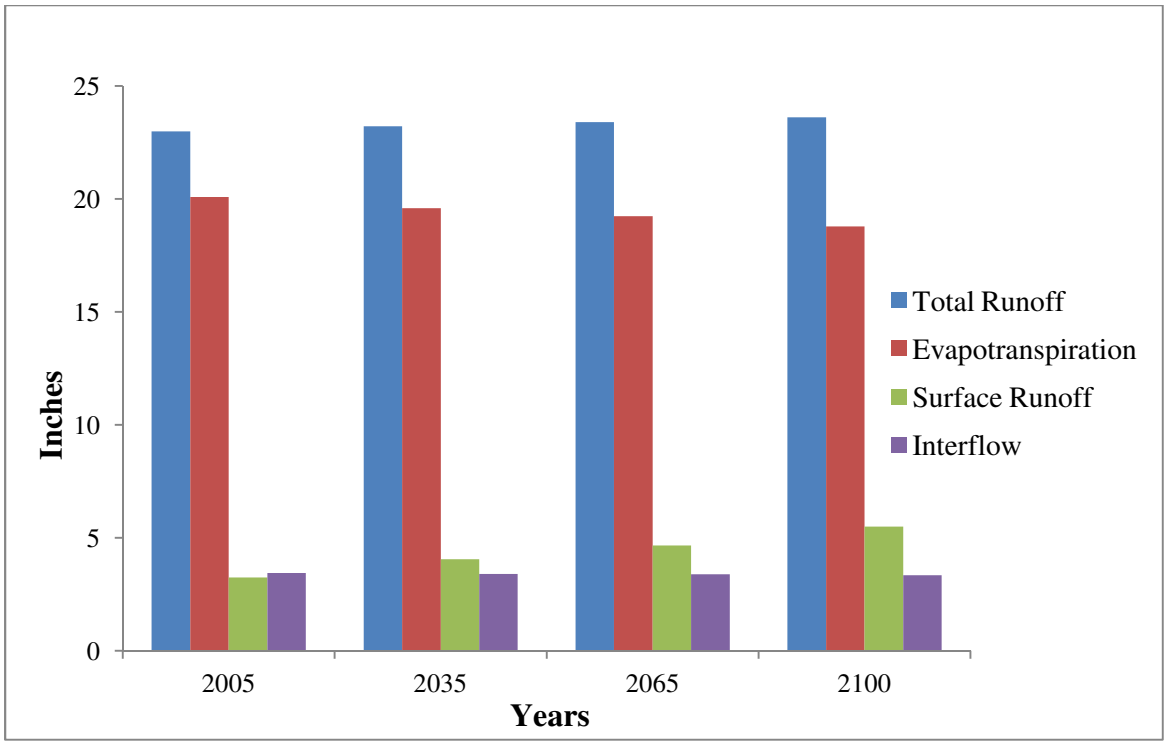

Figure 23: Changes in Annual Average Water Balance with Future Land Cover Change

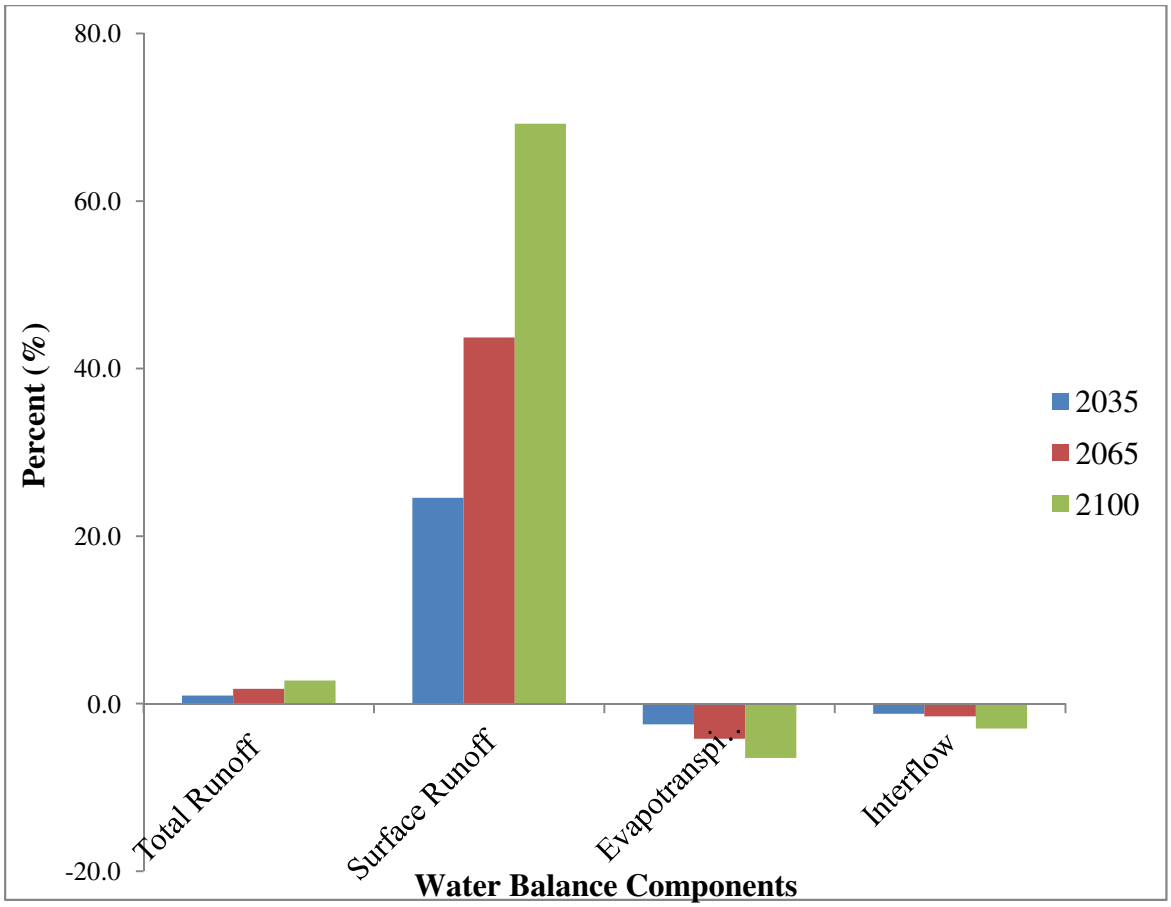

Figure 24 : Percent Changes in Water Balance with Future Land Cover Change

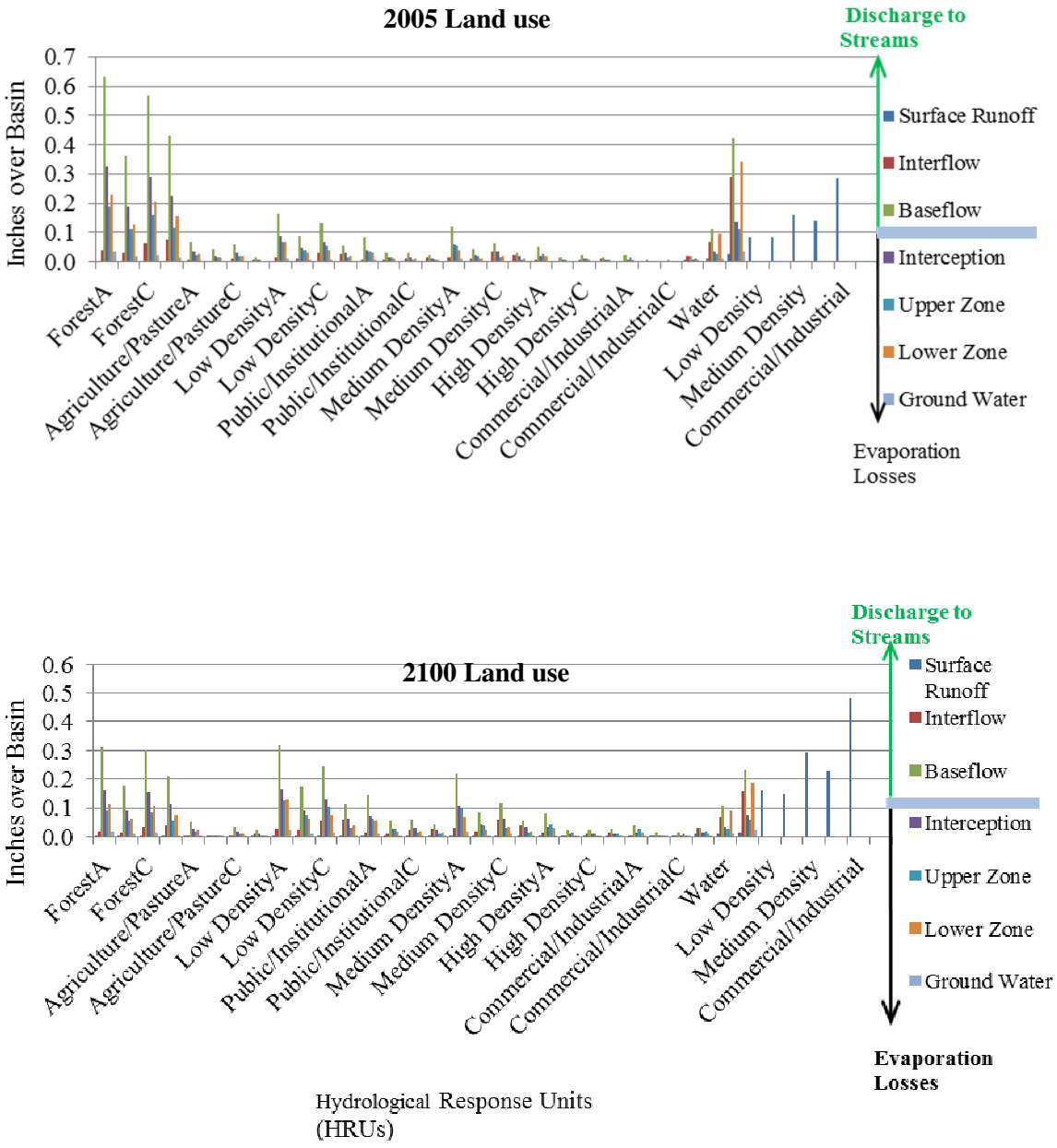

Figure 25: Water-budget outflow components by Hydrologic Response Unit (HRU) simulated by the Hydrological Simulation Program–FORTRAN (HSPF) in SuAsCo watershed under 2005 land use and projected 2100 land-use conditions

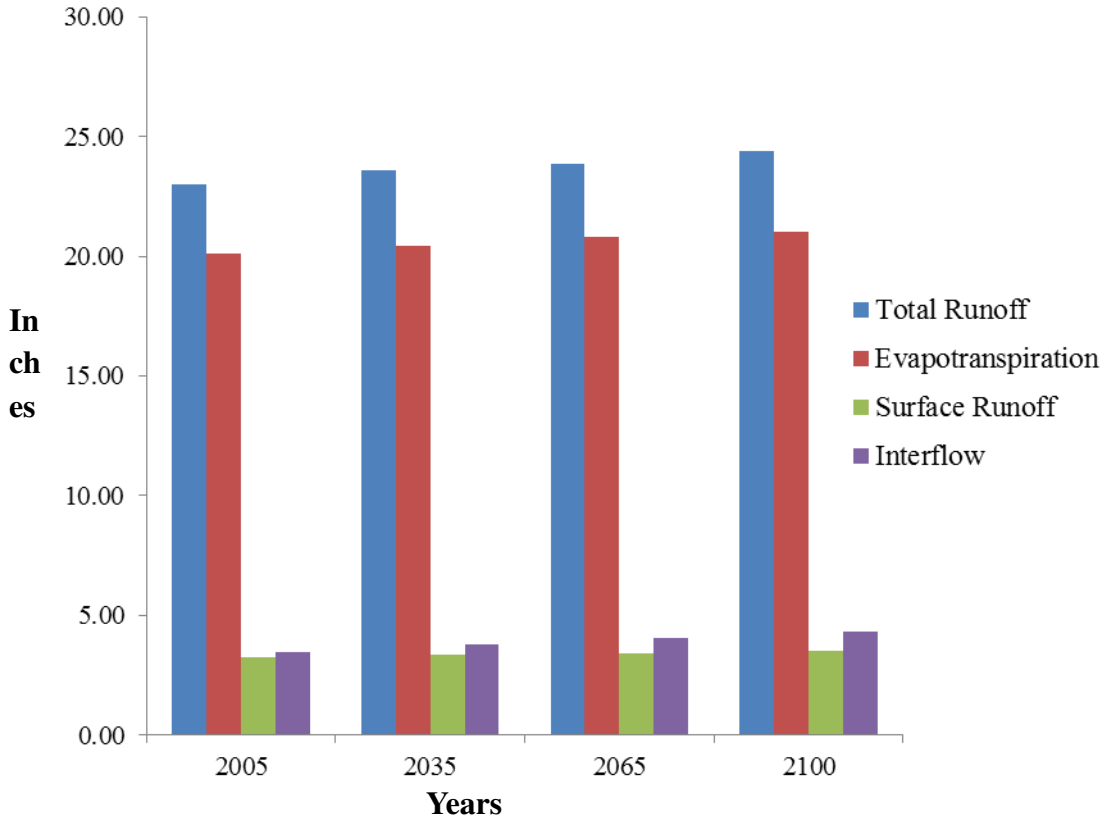

Figure 26: Changes in Annual Average Water Balance with Future Climate Change Scenario (RCP4.5)

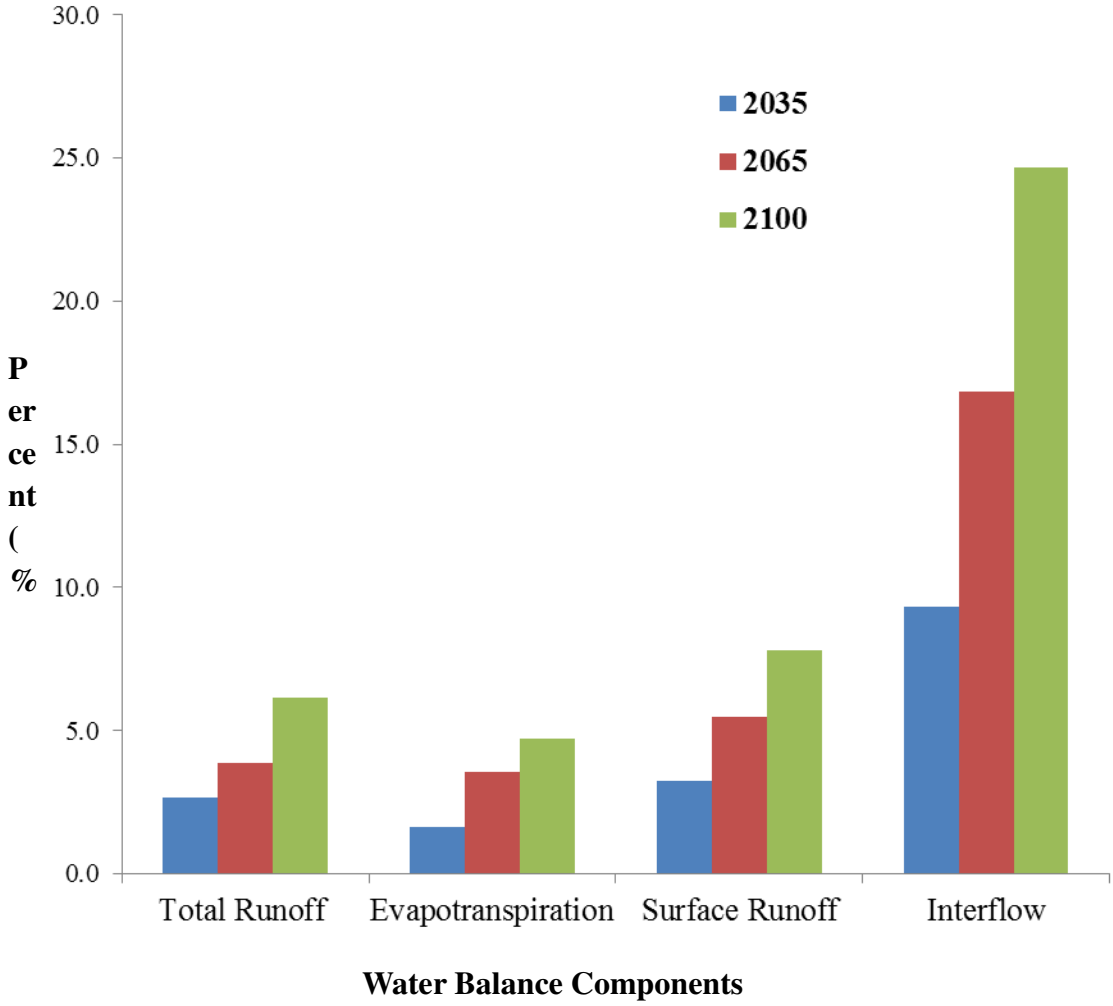

Figure 27: Percent Changes in Water Balance with Future Climate Change Scenario (RCP4.5)

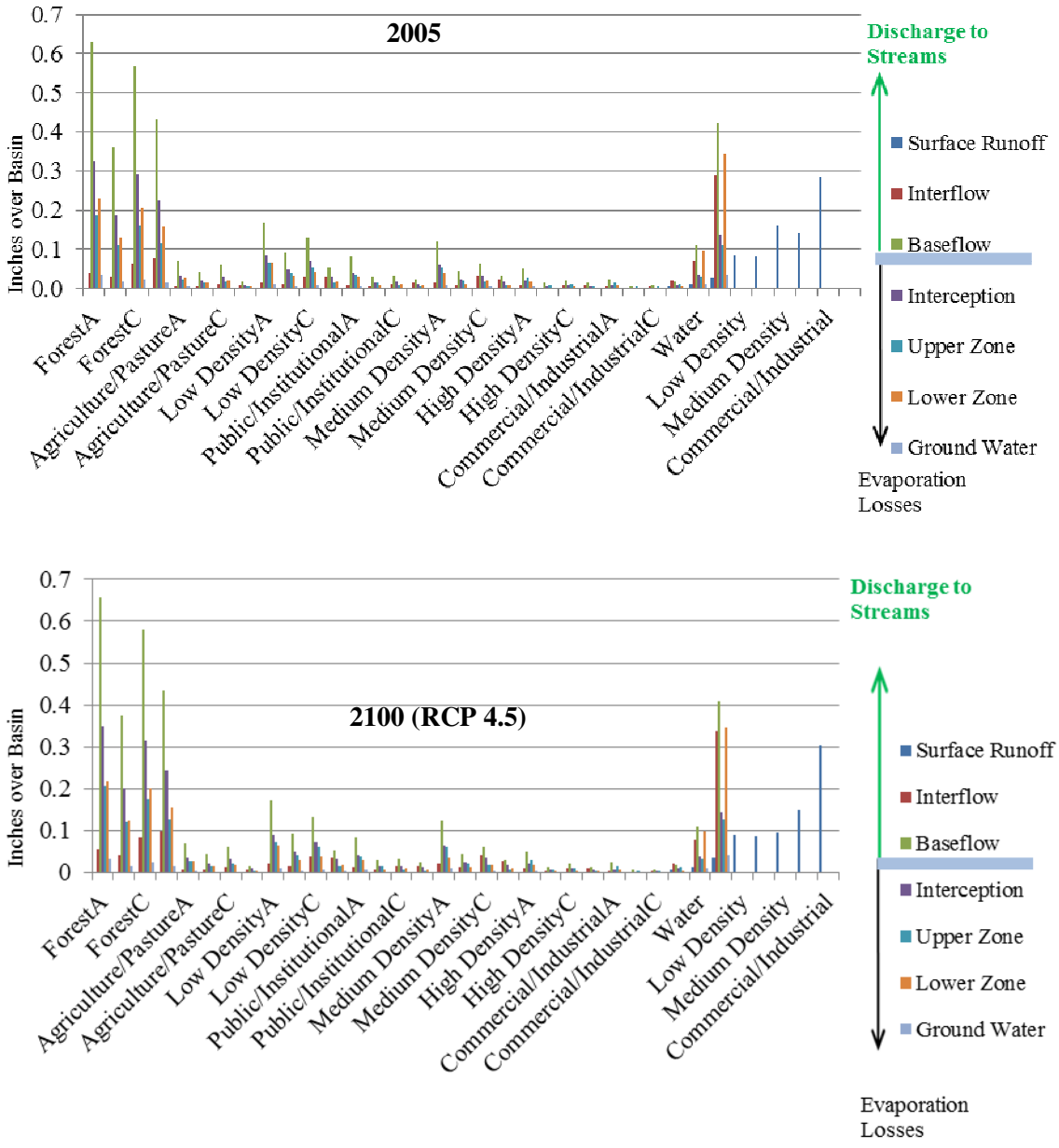

Figure 28: Water-budget outflow components by Hydrologic Response Unit (HRU) simulated by the Hydrological Simulation Program–FORTRAN (HSPF) in SuAsCo watershed under 2005 and projected 2100 Climate Change (RCP 4.5) Scenario

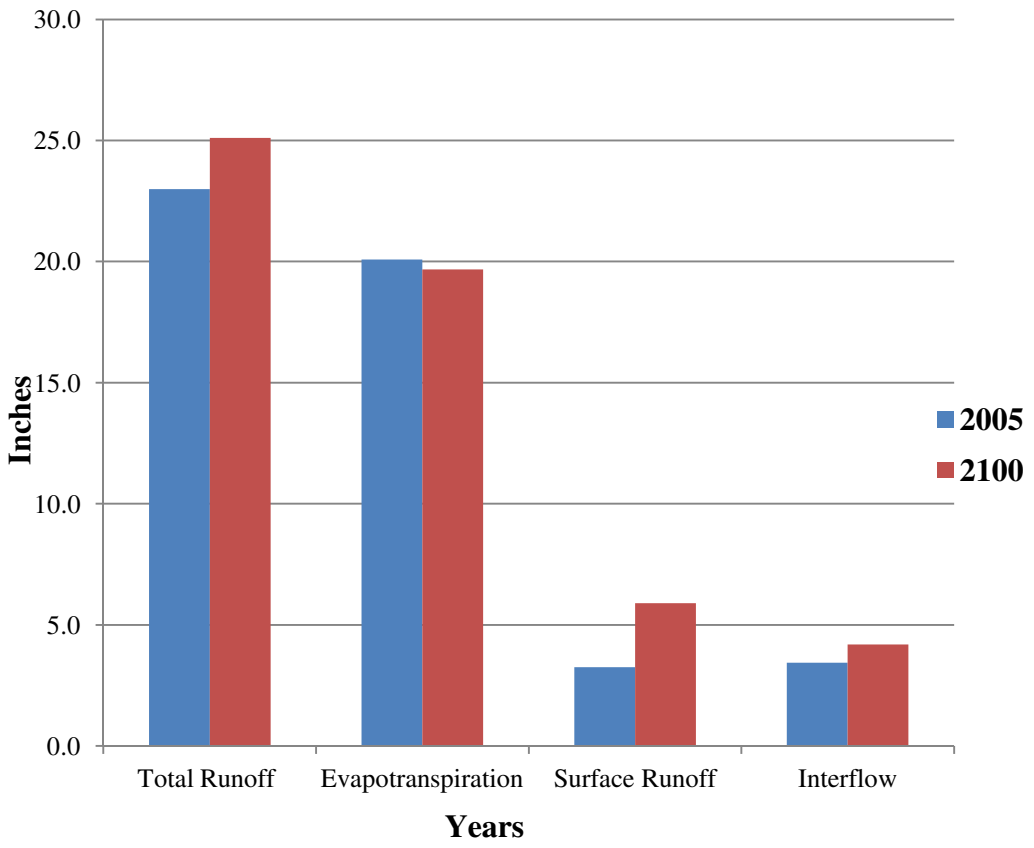

Figure 29: Changes in Annual Average Water Balance with Future Climate Change and Land Use Change

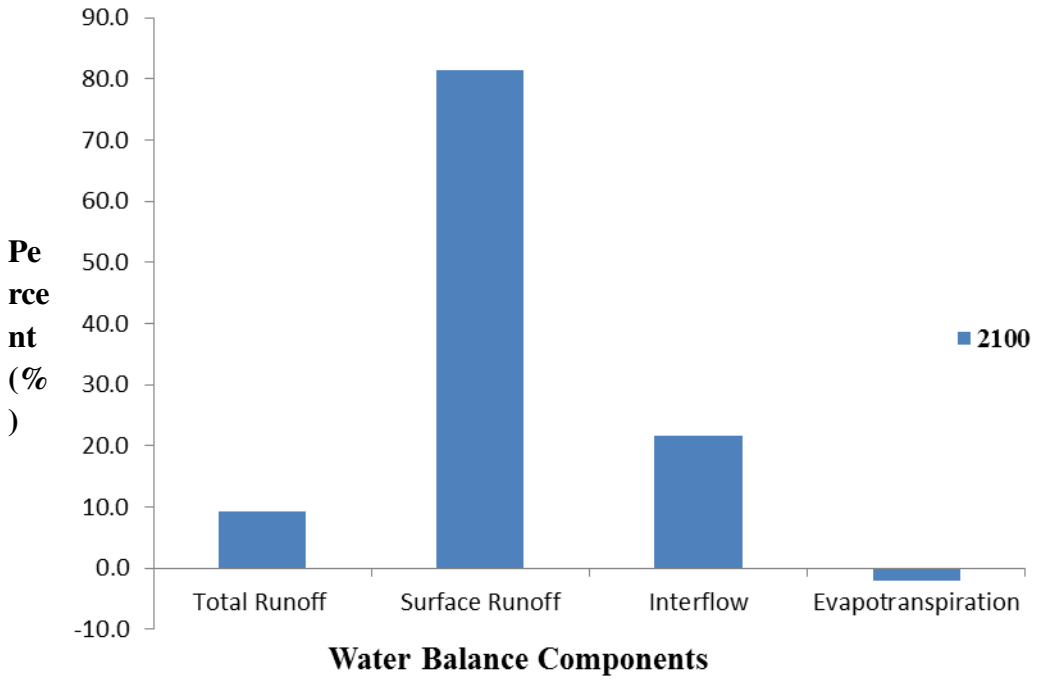

Figure 30 : Percent Changes in Water Balance with Future Land use change and Climate Change Scenario

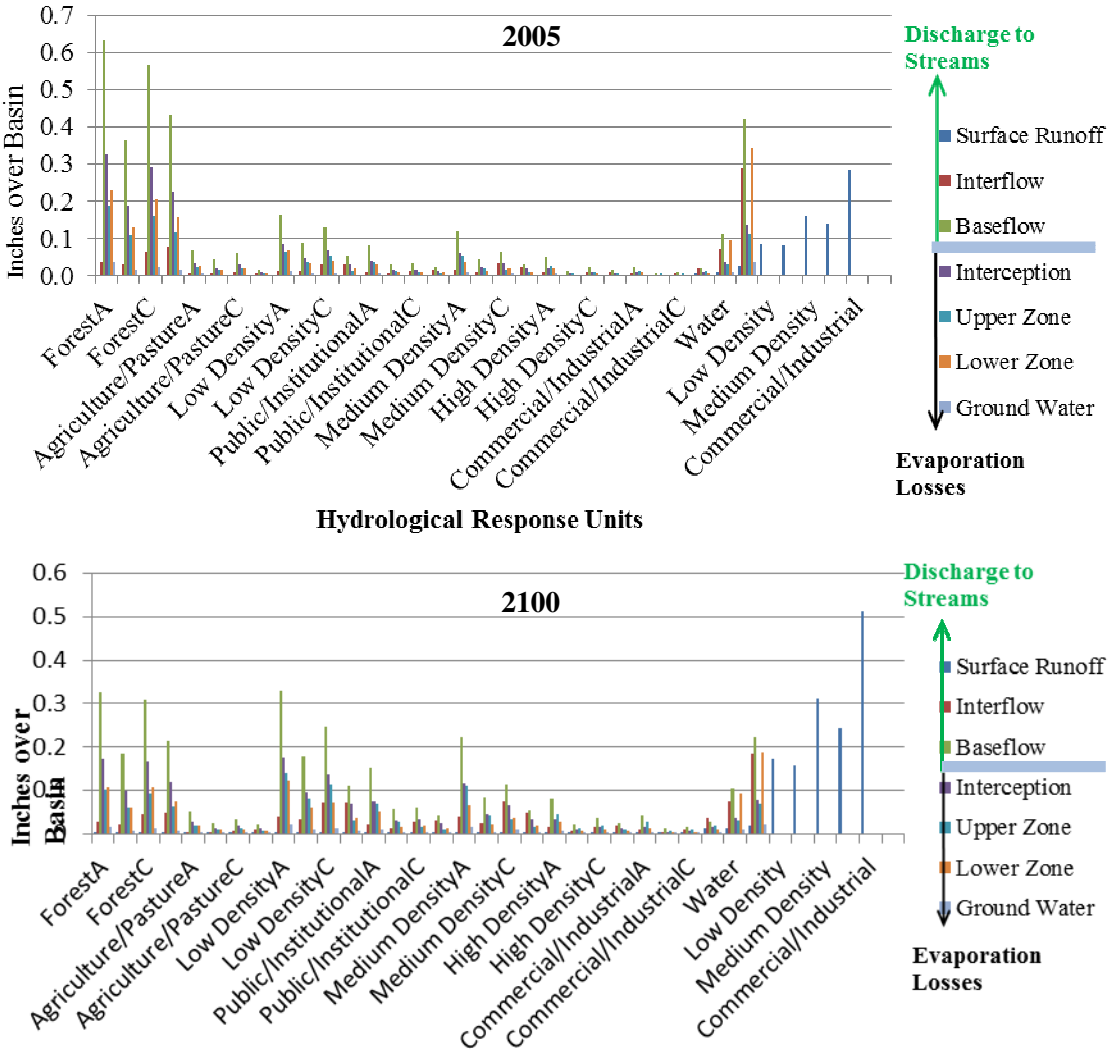

Figure 31 : Water-budget outflow components by Hydrologic Response Unit (HRU) simulated by the Hydrological Simulation Program–FORTRAN (HSPF) in SuAsCo watershed under 2005 and projected 2100 Land Use and Climate Change Scenario

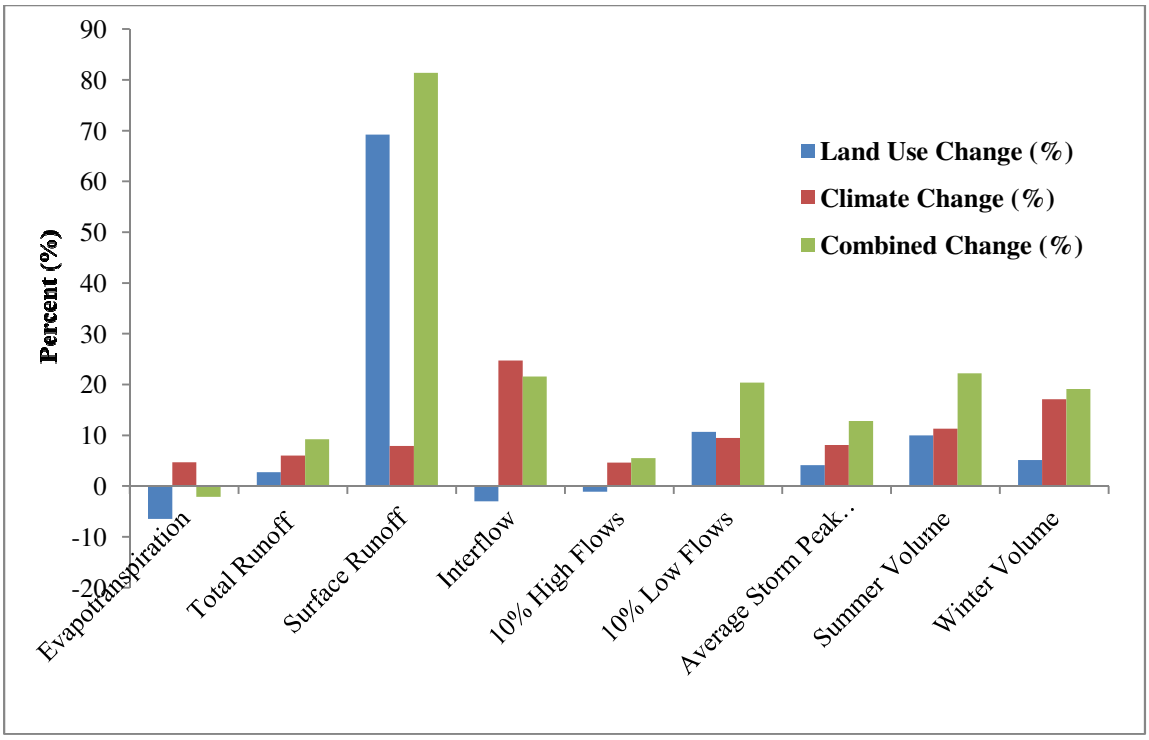

Figure 32: Comparison of independent change in land cover and climate with combined change in land cover and climate

BIBLIOGRAPHY

Abbaspour, K. C., M. Faramarzi, S. S. Ghasemi, and H. Yang (2009), Assessing the impact of climate change on water resources in Iran*, Water Resour. Res., 45*, W10434.

Adam, J. C. and Lettenmaier, D. P. (2003), Adjustment of global gridded precipitation for systematic bias, J. *Geophys. Res*., 108, 1–14.

Aguilera, R., R. Marcé, and S. Sabater (2012), Linking in-stream nutrient flux to land use and inter-annual hydrological variability at the watershed scale*, Sci. Total Environ., 440*, 72-81.

Ahiablame, L. M., B. A. Engel, and I. Chaubey (2013), Effectiveness of low impact development practices in two urbanized watersheds: Retrofitting with rain barrel/cistern and porous pavement*, J. Environ. Manage., 119*, 151-161.

Albek, M., Ü. Bakır Öğütveren, and E. Albek (2004), Hydrological modeling of Seydi Suyu watershed (Turkey) with HSPF*, Journal of Hydrology, 285*, 260-271.

Anchorage, AKNash, J. and J. Sutcliffe (1970), River flow forecasting through conceptual models part I—A discussion of principles*, Journal of hydrology, 10*, 282-290

Artola, C. G., B. L. Pareja, and P. G. Garcia (1995), Impact on hydrology and nutrient movements of developments in river basins draining into reservoirs*, Water Res., 29*, 601-609.

Barbaro, J. R. and Zarriello, P. J. 2007. A Precipitation-Runoff Model for the Blackstone River Basin, Massachusetts and Rhode Island.

Barbaro, J. R. and Sorenson, J. R. 2013. Nutrient and Sediment Concentrations, Yields, and Loads in Impaired Streams and Rivers in the Taunton River Basin, Massachusetts, 1997–2008.

Barrington, D. J., A. Prior, and G. Ho (2013), The role of water auditing in achieving water conservation in the process industry*, J. Clean. Prod., 52*, 356-361.

Berris, S. N. (1995)*, Conceptualization and Simulation of Runoff Generation from Rainfall for Three Basins in Thurston County, Washington*, US Geological Survey.

Bicknell, B., Imhoff, J., Kittle Jr, J., Donigian, A., Johanson, R. 1993. Hydrological Simulation Program—Fortran, Users Manual for Release 10: EPA-600.

Bicknell, B. R., J. C. Imhoff, J. L. Kittle Jr, T. H. Jobes, A. S. Donigian Jr, and R. Johanson (2001), Hydrological Simulation Program–FORTRAN: HSPF Version 12 User's Manual*, AQUA TERRA Consultants, Mountain View, California*.

Boyer, C., D. Chaumont, I. Chartier, and A. G. Roy (2010), Impact of climate change on the hydrology of St. Lawrence tributaries, *Journal of Hydrology, 384*, 65-83.

Brath, A., A. Montanari, and G. Moretti (2006), Assessing the effect on flood frequency of land use change via hydrological simulation (with uncertainty), *Journal of Hydrology, 324*, 141-153.

Brown, R. (1988), Effects Of Precipitation And Land Use On Storm Runoff, *JAWRA Journal of the American Water Resources Association, 24*, 421-426.

Brun, S. E. and L. E. Band (2000), Simulating runoff behavior in an urbanizing watershed, *Comput. , Environ. Urban Syst., 24*, 5-22.

Campbell, J. L., L. E. Rustad, E. W. Boyer, S. F. Christopher, C. T. Driscoll, I. J. Fernandez, P. M. Groffman, D. Houle, J. Kiekbusch, and A. H. Magill (2009), Consequences of climate change for biogeochemical cycling in forests of northeastern North America This article is one of a selection of papers from NE Forests 2100: A Synthesis of Climate Change Impacts on Forests of the Northeastern US and Eastern Canada., *Canadian Journal of Forest Research, 39*, 264-284.

Carpenter, S. R., N. F. Caraco, D. L. Correll, R. W. Howarth, A. N. Sharpley, and V. H. Smith (1998), Nonpoint pollution of surface waters with phosphorus and nitrogen, *Ecol. Appl., 8*, 559-568.

Carey, R. O., K. W. Migliaccio, Y. Li, B. Schaffer, G. A. Kiker, and M. T. Brown (2011), Land use disturbance indicators and water quality variability in the Biscayne Bay Watershed, Florida, *Ecol. Ind., 11*, 1093-1104.

Chen, L., R. M. Liu, Q. Huang, Y. X. Chen, S. H. Gao, C. C. Sun, Z. Y. Shen, S. Z. Ou, and S. L. Chen (2012), An integrated simulation-monitoring framework for nitrogen assessment: A case study in the Baixi watershed, China, *Procedia Environmental Sciences, 13*, 1076-1090.

Choi, W. and B. M. Deal (2008), Assessing hydrological impact of potential land use change through hydrological and land use change modeling for the Kishwaukee River basin (USA), *J. Environ. Manage., 88*, 1119-1130.

Cloern, J. E. (2001), Our evolving conceptual model of the coastal eutrophication problem, *Mar. Ecol. Prog. Ser., 210*, 223-253.

Codner, G., E. Laurenson, and R. Mein (1988), Hydrologic effects of urbanization: A case study, Hydrology and Water Resources Symposium 1988: Preprints of Papers**.**

Colin, T. (1995), Recent advances in statistical methods for the estimation of sediment and nutrient transport in rivers, *Rev. Geophys., 33*, 1117-1123.

Cuo, L., Y. Zhang, Y. Gao, Z. Hao, and L. Cairang (2013), The impacts of climate change and land cover/use transition on the hydrology in the upper Yellow River Basin, China, *Journal of Hydrology, 502*, 37-52.

Dechmi, F. and A. Skhiri (2013), Evaluation of best management practices under intensive irrigation using SWAT model, *Agric. Water Manage., 123*, 55-64.

Delgado, J. A., M. A. Nearing, and C. W. Rice (2013) , Chapter two - conservation practices for climate change adaptation, in *Advances in Agronomy*, vol. Volume 121Anonymous , pp. 47-115, Academic Press.

Den Biggelaar, C., R. Lal, K. Wiebe, H. Eswaran, V. Breneman, and P. Reich (2003), The Global Impact Of Soil Erosion On Productivity II: Effects On Crop Yields And Production Over Time, *Adv. Agron., 81*, 49-95.

DeGaetano, A. T., Eggleston, K. L., Knapp, W. W. (1994) Daily evapotranspiration and soil moisture estimates for the northeastern United States. Northeast Regional Climate Center, Cornell University, .

Deng, Z., J. L. M. P. de Lima, and H. Jung (2008), Sediment transport rate-based model for rainfall-induced soil erosion, *Catena, 76*, 54-62.

Denny, C. S. (1982) Geomorphology of New England. US Government Printing Office, .

Dodds, W. K. and E. B. Welch (2011), Establishing nutrient criteria in streams.

Donigian Jr, A., Imhoff, J., Kittle Jr, J. 1999. HSPFParm, An Interactive Database of HSPF Model Parameters. Version 1.0. AQUA TERRA Consultants, CA 94043.

Donigian, A.S. Jr., and J.T. Love. 2005. *The Use of Continuous Watershed Modeling to address Issues of Urbanization and Channel Stability in Southern California.* ASCE World Water and Environmental Resources Congress 2005. May 16-19, 2005.

Ducharne, A. (2008), Importance of stream temperature to climate change impact on water quality, *Hydrology and Earth System Sciences Discussions, 12*, 797-810.

Evans, D. J., C. E. Gibson, and R. S. Rossell (2006), Sediment loads and sources in heavily modified Irish catchments: A move towards informed management strategies, *Geomorphology, 79*, 93-113.

Ewen, J. and G. Parkin (1996), Validation of catchment models for predicting land-use and climate change impacts. 1. Method, *Journal of Hydrology, 175*, 583-594.

Ewert, F., M. K. van Ittersum, I. Bezlepkina, O. Therond, E. Andersen, H. Belhouchette, C. Bockstaller, F. Brouwer, T. Heckelei, and S. Janssen (2009), A methodology for enhanced flexibility of integrated assessment in agriculture, *Environ. Sci. & Policy, 12*, 546-561.

Forsee, W. J. and S. Ahmad (2011), Evaluating Urban Storm-Water Infrastructure Design in Response to Projected Climate Change*, J. Hydrol. Eng., 16*, 865-873.

Falkenmark, M. (2003), Freshwater as shared between society and ecosystems: from divided approaches to integrated challenges*, Philosophical Transactions of the Royal Society of London.Series B: Biological Sciences, 358*, 2037-2049.

Fu, B., Y. Wang, Y. Lu, C. He, L. Chen, and C. Song (2009), The effects of land-use combinations on soil erosion: a case study in the Loess Plateau of China*, Prog. Phys. Geogr., 33*, 793-804.

De Girolamo, A. M. and A. Lo Porto (2012), Land use scenario development as a tool for watershed management within the Rio Mannu Basin*, Land Use Policy, 29*, 691-701.

Giles, C. (2005), Concord Watershed 2001 Dwm Water Quality Monitoring Data.

Ghimire, S. R. and J. M. Johnston (2013), Impacts of domestic and agricultural rainwater harvesting systems on watershed hydrology: A case study in the Albemarle-Pamlico river basins (USA)*, Ecohydrology & Hydrobiology, 13*, 159-171.

Goonetilleke, A., E. Thomas, S. Ginn, and D. Gilbert (2005), Understanding the role of land use in urban stormwater quality management*, J. Environ. Manage., 74*, 31-42.

Harris, G. P. (2001), Biogeochemistry of nitrogen and phosphorus in Australian catchments, rivers and estuaries: effects of land use and flow regulation and comparisons with global patterns*, Marine and Freshwater Research, 52*, 139-149.

Henderson-Sellers, A., R. E. Dickinson, T. Durbidge, P. Kennedy, K. McGuffie, and A. Pitman (1993), Tropical deforestation: Modeling local-to regional-scale climate change*, Journal of Geophysical Research: Atmospheres (1984–2012), 98*, 7289-7315.

Horton, P., B. Schaefli, A. Mezghani, B. Hingray, and A. Musy (2006), Assessment of climate-change impacts on alpine discharge regimes with climate model uncertainty*, Hydrol. Process., 20*, 2091-2109.

Hock, R. (2005), Glacier melt: a review of processes and their modelling*, Prog. Phys. Geogr., 29*, 362-391.

Hong, B., K. E. Limburg, M. H. Hall, G. Mountrakis, P. M. Groffman, K. Hyde, L. Luo, V. R. Kelly, and S. J. Myers (2012), An integrated monitoring/modeling framework for assessing human–nature interactions in urbanizing watersheds: Wappinger and Onondaga Creek watersheds, New York, USA*, Environmental Modelling & Software, 32*, 1-15.

Hundecha, Y. and Bárdossy, A. 2004. Modeling of the effect of land use changes on the runoff generation of a river basin through parameter regionalization of a watershed model. Journal of Hydrology 292 (1–4), 281295.

Intergovernmental Panel on Climate Change (IPCC) (2007), *Climate Change: The Physical Science Basis*, edited by S. Solomon et al., 996 pp., Cambridge Univ. Press, Cambridge, U. K.

Jakeman, A. J. and R. A. Letcher (2003), Integrated assessment and modelling: features, principles and examples for catchment management*, Environmental Modelling & Software, 18*, 491-501

Johnson, M. S., W. F. Coon, V. K. Mehta, T. S. Steenhuis, E. S. Brooks, and J. Boll (2003), Application of two hydrologic models with different runoff mechanisms to a hillslope dominated watershed in the northeastern US: a comparison of HSPF and SMR*, Journal of Hydrology, 284*, 57-76.

Kim, J., J. Choi, C. Choi, and S. Park (2013), Impacts of changes in climate and land use/land cover under IPCC RCP scenarios on streamflow in the Hoeya River Basin, Korea*, Sci. Total Environ., 452–453*, 181-195.

Kosmas, C., N. Danalatos, L. H. Cammeraat, M. Chabart, J. Diamantopoulos, R. Farand, L. Gutierrez, A. Jacob, H. Marques, and J. Martinez-Fernandez (1997), The effect of land use on runoff and soil erosion rates under Mediterranean conditions*, Catena, 29*, 45-59.

Kung, H. and L. Ying (1991), A study of Lake Eutrophication in Shanghai, China*, Geogr. J.*, 45-50.

Kundzewicz, Z., L. Mata, N. Arnell, P. Döll, P. Kabat, B. Jiménez, K. Miller, T. Oki, Z. Sen, and I. Shiklomanov (2007), Freshwater resources and their management.[W:] Climate Change 2007: Impacts, Adaptation and Vulnerability. Contribution of Working Group II to the Fourth Assessment Report of the Intergovernmental Panel on Climate Change,(red. Parry, ML, Canziani, OF, Palutikof, JP, Hanson, CE & van der Linden, PJ).

Lane, L. J., M. Hernandez, and M. Nichols (1997), Processes controlling sediment yield from watersheds as functions of spatial scale*, Environmental Modelling & Software, 12*, 355-369.

Legates, D. R. and McCabe, G. J. 1999. Evaluating the use of "goodness-of-fit" measures in hydrologic and hydroclimatic model validation. Water Resources Research 35 (1), 233-241.

Li, Z., W. Liu, X. Zhang, and F. Zheng (2009), Impacts of land use change and climate variability on hydrology in an agricultural catchment on the Loess Plateau of China*, Journal of Hydrology, 377*, 35-42.

Lin, Y., N. Hong, P. Wu, C. Wu, and P. H. Verburg (2007), Impacts of land use change scenarios on hydrology and land use patterns in the Wu-Tu watershed in Northern Taiwan*, Landscape Urban Plann., 80*, 111-126.

Lumb, A. M., McCammon, R. B., Kittle, J. L. (1994) Users Manual for an Expert System (HSPEXP) for Calibration of the Hydrological Simulation Program--Fortran. US Geological Survey Reston, VA, .

Luo, Y., D. L. Ficklin, X. Liu, and M. Zhang (2013), Assessment of climate change impacts on hydrology and water quality with a watershed modeling approach*, Sci. Total Environ., 450–451*, 72-82.

Magnusson, J., T. Jonas, I. Lopez-Moreno, and M. Lehning (2010), Snow cover response to climate change in a high alpine and half-glacierized basin in Switzerland.

Massachusetts Department of Environmental Protection (MassDEP), CONCORD WATERSHED WATER QUALITY MONITORING DATA, SuAsCo Watershed Water Quality Assessment Report.,2001, *82wqar.doc ,DWM CN 92.0* (Available at http:// www.mass.gov/dep/water/resources/82wqar1/.

Massachusetts Department of Environmental Protection (MassDEP), DEP's Proposed Total Maximum Daily Loads (TMDL's) Strategy to Improve the Water Quality of Massachusetts Rivers and Lakes, MA82B-01-2004-01., 2004. (Available at http://www.mass.gov/eea/agencies/massdep/water/watersheds/total-maximum-daily-loads-tmdls.html).

Marshall, E. and T. Randhir (2008), Effect of climate change on watershed system: a regional analysis*, Clim. Change, 89*, 263-280.

Meehl, G. A., C. Covey, K. E. Taylor, T. Delworth, R. J. Stouffer, M. Latif, B. McAvaney, and J. F. Mitchell (2007), The WCRP CMIP3 multimodel dataset: A new era in climate change research*, Bull. Am. Meteorol. Soc., 88*, 1383-1394.

Merritt, W. S., Y. Alila, M. Barton, B. Taylor, S. Cohen, and D. Neilsen (2006), Hydrologic response to scenarios of climate change in sub watersheds of the Okanagan basin, British Columbia*, Journal of Hydrology, 326*, 79-108.

Milliman, J., K. Farnsworth, P. Jones, K. Xu, and L. Smith (2008), Climatic and anthropogenic factors affecting river discharge to the global ocean, 1951–2000*, Global Planet. Change, 62*, 187-194.

Milly, P. C., K. Dunne, and A. V. Vecchia (2005), Global pattern of trends in streamflow and water availability in a changing climate*, Nature, 438*, 347-350.

Moscrip, A. L. and D. R. Montgomery (1997), URBANIZATION, FLOOD FREQUENCY, AND SALMON ABUNDANCE IN PUGET LOWLAND STREAMS1*, JAWRA Journal of the American Water Resources Association, 33*, 1289-1297.

Mozumder, P., E. Flugman, and T. Randhir (2011), Adaptation behavior in the face of global climate change: Survey responses from experts and decision makers serving the Florida Keys*, Ocean Coast. Manage., 54*, 37-44.

Mohamoud, Y. M. and R. S. Parmar (2006), Estimating Streamflow and Associated Hydraulic Geometry, the Mid-Atlantic Region, USA, *Journal of the American Water Resources Association* (JAWRA), *42(3)*:755:768.

Mukundan, R., S. M. Pradhanang, E. M. Schneiderman, D. C. Pierson, A. Anandhi, M. S. Zion, A. H. Matonse, D. G. Lounsbury, and T. S. Steenhuis (2013), Suspended sediment source areas and future climate impact on soil erosion and sediment yield in a New York City water supply watershed, USA*, Geomorphology, 183*, 110-119.

Maurer, E.P. and H.G. Hidalgo (2008), Utility of daily vs. monthly large-scale climate data: an intercomparison of two statistical downscaling methods, *Hydrology and Earth System Sciences* Vol. 12, 551-563.

Niehoff, D., Fritsch, U., Bronstert, A. 2002. Landuse impacts on stormrunoff generation: scenarios of landuse change and simulation of hydrological response in a mesoscale catchment in SWGermany. Journal of Hydrology 267 (1–2), 8093.

Nie, W., Y. Yuan, W. Kepner, M. S. Nash, M. Jackson, and C. Erickson (2011), Assessing impacts of Landuse and Landcover changes on hydrology for the upper San Pedro watershed*, Journal of Hydrology, 407*, 105-114

Obropta, C. C. and J. S. Kardos (2007), Review of Urban Stormwater Quality Models: Deterministic, Stochastic, and Hybrid Approaches1*, JAWRA Journal of the American Water Resources Association, 43*, 1508-1523.

Ozturk, M., N. K. Copty, and A. K. Saysel (2013), Modeling the impact of land use change on the hydrology of a rural watershed*, Journal of Hydrology, 497*, 97-109.

Ozaki, N., T. Fukushima, H. Harasawa, T. Kojiri, K. Kawashima, and M. Ono (2003), Statistical analyses on the effects of air temperature fluctuations on river water qualities*, Hydrol. Process., 17*, 2837-2853.

Park, J., L. Duan, B. Kim, M. J. Mitchell, and H. Shibata (2010), Potential effects of climate change and variability on watershed biogeochemical processes and water quality in Northeast Asia*, Environ. Int., 36*, 212-225.

Parry, M. L. (2007)*, Climate Change 2007: Impacts, Adaptation and Vulnerability: Working Group II Contribution to the Fourth Assessment Report of the IPCC Intergovernmental Panel on Climate Change*, vol. 4, Cambridge University Press.

Pielke, R. A. and R. Avissar (1990), Influence of landscape structure on local and regional climate*, Landscape Ecol., 4*, 133-155.

Quevauviller, P. (2011), Adapting to climate change: reducing water-related risks in Europe – EU policy and research considerations*, Environ. Sci. & Policy, 14*, 722-729.

Ramin, B. and A. McMichael (2009), Climate Change and Health in Sub-Saharan Africa: A Case-Based Perspective*, EcoHealth, 6*, 52-57.

Randhir, T. (2003), Watershed-scale effects of urbanization on sediment export: Assessment and policy, *Water Resour. Res., 39*, 1169.

Randhir, T. O. and A. G. Hawes (2009), Watershed land use and aquatic ecosystem response: Ecohydrologic approach to conservation policy, *Journal of Hydrology, 364*, 182-199.

Randhir, T. O. and O. Tsvetkova (2011), Spatiotemporal dynamics of landscape pattern and hydrologic process in watershed systems, *Journal of Hydrology, 404*, 1-12.

Ribarova, I., P. Ninov, and D. Cooper (2008), Modeling nutrient pollution during a first flood event using HSPF software: Iskar River case study, Bulgaria, *Ecol. Model., 211*, 241-246.

Riskin, M. L., J. R. Deacon, M. L. Liebman, and K. W. Robinson (2003), *Nutrient and Chlorophyll Relations in Selected Streams of the New England Coastal Basins in Massachusetts and New Hampshire, June-September 2001*, vol. 3, US Geological Survey.

Runkel, R. L., C. G. Crawford, and T. A. Cohn (2004), *Load Estimator (LOADEST): A FORTRAN Program for Estimating Constituent Loads in Streams and Rivers*, US Department of the Interior, US Geological Survey.

Santhi, C., R. Srinivasan, J. G. Arnold, and J. R. Williams (2006), A modeling approach to evaluate the impacts of water quality management plans implemented in a watershed in Texas, *Environmental Modelling & Software, 21*, 1141-1157.

Sauer, T. J., R. B. Alexander, J. V. Brahana, and R. A. Smith (2008), Chapter 8 - the importance and role of watersheds in the transport of nitrogen, in *Nitrogen in the Environment (Second Edition)*, edited by J.L. Hatfield and R.F. Follett, pp. 203-240, Academic Press, San Diego.

Schueler, T. and R. Claytor (1997), Impervious cover as a urban stream indicator and a watershed management tool, Effects of Watershed Development and Management on Aquatic Ecosystem.

Shen, Z., Q. Hong, Z. Chu, and Y. Gong (2011), A framework for priority non-point source area identification and load estimation integrated with APPI and PLOAD model in Fujiang Watershed, China, *Agric. Water Manage., 98*, 977-989.

Shi, Z. H., L. Ai, X. Li, X. D. Huang, G. L. Wu, and W. Liao (2013), Partial least-squares regression for linking land-cover patterns to soil erosion and sediment yield in watersheds, *Journal of Hydrology, 498*, 165-176.

Shrestha, R. R., Y. B. Dibike, and T. D. Prowse (2012), Modelling of climate-induced hydrologic changes in the Lake Winnipeg watershed, *J. Great Lakes Res., 38, Supplement 3*, 83-94

Singh, R., K. Subramanian, and J. C. Refsgaard (1999), Hydrological modelling of a small watershed using MIKE SHE for irrigation planning*, Agric. Water Manage., 41*, 149-166.

Singh, J., Knapp, H. V., Arnold, J., Demissie, M. 2005. Hydrological modeling of the iroquois river watershed using HSPF and SWAT1.

Singh, R. K., R. K. Panda, K. K. Satapathy, and S. V. Ngachan (2011), Simulation of runoff and sediment yield from a hilly watershed in the eastern Himalaya, India using the WEPP model*, Journal of Hydrology, 405*, 261-276.

Singh, V. P. and V. P. Singh (1997)*, Kinematic Wave Modeling in Water Resources: Environmental Hydrology*, Wiley New York.

Smith, M. P. (2000), Watershed Teams Take Charge: Results from the Massachusetts Watershed Initiative*, Proceedings of the Water Environment Federation, 2000*, 341-355.

Stocker, T., Qin, D., Plattner, G., Tignor, M., Allen, S., Boschung, J., Nauels, A., Xia, Y., Bex, B., Midgley, B. 2013. IPCC, 2013: climate change 2013: the physical science basis. Contribution of working group I to the fifth assessment report of the intergovernmental panel on climate change.

Stohlgren, T. J., T. N. Chase, R. A. Pielke, T. G. Kittel, and J. Baron (1998), Evidence that local land use practices influence regional climate, vegetation, and stream flow patterns in adjacent natural areas*, Global Change Biol., 4*, 495-504.

Sutherland, R. 2000. Methods for Estimating Effective Impervious Cover. The Practice of Watershed Protection

Tang, Z., B. Engel, B. Pijanowski, and K. Lim (2005), Forecasting land use change and its environmental impact at a watershed scale*, J. Environ. Manage., 76*, 35-45.

Therond, O., H. Belhouchette, S. Janssen, K. Louhichi, F. Ewert, J. Bergez, J. Wery, T. Heckelei, J. A. Olsson, and D. Leenhardt (2009), Methodology to translate policy assessment problems into scenarios: the example of the SEAMLESS integrated framework*, Environ. Sci. & Policy, 12*, 619-630

Tong, S. T. Y., Y. Sun, T. Ranatunga, J. He, and Y. J. Yang (2012), Predicting plausible impacts of sets of climate and land use change scenarios on water resources*, Appl. Geogr., 32*, 477-489.

Tran, L. T. and R. V. O'Neill (2013), Detecting the effects of land use/land cover on mean annual streamflow in the Upper Mississippi River Basin, USA*, Journal of Hydrology, 499*, 82-90.

US Environmental Protection Agency (1999), National water quality inventory: *1998 report to congress EPA, 841-R-00-001. Washington, DC.*

US Environmental Protection Agency (2011), Integrated reporting categories 303(d) submission U.S. *EPA,, Washington, DC*, [http://www.epa.gov/waterscience/standards/academy/supp/tmdl/page7.htm, accessed 04/2011]

Vaze, J., D. A. Post, F. H. S. Chiew, J. -. Perraud, N. R. Viney, and J. Teng (2010), Climate non-stationarity – Validity of calibrated rainfall–runoff models for use in climate change studies*, Journal of Hydrology, 394*, 447-457.

Wang, S., X. Qian, Q. H. Wang, and W. Xiong (2012), Modeling Turbidity Intrusion Processes in Flooding Season of a Canyon-Shaped Reservoir, South China*, Procedia Environmental Sciences, 13*, 1327-1337.

White, M. D. and K. A. Greer (2006), The effects of watershed urbanization on the stream hydrology and riparian vegetation of Los Penasquitos Creek, California*, Landscape Urban Plann., 74*, 125-138.

Wasige, J. E., T. A. Groen, E. Smaling, and V. Jetten (2013), Monitoring basin-scale land cover changes in Kagera Basin of Lake Victoria using ancillary data and remote sensing*, International Journal of Applied Earth Observation and Geoinformation, 21*, 32-42.

Williamson, C. E., W. Dodds, T. K. Kratz, and M. A. Palmer (2008), Lakes and streams as sentinels of environmental change in terrestrial and atmospheric processes*, Frontiers in Ecology and the Environment, 6*, 247-254.

Wilson, C. O. and Q. Weng (2011), Simulating the impacts of future land use and climate changes on surface water quality in the Des Plaines River watershed, Chicago Metropolitan Statistical Area, Illinois*, Sci. Total Environ., 409*, 4387-4405.

Wischmeier, W. H. and D. D. Smith (1978), Predicting rainfall erosion losses-A guide to conservation planning.*, Predicting rainfall erosion losses-A guide to conservation planning*.

Wolter, P. T., C. A. Johnston, and G. J. Niemi (2006), Land Use Land Cover Change in the U.S. Great Lakes Basin 1992 to 2001*, J. Great Lakes Res., 32*, 607-628.

Wood, A. W., Leung, L. 5 R., Sridhar, V., and Lettenmaier, D. P.: Hydrologic implications of dynamical and statistical approaches to downscaling climate model outputs, *Climatic Change*, 62, 189–216, 2004.

Xia, L. L., R. Z. Liu, and Y. W. Zao (2012), Correlation Analysis of Landscape Pattern and Water Quality in Baiyangdian Watershed*, Procedia Environmental Sciences, 13*, 2188-2196.

Yan, B., N. F. Fang, P. C. Zhang, and Z. H. Shi (2013), Impacts of land use change on watershed streamflow and sediment yield: An assessment using hydrologic modelling and partial least squares regression*, Journal of Hydrology, 484*, 26-37.

Yang, Y., Z. He, Y. Wang, J. Fan, Z. Liang, and P. J. Stoffella (2013), Dissolved organic matter in relation to nutrients (N and P) and heavy metals in surface runoff water as affected by temporal variation and land uses – A case study from Indian River Area, south Florida, USA*, Agric. Water Manage., 118*, 38-49.

Zarriello, P. J. and K. G. Ries (2000)*, A Precipitation-Runoff Model for Analysis of the Effects of Water Withdrawals on Streamflow, Ipswich River Basin, Massachusetts*, US Department of the Interior, US Geological Survey.

Zarriello, P. J., Parker, G. W., Armstrong, D. S., Carlson, C. S. (2010) Effects of Water Use and Land Use on Streamflow and Aquatic Habitat in the Sudbury and Assabet River Basins, Massachusetts. US Department of the Interior, US Geological Survey, .

Zentner, R., G. Lafond, D. Derksen, C. Nagy, D. Wall, and W. May (2004), Effects of tillage method and crop rotation on non-renewable energy use efficiency for a thin Black Chernozem in the Canadian Prairies*, Soil Tillage Res., 77*, 125-136.

Zhang, S., B. Ye, S. Liu, X. Zhang, and S. Hagemann (2012), A modified monthly degree-day model for evaluating glacier runoff changes in China. Part I: model development*, Hydrol. Process., 26*, 1686-1696